DOCTORAL THESIS IN CHEMICAL ENGINEERING
STOCKHOLM, SWEDEN 2016

Application of Nanomaterials for the Removal of Hexavalent Chromium and their Biological Implications

Terrance Burks

KTH ROYAL INSTITUTE OF TECHNOLOGY
SCHOOL OF CHEMICAL SCIENCE AND ENGINEERING

TRITA-CHE Report 2016:4
ISSN 1654-1081
ISBN 978-91-7595-813-2

Akademisk avhandling som med tillstånd av Kungl Tekniska Högskolan framlägges till offentlig granskning för avläggande av teknologie doktorsexamen i kemiteknik den 29 januari 2016 klockan 10:00 i sal D2, Lindstedtsvägen 5, Kungl Tekniska Högskolan, Stockholm, Sweden.

Tryck: Universitetsservice US-AB

Abstract

The International Agency for Research on Cancer (IARC) stated that chromium in the form of Cr(VI) has been deemed to be a class-A human carcinogen. It has been a major contaminant associated with wastewater. Moreover, the existence of heavy metals in aquatic systems is a critical concern for the environment as well as industries that manufacture or consume these particular elements. In order to remove these particular toxic metals, several well-known conventional methods including ion-exchange, filtration and adsorption are used. Amongst these methods, adsorption offers significant advantages such as the low-cost materials, ease of operation and efficiency in comparison to the other conventional methods.

The aim of this work was to develop nanomaterials (particles and fibers) to address some critical issues for the treatment of heavy metals, especially chromium in aqueous systems. Furthermore, the use of nanomaterials and how they relate to nanoscale operations at the biological level has generated considerable concerns in spite of their novel properties.
The first part of this thesis deals with the synthesis and characterizations of Fe_3O_4, magnetite, as nanoparticles which were further coated with surfactants bis(2,4,4-trimethylpentyl)dithiophosphinic acid, Cyanex-301, and 3-Mercaptopropionic acid with the active compound being the thiol (SH) groups, that will suffice as a viable material for Cr(VI) removal from aqueous solutions. The proposed mechanism was the complexation between the thiol group on Cyanex-301 and 3-Mercaptopropionic acid, respectively. The effect of different parameters on the adsorption including contact time, initial and final Cr(VI) ion concentration and solution pH was investigated.

The second part of this thesis encompassed the fabrication of flexible nanocomposite materials, with a large surface area and architecture for the removal of Cr(VI) in batch and continuous flow mode. A technique known as electrospinning was used to produce the nanofibers. The flexible yet functional materials architecture has been achieved by growing ZnO nanorod arrays through chemical bath deposition on synthesized electrospun poly-L-lactide nanofibers. Moreover, polyacrylonitrile nanofibers (PAN) were synthesized and adapted by the addition of hydroxylamine hydrochloride to produce amidoxime polyacrylonitrile nanofibers (A-PAN). Scanning electron microscopy (SEM) and transmission electron microscopy (TEM) were used to identify the morphologies and particle sizes whereas Fourier-Transform Infrared spectroscopy (FT-IR) was used to identify either the presence or absence of functional groups for the formation of PAN and A-PAN nanofibers. The optimization of functionalized nanoadsorbents to adsorb Cr(VI) was also carried out to investigate the effect of experimental parameters: contact time, solution pH, initial, final and other metal ion concentration. Commercially manufactured pristine engineered (TiO_2, ZnO and SiO_2) nanoparticles and lab-made functionalized (Fe_3O_4 and CeO_2) nanoparticles were studied while the powders were suspended in appropriate media by Dynamic Light Scattering (DLS) to identify their cytotoxicity effects.

Keywords: Adsorption, Chromium(VI), toxicology, extractant, nanofiber, engineered and lab-made nanoparticles, desorption

Sammanfattning

Internationella centrumet for cancerforskningen (IARC) uppgav att krom i form av Cr (VI) har bedömts vara en klass-A cancerframkallande ämne hos människor. Cr (VI) har förkommer som en stor förorening i samband med utsläpp av avloppsvatten. Förkomsten av tungmetaller i akvatiska system anses vara en kritisk oro för miljön samt industrier som tillverkar eller förbrukar just dessa element. För att avlägsna dessa giftiga metaller, är flera välkända och konventionella metoder inklusive jonbyte, filtrering och adsorption användbara i gagens system. Bland dessa metoder erbjuder adsorption betydande fördelar såsom billiga material, enkelt handhavande och effektivitet i jämförelse med andra de andra metoder.

Syftet med detta arbete är att utveckla nanomaterial (partiklar och fibrer) föt att ta itu med i fråga om några kritiska parametrar för behandling av tungmetaller, särskilt krom i vattenbaserade system. Vidare har användningen av nanomaterial och hur de relaterar till på biologiska nivå studerats trots att nanomaterial har genererat unika egenskaper.

Första delen av denna avhandling handlar om syntes och karakterisering av Fe_3O_4, magnetit, som nanopartiklar var vidare belagda med tensider bis (2,4,4-trimetylpentyl) dithiophosphinic syra, Cyanex-301, och 3-merkaptopropionsyra med den aktiva föreningen av tiol (SH)-grupper. Dessa har visats vara en praktisk material för att avlägsna Cr (VI) från akvatiska system. Den föreslagna mekanismen var en komplex bildning mellan tiolgruppen på Cyanex-301 och 3-merkaptopropionsyra. Effekten av olika parametrar på adsorptionen inklusive kontakttiden, ininitiala och slut knocentrationen på Cr (VI) samt lösningens pH har undersöktes.

Den andra delen av denna avhandling omfattar tillverkning av flexibla nanokompositmaterial, med en stor yta och arkitektur för att avlägsna Cr (VI) i satsvis och kontinuerligt flöde. En teknik känd som elektrospinning användes för att framställa nanofibrer. Den flexibla och funktionella material arkitektur uppnåddes genom att låta ZnO nanostavar växa i ett kemiskt bad och genom utfällning på de syntetiserade elektrospunna poly-L-laktid nanofibrerna. Dessutom har polyakrylnitril nanofibrer (PAN) syntetiseras och anpassats genom tillsats av hydroxylaminhydroklorid för att producera amidoximen polyakrylnitril nanofibrer (A-PAN). Svepelektronmikroskopi (SEM) och transmissions elektronmikroskopi (TEM) utfördes för att identifiera morfologin och partikelstorlekar medan Fourier-Transform Infraröd spektroskop (FT-IR) användes för att identifiera antingen närvaro eller frånvaro av funktionella grupper för bildandet av PAN och A-PAN nanofibrer. Optimeringen av funktionella nanoadsorbent för att adsorbera Cr (VI) genomfördes för att undersöka effekten av olika parametrar: kontakttid, lösningens pH, begynnelse och slut och andra metall-jonkoncentrationer. Kommersiellt tillverkade och anordande nanopartiklar (TiO_2, ZnO och SiO_2) samt labbtillverkade nanopartiklar (Fe_3O_4 och CeO_2) studerades gernom att suspendera i lämplig västka genom Dynamic Light Scattering (DLS) teknik för att iaktta cytotoxiska effekter.

Nyckelord: adsorption, krom (VI), toxikologi, extraktant, nanofiber, anordnade och labbtillverkade nanopartiklar, desorption

And we know that in all things God works for the good of those who love the Lord who have been called according to His purpose…..Romans 8:28

To my parents: Mr and Mrs W.L. and Mary Burks; Atty. and Mrs. Landman and Peggy Teller and my loving brothers, sisters, nephews, nieces and extended family

List of Publications

I. M.Avila, **T.Burks**, F.Akhtar, M.Göthelid, P.C.Lansåker, M.S.Toprak, M. Muhammed and A.Uheida. Surface functionalized nanofibers for the removal of Chromium(VI) from Aqueous Systems. Chemical Engineering Journal, vol. 245, pp201-209, 2014.

II. **T.Burks**, M.Avila, F.Akhtar, M.Göthelid, P.C.Lansåker, M.S.Toprak, M. Muhammed and A.Uheida. Studies on the adsorption of Chromium(VI) onto 3-Mercaptopropionic acid coated superparamagnetic iron oxide nanoparticles, Journal of Colloid and Interface Science, vol.425, pp36-43, 2014.

III. **T.Burks**, A.Uheida, M.Saleemi, M.Eita, M.S.Toprak, and M.Muhammed. Removal of Chromium(VI) using Surfaced Modified Superparamagnetic Iron Oxide Nanoparticles. Journal of Separation and Science Technology, vol.48, no.8, pp1243-1251, 2013.

IV. J.Shi, H.Karlsson, K.Johansson, V.Gogvadze, L.Xiao, J.Li, **T.Burks**, A. Uheida, M.Muhammed, S.Mathur, R.Morgenstern, V.Kagan, B.Fadeel, Microsomal Glutathione Transferase1 Protects Against Silica Nanoparticle-Induced Cytotoxicity, ACS Nano, vol.6, no.3, pp1925-38, 2012.

V. Murray A.R., Kisin E., Inman A., Young S.H., Muhammed M., **Burks T.**, Uheida A., Tkach A., Waltz M., Castranova V., Fadeel B., Kagan V.E., Riviere J.E., Monteiro-Riviere N., Shvedova A.A., Oxidative stress and dermal toxicity of iron oxide nanoparticles in vitro, Cell Biochem Biophys, vol.67, no.2, pp461-76, 2013.

VI. **T.Burks**, F.Akthar, M.Saleemi, M.Avila, Y.Kiros. The Extraction and Regeneration of Cr(VI) Utilizing A Highly Flexible ZnO-PLLA Nanofiber Nanocomposite for Continuous Flow Mode Purification of Water, Journal of Environmental and Public Health, vol.2015, 2015.

Contributions of the Author

I. Planning and performing of the experiments, analysis of the samples, evaluation of some of the results and writing.

II. Planning and performing of the experiments, analysis of the samples, evaluation of the results and writing.

III. Planning and performing of the experiments, analysis of the samples, evaluation of the results and writing.

IV. Performing dissolution experiment, characterization and analysis of samples Characterization and analysis of samples.

V. Characterization and analysis of the samples.

VI. Planning and performing of the experiments, analysis of the samples and evaluation of the results and writing.

Other papers not included

I. **T.Burks,** M.Saleemi and F.Akhtar, Synthesis and Characterization of Cellulose Nanofibers and Zeolite Crystals for the removal of Arsenic(V) and Chromium(VI) from Aqueous Solutions. Submitted

II. **T.Burks,** F.Akhtar, M.Avila, M.Saleemi and Y.Kiros, Functionalized Polyacrylonitrile Nanofibers for the removal of Arsenic(V) and Chromium(VI) from Aqueous Solutions. Manuscript

Conference Presentations

I. **T.Burks,** M.Saleemi, and F.Akthar. FTIR and SEM characterization of Cellulose Nanofiber and Commercial Zeolite crystals for the removal of Arsenic (V) and Chromium (VI) from Aqueous Solution. International Materials Research Congress, Cancun, Mexico 2015 (Oral presentation).

II. **T.Burks**, F.Akthar, M.Saleemi, M.Avilia, and Y.Kiros. The Extraction and Regeneration of Cr(VI) Utilizing A Highly Flexible ZnO-PLLA Nanofiber Nanocomposite for Continuous Flow Mode Purification of Water. Young Water Professional Conference. Kuala Lumpor, Malaysia 2015 (Oral presentation).

III. **T.Burks**, M.Avila, M.S.Toprak, A.Uheida and M.Muhammed. Adsorption of Chromium (VI) for Environmental Water Applications. Accepted poster Nanotek Philadelphia, Pennsylvania U.S.A 2012.

IV. **T.Burks**, M.Avila, M.S.Toprak, A.Uheida and M.Muhammed. 3-Mercaptopropionic acid coated Superparamagnetic Iron Oxide Nanoparticles for the removal of Chromium(VI). Accepted poster E-MRS Strasbourg, France 2012.

V. A.R.Murray, E.Kisin, A.Inman, S.H.Young, M.Muhammed, **T.Burks**, A.Uheida, A.Tkach, M.Waltz, V.Castranova1, B.Fadeel, V.E.Kagan, J.E. Riviere, N.Monteiro-Riviere, A.A.Shvedova. Iron Oxide Nanoparticles Cause Oxidative Stress and Dermal Toxicity. Presented at Society of Toxicology Meeting in U.S.A. Sept 2010.

VI. J.Shi, K.Johansson, V.Gogvadze, L.Xiao, J.Li, **T.Burks**, A.Uheida, M. Muhammed, S.Mathur, R.Morgenstern, V.Kagan, B.Fadeel. Microsomal Glutathione Transferase1 Protects Against Silica Nanoparticle-Induced Cytotoxicity Presented at Nanotoxicology. Edinbergh, Scotland 2010.

VII. **T.Burks**, A.Uheida, M.Saleemi, A.Sugunan, M.S.Toprak and M.Muhammed. Highly flexible nanofiber nanocomposite for the removal of Cr(VI) from aqueous solutions. Presented poster at Nanostructured Materials. Rome, Italy 2010.

Symbols and Abbreviations

q_e	Amount of solute adsorbed per unit weight of sorbent (mgL g^{-1})
C_e	Equilibrium metal concentration (mg L^{-1})
K,K_L	Langmuir constant (L mg-1)
C_i	Initial solute concentration (mg L^{-1})
C_e,C_t	Solute concentration in the aqueous phase at equilibrium (mg L^{-1})
C_o	Initial concentration of solute (mg L^{-1})
V	Total aqueous volume (L)
m	Weight of the solid (g)
q_{max}	Maximum adsorption capacity (mg g^{-1})
k_L and Q_o	Langmuir constant (L mg^{-1})
q_f	Amount of metal ion adsorbed in (mg g^{-1})
C_f	Concentration of metal ion at equilibrium (mg L^{-1})
K_f	Freundlich constant (mg g^{-1})
C_S	Adsorbate monolayer saturation concentration (mg L^{-1})
t	Time (min)
n	Freundlich isotherm exponent; heterogeneity factor
k_1	Pseudo-first-order rate constant (min^{-1})
q_t	Adsorption capacity of solute (mg g^{-1})
k,k_2	Pseudo-second-order rate constant (g mg^{-1} min^{-1})
R_2	Correlation factor
D	Distribution ratio
A_1	Concentration of material in phase 1
A_2	Concentration of material in phase 2
A^+	Counterion in liquid
R^-	Fixed negative charge
B^+	Counterion in solid
d_{hkl}	Miller indices
λ	Wavelength
Θ	Angle
R_L	Separation factor
X-	Coion
N	Integer
NF-κB	Eukaryotic transcription factor

Table of Contents

1. Background

Clean water can be defined as water which is liberated from harmful or toxic chemicals. Water that is free of toxic chemicals and pathogens is crucial to human health and to a variety of industrial processes. As a scarce resource and an issue in developing countries, water is the most essential element to human life and ecosystem [1]. In 2015, it was estimated that 3900 children die daily from a lack of clean water and 672 million inhabitants will not have access to clean potable water [2],[3]. The amount of contaminated water is drastically increasing as a result of world population growth [4],[5], global warming [6] and industrial growth [7],[3],[8].

In wastewater, contaminants can include heavy metals, organic and inorganic compounds [9-11]. When released into the environment (i.e. aquatic systems), they can produce harmful effects to human beings and the environment. Therefore, access to clean and safe drinking water is receiving huge attention. The necessity to improve and develop new and more efficient water cleaning processes has vastly intensified.

1.1 Heavy metals in aquatic solutions

Heavy metal(s) can be defined as a metallic chemical element that has a high density. These metal(s) are toxic or even poisonous at relatively low concentrations. The term heavy metal is a generic word for any element that is metal. It has the atomic mass higher than that of calcium [12]. Heavy metals are natural components of the earth's crust; they cannot be degraded or destroyed due to their variation in concentration. It is the properties of the metals that govern the distribution of the metals in the environment and therefore influencing environmental factors [13]. The heavy metals contaminated chain more than likely follows a cyclical order: industry, atmosphere, soil, water, foods and humans [14].

As trace elements, some heavy metals (e.g. copper, selenium, zinc) are essential to maintain the metabolism of the human body. However, at higher concentrations they can lead to poisoning. From drinking-water contamination (e.g. lead pipes), high ambient air concentrations (near emission sources), or intake via the food chain could result in heavy metal poisoning. In chemical reactions, metals, which carry a positive charge, can act as a donor of electrons. Moreover, they cause the formation of salt compounds.

Heavy metals are dangerous because they tend to bioaccumulate, i.e. increase their concentration over time in soft tissues. Hence, heavy metals are taken up and stored faster than they are broken down (metabolized) or excreted [15].

Heavy metals can enter a water supply by industrial and consumer waste and/or even from the acid rain breaking down the soil and releasing the heavy metals into streams, lakes, rivers, and groundwater as seen in Table 1.

Table 1. Heavy metal effects on humans as pertaining to industrial applications [16].

Metal	Source	Toxic effect	Reference
Lead	Electroplating, manufacturing of batteries, pigments and ammunition	Anemia, brain damage, anorexia, malaise, loss of appetite, diminishing IQ	[17-19]
Cadmium	Electroplating, smelting, alloy manufacturing, pigments, plastic, mining, refining	Carcinogenic, renal disturbances, lung insufficiency, bone lesions, cancer, hypertension, Itai–Itai disease, weight loss	[20, 21,18, 22,23]

Mercury	Weathering of mercuriferous areas, volcanic eruptions, naturally-caused forest fires, biogenic emissions, battery production, fossil fuel burning, mining and metallurgical processes, paint and chloralkali industries	Neurological and renal disturbances, impairment of pulmonary function, corrosive to skin, eyes, muscles, dermatitis, kidney damage	[24-26]
Chromium (VI)	Electroplating, leather tanning, textile, dyeing, electroplating, metal processing, wood preservatives, paints and pigments, steel fabrication and canning industry	Carcinogenic, mutagenic, teratogenic, epigastric pain nausea, vomiting, severe diarrhea, producing lung tumors	[27-30]
Arsenic	Smelting, mining, energy production from fossil fuels, rock sediments	Gastrointestinal symptoms, disturbances of cardiovascular and nervous system functions, bone marrow depression, hemolysis, hepatomegaly, melanosis, polyneuropathy and encephalopathy, liver tumor	[31-33]
Copper	Printed circuit board manufacturing, electronics plating, plating, wire drawing, copper polishing, paint manufacturing, wood preservatives and printing operations	Reproductive and developmental toxicity, neurotoxicity, and acute toxicity, dizziness, diarrhea	[34-36]
Zinc	Mining and manufacturing processes	Causes short term 'metal-fume fever', gastrointestinal distress, nausea and diarrhea	[37]
Nickel	Non-ferrous metal, mineral processing, paint formulation, electroplating, porcelain enameling, copper sulphate manufacture and steam-electric power plants	Chronic bronchitis, reduced lung function, lung cancer	[38 39]

When heavy metals are accumulated or discarded to the aquatic media in large quantities, they can and often become troublesome to life and the environment. As a result, the WHO and other local and national organizations implemented goals and guidelines (Table 2) ensuring basic and adequate requirements regarding safe water. In 1999, Swedish leaders made a dynamic change by creating guidelines that encompassed drinking and recreational water, wastewater; with the thorough integration of risk assessment and management as well as exposure control of chemical elements [40].

Table 2. Recommended concentrations of various elements for drinking water [41-42].

Element	Guideline value (ppm)	Maximum value (ppm)	Minimum value (ppm)
Antimony	0.02	0.05	0.003
Arsenic	0.01	<0.05	0.007
Barium	0.7	2.0	0.1
Boron	2.4	5.0	0.2
Bromate	0.01	0.025	0.005
Cadmium	0.003	0.05	0.001
Chlorate	0.7	1.0	0.02
Chlorine	5.0	5.0	0.2
Chlorite	0.7	1.0	0.15

Chromium	0.05	0.5	0.04
Copper	2.0	3.0	0.1
Cyanide	0.07	0.6	0.01
Fluoride	1.5	4.0	0.6
Lead	0.01	0.1	0.005
Manganese	0.4	0.5	0.05
Mercury	0.006	0.007	0.0005
Molybdenum	0.07	0.25	0.05
Nickel	0.07	0.1	0.01
Nitrate	50 (NO_3^-)	100 (NO_3^-)	45 (NO_3^-)
Selenium	0.04	0.05	0.007
Uranium	0.03	0.1	0.002

1.2 Chromium

Chromium (Cr) is the 24th element of the periodic table. Its name is derived from the Greek word *chroma* which means color due to the fact that many of its compounds are colored [43]. Chromium is a naturally occurring element found in rocks, animals, plants, soil, and in volcanic dust and gases. Chromium can exist in different oxidation states: Cr(0) (metallic chromium), Cr(II) (chromous), Cr(III) (chromic) and Cr(VI) (chromates). Chromium metal is not found naturally in the environment and is produced from other minerals such as chromite (chrome ore) that contains Cr(III). Chromium (III) is the most stable oxidation state and forms coordination complexes with ligands such as water, urea, sulfates, ammonia, and organic acids in exclusively octahedral coordination [44]. Chromium (VI) compounds are produced industrially by heating chromium (III) compounds in the presence of bases (such as soda ash) and atmospheric oxygen. Most chromium (VI) solutions are powerful oxidizing agents under acidic conditions. Depending on the concentration and acidity, chromium (VI) is virtually always bound to oxygen and can exist as either chromate ion (CrO_4^{2-}), or as dichromate ion ($Cr_2O_7^{2-}$). Chromium (VI) ions are strong oxidizing agents and are readily reduced to chromium (III) in acid or by organic matter. Chromium (III) compounds are slightly soluble in water, while most chromium (VI) compounds are readily soluble in water [45].

Jacobs et al. [46] regarded Cr as one of the world's most strategic and critical materials as the stability of chromium aids in protecting materials from environmental degradation [44,47,48], electroplating [49], leather tanning [50], stainless steel [51] or other applications as displayed in Table 3.

Table 3. Applications of chromium compounds (modified from [52]).

Application	**Usage**
Industrial	• Chromates manufacture of refractory tiles. • Chromates metallurgy for alloys used in tools and stainless steel • Furniture linings
Healthcare	• Prosthesis
Public	• Jewelry • Clothing

Chromium is used for corrosion resistance, steel production, and as protective coating for automotive and equipment accessories. It is a permanent and stable inorganic pigment used for paints, rubber, and plastic products.

Cr(III) and Cr(VI) enter the body through inhalation, ingestion and dermal contact. The trivalent and hexavalent forms are believed to be the biologically active species; but, their health impacts are not identical. Chromium (VI) readily penetrates biological membranes while chromium (III) generally does not. Chromium (III) is an essential trace element and the U.S. National Academy of Sciences has established a safe and adequate daily intake of

50-200μg of Cr(III) for adults [53]. Cr(III), a micronutrient, is deemed an essential element to maintain good health. It controls insulin, cholesterol, and fat in human bodies [54]; but, is poisonous at very high concentrations [55]. On the contrary, chromium (VI) is regarded as a toxic element. Research has demonstrated it to be mutagenic [56], teratogenic [57] and carcinogenic [58]. According to the International Agency for Research on Cancer (IARC), chromium (VI) is classified as a class 1 human carcinogen and has been considered as an environmental concern. Table 4 lists some examples of the effect of chromium (VI) when certain organs experience this toxic element [59].

Table 4. Organ response to Cr(VI) in the human body.

Organ	Outcome	Reference
Skin	Chromium (VI) can act as an oxidant directly on the skin surface. Exposure to the skin, especially if damaged, is the most frequently reported human health effect.	[60]
Blood	Once absorbed into the blood system several reducing agents such as glutathione and ascorbate are known antioxidants that rapidly reduce chromium (VI) to chromium (III)	[59]
Lung	Chromium absorbed through the lungs by into the blood system is excreted by the kidneys and the liver.	[59]
Kidney	Absorbs chromium from the blood through the venal cortex and released in the urine	[59]
Intestinal wall	Chromium (VI) can be rapidly absorbed through the intestinal wall, any ingested chromium (VI) is believed to be quickly reduced in the stomach where the pH is around 1 and numerous organic reducing agents can be found.	[61]
Upper respiratory	Ulceration or perforation of the nasal septum and irritation of the upper airways is the oxidative power of chromates that corrodes the epithelium.	[62]

In occupational settings, the most commonly reported chronic effects of chromium (VI) exposure include contact dermatitis, skin ulcers, irritation and ulceration of the nasal mucosa and perforation of the nasal septum. Less common are reports of hepatic and renal damage and pulmonary effects (bronchitis, asthma, and bronchospasm). Therefore, it is important to remove Chromium (VI) from polluted waters, especially those belonging to the electroplating industry.

1.3 (Nano)technology and materials

In terms of a new industrial revolution, this statement can not be true without talking about the driving force, i.e. nanotechnology. The European Union has described nanotechnology as having a disruptive or revolutionary potential as it pertains to the impact it has on industry [63]. The science and art of matter that is manipulated at the atomic and molecular scale is used to define nanotechnology. Hence, regarding the protection of the environment, nanotechnology holds the promise of providing new and unique improvements [64]. The term nanotechnology was coined by Erik Drexler during the 1980's by adding the prefix nano. It was derived from the Greek *nanos* meaning dwarf to the word technology [65]. Some critics claim that in 1974 Norio Taniguchi was the first to use the term nanotechnology at the International Conference on Precision Engineering (ICPE) [66]. The National Nanotechnology Initiative (NNI), created in the U.S.A., was the organization that first provided a definition of the word nanotechnology. According to the NNI, nanotechnology was defined as 'anything smaller than 100nm with novel properties' [67]. The European Union defined nanoparticles/nanomaterials as manufactured or natural material, in a state of agglomeration and/or unbounded, where 50% of the material are ≤ 100nm [68]. According to the U.S. National Science Foundation, nanotechnology is estimated to impact the economy globally by a trillion dollars. In addition, this industry

was estimated to employee up to 2 million employees in 2015. The important features of nanotechnology are ascribed to shape [68], size [69] and surface characteristics [70]. It is those properties that allow nanotechnology to become more chemically reactive by changing its strength and other properties. On the contrary, nanotechnology can serve as a powerful tool to address the problems of different sectors. Those sectors can range from biological systems to water treatment facilities.

In the field of nanomedicine, nanoparticles are often used as a tool for drug delivery. Nanotechnology has become a strong vehicle in aiding researchers to conduct diagnoses, treatment and prevention of certain diseases that affect the well being of humans such as cancer [71]. However, the usage of nanomaterials has been highly regulated because of the potential to induce toxicity. Table 5 illustrates some types of nanomaterial and how certain human organs can be adversely affected when exposed to nanoparticles.

Table 5. Nanomaterial application and its toxicity effect [72].

Nanomaterial	Application	Toxicity	Reference
Silica nanoparticles	Diagnostic imaging and Drug delivery	Physiological and reproductive toxicity. Aggregation of platelet	[73-75]
Iron oxide nanoparticles (SPION)	Drug delivery and MRI imaging contrast and enhancement	Oxidative stress	[76-78]
Titanium dioxide nanoparticles	Therapeutics in cancer	Central nervous system	[79-81]

1.3.1 Engineered and functionalized nanoparticles

Engineered nanoparticles are defined as particles which are intentionally produced of characteristic dimensions ranging from 1-100nm; differentiating them from materials with the same chemical composition but with a larger size [82]**.** Nanoparticles are of great scientific interest. They are effectively seen as a bridge between bulk materials and atomic or molecular structures [83]. A bulk material should have constant physical properties regardless of its size. At the nano-scale level, it is often not the case [84]. The key benefits of nanoparticles include altering the properties of materials in relation to their size and the ability to manipulate fundamental properties (i.e. magnetization) [66]. Studies have shown that nanomaterials are now considered as the most promising approach in applications such as: antibacterial materials [85], cosmetics [86], sunscreens [87], drug delivery [88], water purification [89], audio and video tapes [90] and magnetic fluids [91]. Research attention on nanomaterials, magnetite (Fe_3O_4) nanoparticles has been of significant use. Large surface area, high surface reactivity, high catalytic activity and strong adsorption ability are unique properties of nanomaterials.

1.3.1.1 Superparamagnetic iron oxide nanoparticles (SPION)

Magnetite is one of three types of iron oxide that exist in nature. Magnetite contains both Fe^{2+} and Fe^{3+} ions. It has the strongest magnetism compared to α-Fe_2O_3 and γ-Fe_2O_3 because its form is more stable [92]. Magnetite, a classified as magnetic material, is dependent upon its magnetic susceptibility (χ). Moreover, iron oxide nanoparticles can be divided into magnetic classes: paramagnetism, ferromagnetism and superparamagnetism.

Supermagnetism occurs when dipoles align themselves in a parallel orientation to an applied field. In the absence of the magnetic field, magnetite's direction is disorganized due to the thermal energy [93]. The advantages of magnetic nanoparticles are the size of

the particles that enhances the surface to volume ratio. The superparamagnetic properties are believed to be very suitable for the extraction of different types. In addition, magnetite nanoparticles can be easily separated and collected by applying an external magnetic field.

1.3.1.2 Cerium oxide nanoparticles (CON)

In industries pertaining to the automobile, ceria nanoparticles are extensively used in areas such as the catalytic converters for the exhaust system. Ceria can also be found in fuels cell where the naoparticles are used as an electrolyte [94,95]. Under oxidation and reduction conditions, it is the conversion of the valence states of the ions, Ce^{+3} and Ce^{+4}, which establishes cerium as important and viable [96]. In his work, Shi et al. investigated the induction of cytotoxicity and oxidative stress through the evaluation of commercial nanoparticles [97]. The ability of the surface vacancies of the oxygen from cerium oxide nanoparticles has become important in the biomedical research field [98]. The oxygen can merge and vary the free radicals. Factors such as pH play a very important role in determining the behavior of ceria nanoparticles, both as an oxidant or antioxidant (Figure1). Ceria nanoparticles used as a therapeutic agent have been used to treat cancer [99]. Conversely, research studies conducted *in-vitro* and *in-vivo* have deemed ceria as toxic to cancer cells. However, in healthy cells, reactive oxygen species (ROS) are controlled. It is the ability to alter the redox state within the cells that results in ROS level being de-regulated or affected by different treatments.

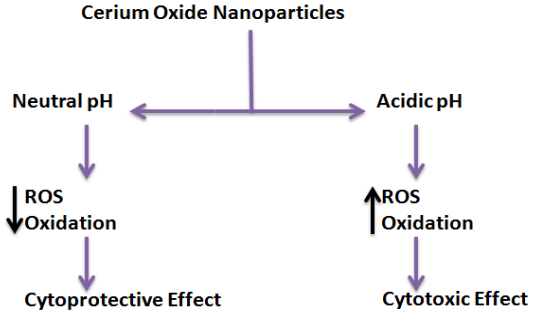

Figure 1. pH dependence upon CON's determination of cytoprotective or cytotoxic effects

1.3.1.3 Titanium oxide nanoparticles (TON)

TONs are amongst the earliest nanoparticles/nanomaterials that have been industrially manufactured. The U.S National Nanotechnology Initiative has deemed TON as being one of the most frequently manufactured nanomaterials in the world [67]. TONs are found in the form of anatase, rutile, brookite and ilmenite; but, commercial rutile and anatase are the most prevalent. Because of TONs physiochemical properties i.e. good fatigue strength, biocompability, photocatalytic and resistance to corrosion, TON can be found in various products such as: paints [100], sunscreens [101,102], wastewater [103], cosmetics and pharmaceuticals [104,105]. It is the characteristics and size of TONs, which make these the nanoparticles great candidates for many biological studies. TON is considered to be a negative control due to the fact that the nanoparticles are characteristically insoluble and thermally stable oxides. Studies conducted *in-vivo* and *in-vitro* have shown the toxicity of titania to be low [106]. Moreover, it was the work of Maness et al. that reported how TiO_2 was instrumental in eradicating bacterial cells as a result of lipid peroxidation reaction species [107].

1.3.1.4 Silica oxide nanoparticles (SON)

Due to the characteristics exhibited by silica nanopartacles such as its hydrophilic surface, low cost and surface functionalization, it has become formidable in the field of

nanomedicine [108]. Two types of nanoparticles mainly exist in biological applications which are denoted as mesoporous or solid (nonporous). Mesoporous SON's are those nanoparticles that exist in the range of 2 to 50nm in size (diameter) and are utilized in physical or chemical adsorption. However; nonporous SON's are used as an encapsulation method in drug delivery. Not only silica particles but their different shapes are of great interest. Silica as nanomaterials, in the shape of rods have been used in detecting the trafficking of cells, cancer cell metastis and drug delivery [109]. In addition to nanomedicine, the size and distribution of silica nanoparticles are of the utmost importance. Silica nanoparticles can be found in various industrial applications such as: thermal insulations [110], electronic [111] and thin film substrates [112].

1.3.2 (Nano)fibers

Nanofibers are highly engineered fibers with diameter less than 1 micron. Nanofibers possess outstanding characteristics such as very large surface area to volume ratio, flexibility in surface functionalities, and superior mechanical performance (e.g. stiffness and tensile strength) compared with any other known forms of othermaterials. Owing to its excellent characteristics, polymer nanofibers have applications in many different fields: health care [113], chemical industry [114], textile industry [115], environment [116] and electronics [117]. Several techniques in addition to electrospinning, such as template synthesis [118], drawing [119], phase separation [120] and self assembly [121] can be used for the preparation of nanofibers. However, the electrospinning technique is the most efficient among them [122,123]. It was not until the early 1990 that the work of Cooley [124] and Morton [125] gave birth to the actual production of fibers by electrospinning. Although electrospinning had been discovered earlier, research and publications utilizing this technique was insufficient due to the difficulties in producing an acceptable jet [126]. Electrospinning is defined as a process based upon the uniaxial stretching of a viscoelastic solution thus producing a highly robust flexible, nonwoven fabric of nano sized fibers [126]. The electrospinning process is accomplished by pushing a liquid solution through the tip of a metal needle that is attached to a syringe [122]. When in the presence of the electric field, the jet migrates towards the lower region of lower potential, which is a plate, the nanofibers are collected (Figure 2).

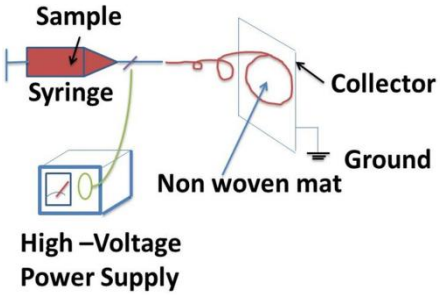

Figure 2. Schematic drawing of electrospinning process

There are many factors determining the construction of nanofibers including but not limited to solution viscosity [127], surface tension [128], conductivity [129], applied voltage [130], tip-to-collector distance [131] and humidity [132]. A high voltage, typically >5kV is applied to the solution to ensure the repulsive force within the charged solution, which is larger than its surface tension to produce the dispensing of the jet, resulting in the formation of the Taylor's cone as observed in Figure 3 [133].

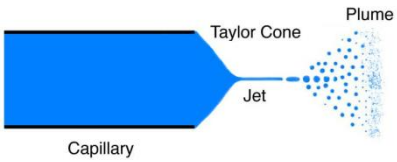

Figure 3. Schematic drawing of Taylors cone

The properties of the polymer solution have the greatest influence on the formation and morphology of the nanofibers as the stretching of the solution is governed by electrical properties, surface tension and viscosity of the solution [134].

1.4 Techniques for the removal of heavy metals

Several conventional methods such as ion-exchange [135], solvent extraction [136] and filtration [137] have been reported for the removal of heavy metals; but, the cost is relatively high. In addition to these conventional methods, the adsorption method has been employed for many years and is considered as one of the most promising methods for the removal of chromium from wastewater systems. An advantage of this method is that it cannot only remove heavy metals; but it can also be recovered or recycled back into the process [138], [139], [140].

The presence of heavy metals is a major concern for humans and the environment. Moreover, most of the heavy metals are well-known carcinogens and toxic. The removal of these metals from aqueous solutions is of utmost importance. Among the methods proposed for the removal of heavy metals from wastewater such as, filtration, solvent extraction [141], ion-exchange [142] and adsorption [143], the pros and cons of using these technologies in relation to adsorption for the removal of heavy metals from water treatment systems are shown in Table 6.

Table 6. Some pros and cons of various conventional technologies for the removal of heavy metals from water treatment systems [144].

Treatment method	Advantages	Disadvantages	References
Chemical precipitation	Low capital cost, simple operation	Sludge generation, extra operationalcost for sludge disposal	[145]
Adsorption with new Adsorbents	Low-cost, easy operating conditions, broad pH range, high metal binding capacities	Low selectivity, production of waste products	[146,147]
Membrane filtration	space requirement is unimportant, low pressure, high separation selectivity	High operational cost as a result of membrane fouling	[145]
Electrodialysis	High separation selectivity	High operational cost resulting from membrane fouling and energy consumption	[148]
Photocatalysis	Removal of metals and organic pollutant simultaneously, less harmful by-products	Extended duration time, limited applications	[149,150]
Adsorption	High surface area, accessible surface sites, short intraparticle diffusion distance	Non-selective in adsorption of metals	[151]

For a nanomaterial to be considered an efficient adsorbent, according to Huang et al., it must characteristically have a large surface area and appropriate functional groups [152].

Compared to conventional or well known materials used for adsorption, activated carbon is the most common adsorbent because of the abundant presence of a variety of functional groups on the surface (i.e. carboxylic groups [153]. Although it has high surface area, sorbent porosity, and capacity to adsorb a wide range of pollutants; it is considered to be expensive, non-selective and generates sludge that requires further treatment [154]. Further enhancement of other materials exhibit even higher removal percentage of pollutants if the nanomaterial is surface coated to be used as an adsorbent [155]. Biosorbents have drawn increased attention in water purification as they have shown to have removal and regeneration capabilities. However, its main disadvantage compared to activated carbon is low adsorption capacity due to its surface properties [156].

1.4.1 Solvent extraction

Solvent extraction or liquid-liquid extraction is a well-known technique that involves the selective removal of a solute from a liquid solution using a solvent. With the development of chelating agents [148], solvent extraction became very useful to remove trace metals from aqueous solutions. In general, the solvent extraction process takes place in three steps: extraction, scrubbing and stripping. In the extraction step the metal of interest dissolved in the aqueous phase is contacted several times with the organic phase containing the extractant. The metal from the aqueous phase reacts and is transferred to the organic phase containing the extractant due to the higher affinity of the metal with the extractant than with water. The distribution ratio provides an idea of the affinity of the metal towards the organic phase containing the extractant (equation 1):

$$D = \frac{A_1}{A_2} \qquad (1)$$

where A_1 is the concentration of the material in phase 1 and A_2 is the concentration of the material in phase 2. Traditionally phase 1 and phase 2 are referred to as aqueous and organic phases, respectively.

Some advantages of solvent extraction include (i) rapid, very selective and highly efficient separations and (ii) wide applications varying the composition of the organic phase and the nature of the binding agent. Conversely, depending upon the application, solvent extraction is not the appropriate method if the number of samples required may become too large; therefore, time can become a concern. Also, the materials can be very costly. Nonetheless, solvent extraction continues to be a powerful technique worthy to be considered when the removal of a target metal is defined.

1.4.2 Ion exchange

Ion exchange is defined as the process where an insoluble substance removes ions of positive or negative charge from an electrolytic solution and releases other ions of the same charge into solution in a chemically equivalent amount [157]. Typically, the solid substrate is a resin that does not undergo structural change. Fundamentally, an ion is removed from a solution when the solution is passed through a bed of exchangeable ions (resin). The process can be schematized as follows:

$$A^+ + R^-B^+ + X^- \leftrightarrow R^-A^+ + B^+ + X^- \qquad (2)$$

where R^- is the fixed negative charge on the resin, A^+ is a counterion present in the liquid stream on the reactant side, B^+ is a counterion present in the solid stream on the reactant side and X^- is the coion.

Acidic resins are those having a negative fixed charge that can be used for the exchange of cations. Conversely, basic resins are those with a fixed positive charge used for anion

exchange. The exchanges can also be weak and strong. Ion exchangers, amongst other technologies, can be utilized in environmental sectors such as environmental remediation, purification, recycling and decontamination processes with the purpose of removing precious materials that are deemed expensive, recycling and regenerating materials from wastewater [158]. In reference to ion exchangers, they do also have disadvantages such as, loss of sensitivity when targeting ions, increase of downtime while regenerating of the exchanger and waste accumulation as a result of regeneration [159].

1.4.3 Adsorption

Adsorption, termed as a surface phenomenon, is the transfer of molecules and atoms from one phase to another [160]. This separation process typically involves a metal (such as copper, lead, arsenic, chromium, etc) of interest. The metal is dispersed in an aqueous phase that is being transported to the surface of the solid material (adsorbent) such as nanomaterials, biomaterials and activated carbon. Adsorption is commonly utilized in the gas phase; but, its disadvantage of being a non-selective process is a major advantage for effectively adopting this technology, for non-selective process in water and wastewater treatment. From the molecular perspective, adsorption results from the attractive interactions between the adsorbate being extracted from aqueous solutions and the surface of the adsorbent. This form of adsorption occurs in two forms being chemical or activated adsorption and physical adsorption and some of the examples of each are displayed in Table 7.

Table 7. Differences between physiosorption and chemisorption [161]

Chemical Adsorption	**Physical Adsorption**
Chemical bonding is involved in the interaction between adsorbates and the surface of the adsorbents	Intermolecular forces are involved in the interaction between adsorbates and the surface of the adsorbents
Highly specific	Nonspecific
Monolayer	Can be both monolayer or multi-layer
Dissolution can occur	No dissociation of adsorbed
Adsorption can occur over a wide temperature range	Occurs at low temperature
Adsorption may be slow and is irreversible	Adsorption is fast and the interaction is reversible
Bonds are formed as a result of electron transfer	No transfer of electrons

Moreover, targeting selected heavy metals such as Cr(VI), biosorption technology, with its environmentally friendly approach, utilizes microorganism to remediate toxic metals from aquatic systems. The advantages are essentially the same as adsorption being that the initial cost, design is simplistic and flexible, operation ease, and unsusceptibility to pollutants that are toxic. Furthermore, the adsorption process does not result in the formation of substances that are deemed harmful [162].

The adsorption method coupled with surface coated nanomaterials can be an efficient and cost effective method. There are principles that must be adhered to in order to design a robust system to achieve the desired outcome. Those principles or guides include knowledge of the equilibrium, as it pertains to the adsorbent and adsorbate in solution, and the properties of the adsorbate: concentration, selectivity, temperature, and capacity based upon performance processes that is dependent upon solid-liquid equilbria and mass transfer rates. These driving forces or principles constitute adsorption as a very reliable and useful technique [163]. It is of utmost importance to select which technology is to be used and why. As mentioned previously based upon the characteristics and advantages, adsorption technology has proven to be the better choice when water systems are contaminated with heavy metals.

1.4.3.1 Adsorption of metal ions

The adsorption of Cr(VI) was calculated by the mass balance following equation (3).

$$\%\ \text{Adsorption} = \frac{C_i - C_e}{C_i} \times 100 \qquad (3)$$

where C_i is the initial Cr(VI) concentration in mmol L^{-1}; C_e is Cr(VI) final concentration in mmol L^{-1}.

The amount of Cr(VI) adsorbed (mg g^{-1}) at time t was calculated by using the following equation (4):

$$q_t = \frac{(C_0 - C_t)V}{m} \qquad (4)$$

where C_0 and C_t are Cr(VI) concentrations (mg L^{-1}) initially and at a given time t, V is the volume and m(g) is the mass of the adsorbent.

1.4.3.2 Adsorption isotherms

Adsorption is usually described by the adsorption isotherm between the adsorbate and adsorbent. In general, an adsorption isotherm is an invaluable method describing the phenomenon governing the retention (or release) or mobility of a substance from the aqueous media to a solid-phase at a constant temperature and pH [164]. The construction of the adsorption isotherms is based on the experimental data [165]. There are two main models to describe the adsorption process onto solid surfaces: Langmuir [166] and Freundlich [166]. These models can be applied to a wide range of adsorbate concentrations in order to provide pertinent and important information for design and scale-up. The Langmuir model assumes that the adsorption of heavy metals occurs as a monolayer on a homogeneous surface by the equilibrium distribution of metal ions between the solid and liquid phases and the non-linear form is represented by equation (5):

$$q_e = \frac{q_{max}\ k_L C_e}{1 + k_L C_e} \qquad (5)$$

where q_{max} is the maximum adsorption capacity that corresponds to the site saturation (mg g^{-1}), C_e is the equilibrium metal concentration (mg L^{-1}) and k_L is the Langmuir constant (L mg^{-1}).

The Langmuir isotherm assumes that metal ions are chemically adsorbed, where each site can hold only one adsorbate and all sites are energetically equivalent and that there is no interaction between ions.

Equation 5 can be rearranged to the following linear form to be used for the linearization of the experimental data by plotting C_e/q_e vs C_e:

$$\frac{C_e}{q_e} = \frac{1}{k_L q_{max}} + \frac{C_e}{q_{max}} \qquad (6)$$

The Freundlich model, which is an empirical model, assumes the presence of preferential sites in the adsorbent and can be expressed in the non-linear form of equation 7:

$$q_f = k_f\, C_f^{1/n} \qquad (7)$$

where q_f is defined as the amount of adsorbate adsorbed in mg g^{-1} and C_f is the concentration of adsorbate at equilibrium.

The Freundlich equation 7 can be linearized by taking the logarithm of both sides of the equation where k_f (mg g^{-1}) is the Freundlich constant related to the adsorption capacity and 1/n is the heterogeneity factor:

$$\log q_f = \log k_f + \frac{1}{n} \log C_f \qquad (8)$$

1.4.3.3 Adsorption kinetic equations

Kinetic models are applied to determine and interpret the adsorption mechanisms of the process obtained from batch metal ion removal experimental data. Kinetics, which is considered as a rate of the reaction, is defined as the movement or change in concentration of reactant or product with time [167]. The dynamics of adsorption kinetics describes the rate at which the adsorbate is adsorbed onto the adsorbent, which controls the time at the particle-metal interface [168]. In order to investigate the mechanism of sorption, two kinetic models have been considered: [169] (i) pseudo-first-order kinetic model [170] and (ii) pseudo-second-order kinetic model [171].

Lagergren's (pseudo-first-order) model is a model that depends upon the amount of metal ion adsorption raised to the first power and is expressed as follows:

$$\frac{dq_t}{dt} = k_1(q_e - q_t) \quad (9)$$

When applying the initial conditions for the definite integration q = 0 at t = 0 and $q = q_t$ at $t = t$. Equation 9 is linearized to (equation10):

$$\log(q_e - q_t) = \log q_e - \left(\frac{k_1}{2.303}\right) t \quad (10)$$

where k_1 is the pseudo-first-order rate constant (min^{-1}) of adsorption, while q_e and q_t are the adsorption capacities of Cr(VI) (mg g^{-1}) at equilibrium and at time t (min).

The pseudo-second-order model is a model that depends upon the amount of metal ions on the surface of the adsorbent at time t and that adsorbed at equilibrium adsorption raised to the second power is expressed as follows:

$$\frac{dq_t}{dt} = k_2(q_e - q_t)^2 \quad (11)$$

When applying the initial conditions for the definite integration q = 0 at t = 0 and $q = q_t$ at $t = t$, equation 11 is linearized to eq.12:

$$\frac{t}{q_t} = \frac{1}{k_2 q_e^2} + \left(\frac{1}{q_e}\right) t \quad (12)$$

where k_2 is the pseudo-second-order rate constant of adsorption ($g \cdot mg^{-1} \cdot min^{-1}$).

The mechanism for adsorption of metals onto adsorbents involve four main steps: (i) migration of the target metal from the bulk of the solution to the surface of the adsorbent (bulk diffusion); (ii) diffusion of the metal ions from the polymeric film to the adsorbent (diffusion); (iii) adsorption of the metal ion at an active site on the surface of material and (iv) uptake (chemical reaction via complexation and/or chelation, chemisorption) [172].

1.5 Objectives

The aim of this thesis is to design novel nanomaterials for the removal of heavy metals from wastewater with enhanced capacities that are simple, cost effective and environmentally friendly. The first part of this study was the synthesis of SPION followed by functionalization with appropriate molecules (bis(2,4,4-tri-methylpentyl) dithiophosphinic acid (Cyanex-301) and 3-Mercaptopropionic acid containing a thiol group that will serve as a surfactant. The second part of this work was the production of electrospunned PLLA nanofibers functionalized with ZnO nanorods for the removal of Cr(VI) and desorb it from the adsorobent in order to collect Cr(VI). This collection is done in an attempt to enable the resale or the reduction of Cr(VI) to Cr(III), which is a benefit to society in general and industry in particular. PAN nanofibers followed by chemical treatment with hydroxylamine hydrochloride to produce amidoxime PAN nanofibers (A-PAN) were also investigated. The nitrile group from PAN nanofibers gave segue to the conversion of amine group, which is highly active in forming strong complexes with metal ions. pH is one of several key parameters that provides pertinent information on the adsorption of heavy metals from aquatic systems. As the particle size decreases, there is a tendency for the increase of cytoxicity. A series of experiments were preformed to investigate the dissolution of commercial ZnO, TiO_2 and SiO_2 and lab-made (CeO_2 and surface coated Fe_3O_4) nanoparticles dispersed in different media (water, cell media and PBS) as temperature was adjusted to 25 ^{o}C and 37 ^{o}C and their effect on cyto and dermal toxicity.

2. Experimental

2.1 Synthesis of superparamagnetic iron oxide nanoparticles (SPION)

The synthesis of superparamagnetic iron oxide nanoparticles were prepared by the co-precipitation method described by [173]. It consists of a 2:1 molar ratio of Fe^{+3} to Fe^{+2} chlorides dissolved in a deoxygenated aqueous solution in a low concentration of 0.2M hydrochloric acid (HCl). HCl was added to the iron (II and III) solutions to prevent the initial formation of iron hydroxides. The Fe^{+2} and Fe^{+3} solution was added to a concentrated aqueous solution of 1.5M NaOH solution for 45 minutes at T=80°C under a constant stirring speed of 500rpm in the presence of N_2 gas. After synthesis, the particles were collected by an external magnet and washed 3 times with deoxygenated water. The particles were suspended in 0.01M tetra-ammonium hydroxide (TMAOH) to reduce particle aggregation.

2.1.1 Cyanex-301 coated SPION

The coating of SPION with Cyanex-301 was achieved by mixing a known amount of SPION with 100mL of 150mM of Cyanex-301 diluted in toluene using a rotary shaker for 24h. After aqueous and organic phase separation, the Cyanex-301 coated SPION remained in the aqueous phase and by use of a magnet, the particles were settled and separated. The Cyanex-301 coated SPION particles were washed with toluene three times and dried overnight at room temperature (23±1 ºC).

For the adsorption experiments, a stock solution of Cr(VI) 1000ppm was prepared by dissolving $K_2Cr_2O_7$ in sodium nitrate (0.1M) and this stock solution was diluted to obtain working solutions containing 10-500mg L^{-1} of Cr(VI). Different parameters such as effect of contact time, pH and initial concentration were performed by mixing a fixed amount of Cyanex-301 coated SPION (mg) with an aqueous solution of 0.1M Cr(VI) using a rotary shaker (Multi-Wrist Shaker) at room temperature (23±1ºC) and keeping the ionic strength at 0.01M with $NaNO_3$ after mixing for a different time periods of each sample. In the case of selectivity study of Cyanex-301 coated SPION, two sets of experiments were carried out at different concentrations at the optimized conditions of pH and contact time.

To ensure complete stripping of the Cr(VI) adsorbed onto Cyanex-301 coated SPION, the desorption study was conducted to determine the most suitable eluting solution. The study consisted of 10mg L^{-1} Cyanex-301 coated SPION loaded with Cr(VI), which were stripped using 10mL of HNO_3 (2.0M), NaOH (0.1M), NaCl (0.1M) or H_2O for the duration of 2h.

2.1.2 3-Mercaptopropionic acid (3-MPA) coated SPION

Different coatings of 3-MPA onto SPION were prepared using different initial concentration of 3-MPA: 0.05M, 0.15M, 0.5M and 1.0M diluted in water. SPION with each solution was placed in a rotary shaker for 24h. Subsequently, SPION coated 3-MPA was settled and separated by a magnet, heated at 70°C for 4h and washed with ethanol to remove the excess of 3-MPA and TMAOH.

To investigate the effect of SPION coated 3-MPA, 5mg of each SPION coated 3-MPA were mixed with 10ml of Cr(VI), 10 mg L^{-1}, at pH=3 for 3h, to reach equilibrium, using a rotary shaker (Multi-Wrist Shaker) at room temperature (23±1ºC). The ionic strength was kept constant at 0.01 M with $NaNO_3$. The experiments used to determine the effect of initial concentration, pH and contact time were performed on 10ml solutions of 10mg L^{-1} Cr(VI) at pH ranging from 1.0 to 6.0 mixed with a fixed amount of SPION coated 3-MPA. After the mixing stage, SPION coated particles were separated by an external magnet and centrifuged at 14000rpm.

Inductively Coupled Plasma Optical Emission Spectroscopy (ICP-OES, iCAP 6500, Thermo Fisher), using the following equations (13, 14) to determine the amount of Cr(VI) in the initial and final solution

$$q_t = \frac{(C_0 - C_t)V}{m} \quad (13)$$

$$\% \text{ Adsorption} = \frac{C_i - C_e}{C_i} \times 100 \quad (14)$$

2.1.3 Synthesis of SPION coated dextran

Analytical grade solutions of $FeCl_2$, $FeCl_3$, hydrochloric acid, ammonium hydroxide and dextran were used. A stock solution of iron (III) and iron (II) in chloride media was prepared. The respective salts were dissolved with deoxygenated 0.1M HCl aqueous solution to a final concentration of 1.0M and 0.5M. This solution was added to a deoxygenated solution containing 0.7M NH_3 under mechanical stirring at ca. 250rpm. The particles were aged in the solution for about 45min, decanted by magnetic settling and washed with deoxygenated water three times. After the triple wash, 10.9g of Dextran (Mw: 6000, 40,000, and 70,000Da) was added to 45ml of magnetite nanoparticles. SPION and dextran were mixed using Multi-Wrist Shaker for 24h. The final product was placed into Spectra Pro MWCO 25,000 membrane for dialysis for 3 days, while changing the water every 3h.

2.2 Synthesis of commercial nanoparticles

20mg of metal oxide nanoparticles (TiO_2, SiO_2, ZnO and α-Fe_2O_3) was weighed and added to 20mL of the selected media (water, cell media and PBS). The desired concentration of the metal oxide of 1.0mg mL^{-1} was achieved. The temperature of the mixture was kept constant by placing the flask tube in a glycerol oil bath and onto a thermal heater (Heidolph MR Hei-Standard). For the mixing system, a motor with stirrer (teflon) was attached. The stirring rate was kept constant at 500rpm. This was chosen to ensure sufficient contact between nanoparticles and selected medium. The mixing was carried out for 24h.

2.3 Preparation of commercial nanoparticles for DLS analysis

To study the effect of the particle in cell media, 5mg of each sample was separately suspended in vials containing 5mL of cell media (DMEM). The cell media contained sodium pyruvate and PEST without serum. The first samples, SiO_2 5-15nm, SiO_2 20nm and SiO_2 80nm, were placed in a bath sonicator and were allowed to sonicate for 20 minutes before analysis. In addition to the previous 3 samples, the remaining 3 samples were allowed to sonicate using the tip sonicator for 20mins.

2.4 Synthesis of polyacrylonitrile (PAN) nanofibers

A solution of 10% (w/w) polyacrylonitrile (Figure 4) was prepared by dissolving polyacrylonitrile in dimethylformamide (DMF) for 4h at 40°C.

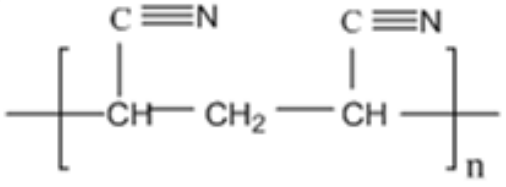

Figure 4. Chemical structure of PAN

The sample was loaded into a syringe composed of a (0.8mm in diameter) stainless steel needle. The syringe was connected to the anode of voltage supply (Brandenburg). The collector's plate was covered with aluminum foil and connected with the cathode from the voltage supply. A voltage of 10kV was applied between the needle and collector. The needle containing the polymer solution was mounted to a syringe pump (Cole-Parmer) in a vertical position. The distance from the needle tip to the collector was 15cm with a flow rate of 0.5mL h^{-1}.

2.4.1 Modification of polyacrylonitrile nanofiber

Figure 5 illustrates the reaction of polyacrylonitrile with hydroxylamide hydrochloride resulting in polyacrylonitrile-amine nanofiber by the addition of 8g of hydroxylamide hydrochloride with 6g of sodium carbonate. The PAN nanofiber and chemicals were added to a 100mL beaker and sealed in order for the reaction to take place at 70°C for 3h.

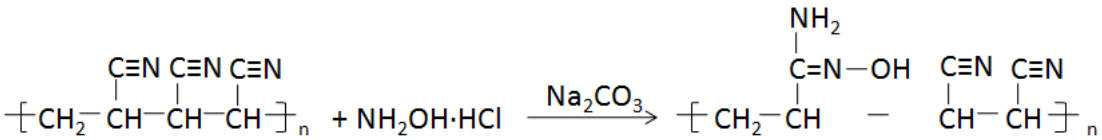

Figure 5. Reaction of PAN with hydroxylamine hydrochloride in the presence of sodium carbonate.

The reaction of A-PAN nanofiber with sodium hydroxide to produce carboxylic acid functional groups was accomplished by the addition of 10mL of 0.05M NaOH into a 25mL beaker for 5mins. The amount of chromium released from the A-PAN nanofibers into the aqueous solutions was quantified. The procedure consisted in the mixing and shaking of the adsorbent with Cr(VI) adsorbed; respectively, followed by magnetic separation of the particles, centrifugation and measurement of the Cr(VI) released to the aqueous solution by ICP-OES.

2.5 Synthesis of poly-L-lactide (PLLA) nanofibers

Poly-L-lactide (Aldrich, Mw = 100000) nanofibers were produced by a technique known as electrospinning. Chloroform was used to dissolve the polymer (7 wt %) while stirring for 24h. The sample was loaded into a syringe composed of a stainless steel needle (0.8 mm in diameter). The syringe was connected to the anode of voltage supply (Brandenburg). The collector's plate was covered with aluminum foil and was connected with the cathode of voltage supply. A voltage of 9-10kV was applied between the needle and the collector. The needle containing the polymer solution was mounted to a syringe pump (Cole-Parmer) in a horizontal direction. The distance from the tip of the needle to the collector was 10cm with a flow rate of 1mL h^{-1}. Bestowing high voltage power supply, the potential was applied to the hypodermic needle (Admix) at the end of the syringe.

2.5.1 Modification of poly-L-lactide (PLLA) nanofibers

For a total time of 30mins, the PLLA nanofibers were immersed into a colloidal ZnO suspension prepared by modifying a method described by Bahnemann et al.; subsequently, allowing it to dry [174]. The "seeded" nanofibers were immersed into a mixed aqueous solution of 20mM each of $Zn(NO_3)_2$ and hexamine at 75°C for 6h. The prepared PLLA-ZnO assembled nanostructured material was washed followed by drying in a vacuum oven for 1h.

2.6. Characterization of the materials

To characterize the materials, several techniques have been used such as Transmission Electron Microscopy (TEM) with high resolution (JEM-2100F) at 200kV in order to determine the dry particle sizes and morphologies of the prepared SPION, SPION coated and engineered materials. In addition, Scanning Electron Microscopy (SEM) was also used to verify the particle textures and diameters for successful fabrication of the nanomaterials. Elemental concentrations were detected by means of Energy Dispersive X-ray analysis (EDX) for 3-MPA. Fourier Transform Infrared (FT-IR) spectra of SPION, functionalized coated (Cyanex301and 3-MPA) SPION, nanofibers (PAN/A-PAN/CAO-PAN and cellulose) and zeolite crystals were also recorded using a Thermo Nicolet iS10 equipment. Thermal Gravimetric Analysis (TGA) (TGA-Q500, TA Instruments) of 3-MPA coated SPION was used to determine the amount of SPION, Cyanex 301- coated SPION and 3-MPA coated onto SPION under N_2 atmosphere at a heating rate of 10°C min^{-1} over a temperature range of 30°C-600°C. Nanoparticle materials (e.g. ZnO, TiO_2 and SiO_2) were measured by DLS in different media (water, cell media and PBS). The adsorption of Cr(VI) and the amount of Fe and other elements in ionic form (i.e. Si, Ti and Ce) leached was determined by Inductively Coupled Plasma Optical Emission Spectroscopy (ICP-OES) (iCAP 6500, Thermo Fisher).

3. Results and discussion

In this section of the thesis, the overall goal was to ascertain and utilize newly prepared and commercial nanomaterials. For the extraction of heavy metals from aquatic systems, the nanomaterials were compared to some commonly used adsorbents. The dissolution of commercial metal oxide and lab-made nanoparticles (papers IV and V) was investigated. The evaluation of the extent of dissolution of the metal oxide nanoparticles is useful in toxicity studies. The effect of studying different parameters on the adsorption of heavy metals such as, Cr(VI) (papers I-III,VI) including contact time, initial ion concentrations and solution pH were examples of systems investigated and the results are presented hereafter.

3.1 Surface morphology of nanomaterials

Currently, there are several materials used for the removal of heavy metals from aqueous systems coupled with enhanced properties to remediate and/or eradicate heavy metals. As these materials have proven to be successful, they also have drawbacks. Activated carbon is the most common adsorbent used considering its high surface area, porosity, and capacity to adsorb a wide range of pollutants. However, it is considered to be expensive, non-selective and it generates sludge that requires further treatment [154]. The reagents Cyanex-301 and 3-MPA were used as an extractant. Each extractant contains a thiol functional group (≡SH)..

In observance of the effects of commercial and lab-made nanoparticles for biological applications, it is the surface formulation of the nanoparticles that is of interest. The surface of the nanoparticles interacted with cells (i.e. MCF-7) may induce cytotoxicity within humans or animals.

Transmission electron microscope (TEM) was used to visualize the morphology of the reagents (engineered and lab-made) (Figures 6, 7) and functionalized SPION (Figures 8, 9).

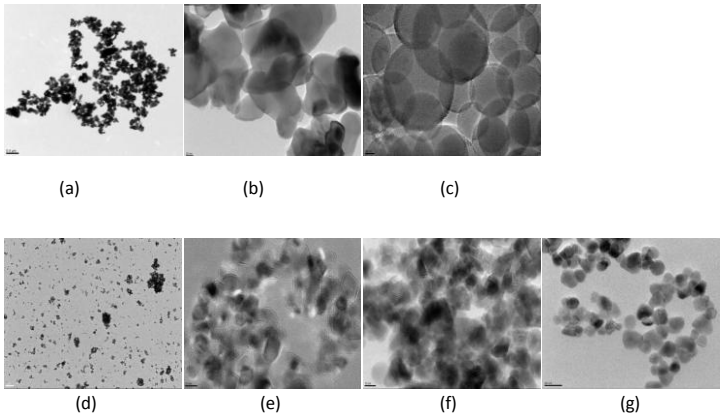

Figure 6. TEM images of the commercial metal oxides nanoparticles used in this work. (a&b) α-Fe_2O_3 (c) SiO_2, (d&e) TiO_2, (f&g) ZnO.

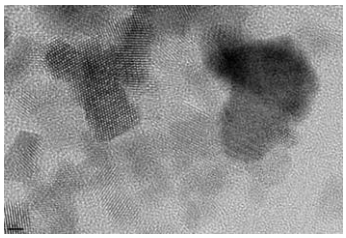

Figure 7. TEM image of the lab-made cerium oxide (CeO_2) nanoparticles

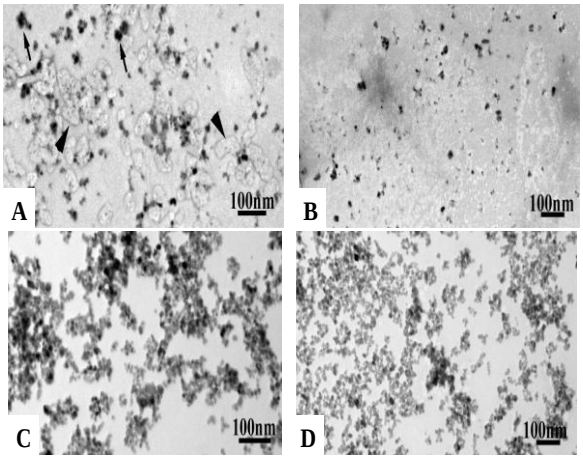

Figure 8. TEM image for lab-made and commercial SPION coated dextran: a) SPION-DEX (20nm) commercial, b) SPION-DEX (50nm) commercial, c) KTH SPION-DEX (15nm) lab-made and d) KTH SPION-DEX (20nm) lab-made.

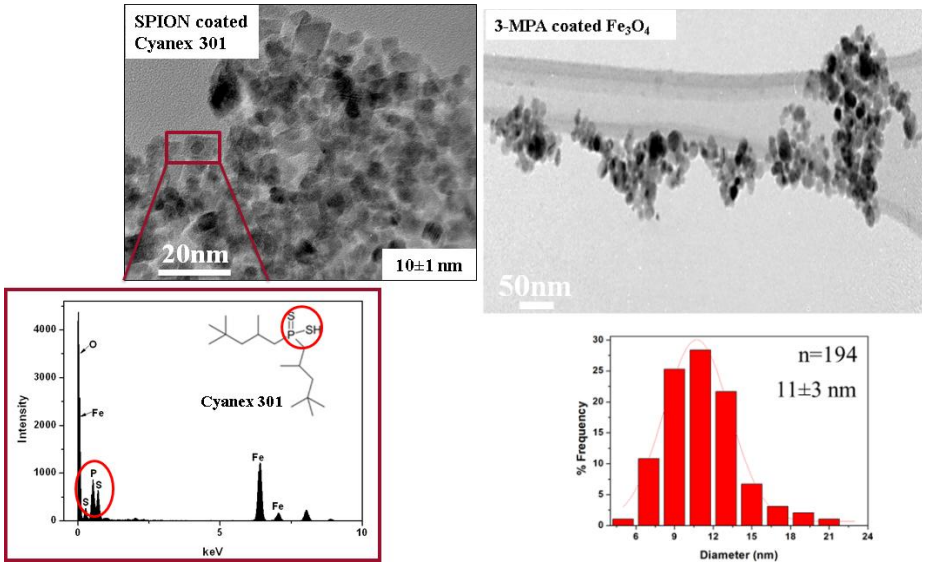

Figure 9. TEM micrographs of Cyanex-301 coated onto magnetite and EDX of the Cyanex-301 coated onto magnetite. 3-MPA coated SPION with size distributions.

The software imageJ was used to compile the micrographs to determine the dry particle size (nm) of the sample (paperII). The particle size showed as though it was not affected by the presence of the ligands. Electron Dispersive X-ray Spectroscopy was employed in order to study if there is any presence of the extractant onto the carrier material (SPION). The results of EDX analysis demonstrated the observed peaks of Fe and O were from

SPION. Moreover, the confirmation of the reagents coated onto SPION was observed by the distribution throughout the sample and exhibited as P and S (Cyanex-301) and Sulfur (3-MPA) along with Fe, O (see Figures 9, 10) and therefore confirming the presence of the reagents.

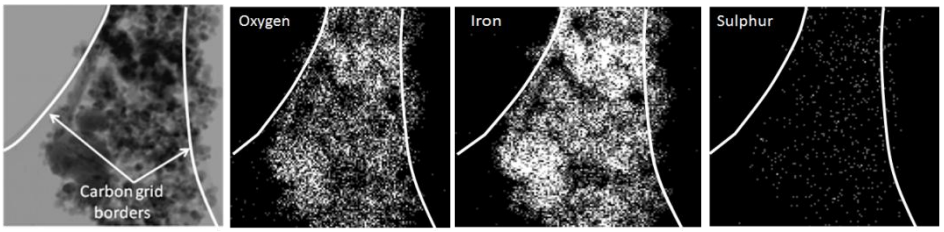

Figure 10. EDX mapping of 3-MPA coated SPION on a Holey- Carbon grid film of Oxygen, Iron and Sulfur

The SEM micrographs illustrated in Figure 11(a, b) represent PAN and A-PAN nanofibers. Depicted in Figure 11a, the surface of PAN nanofiber appears to be smooth and uniform with an average diameter of 309±3nm. As the PAN nanofiber becomes functionalized (Figure 11b), the diameter of the nanofibers increases slightly, which is may be due to the conversion of the nitrile group to amidoxime functional group due to swelling [175]. Despite the increase of the diameter, 326±4nm of A-PAN, the nanofibers did not show any surface degradation or cracking; illustrating similar morphology as the PAN nanofibers.

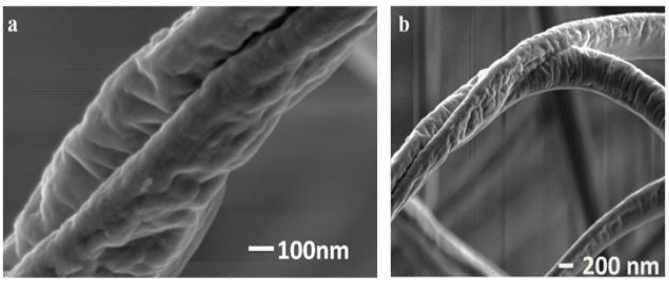

Figure 11. SEM micrographs of nanofibers (a) PAN and (b) A-PAN

After the production of PAN nanofibers, the addition of hydroxylamine hydrochloride with the PAN nanofibers was investigated. The functionalized nanofibers were synthesized to produce ion exchange materials with high adsorption capacity to increase the degree of adsorption of the metal of interest onto the modified nanofiber [176],[177]. Saeed et al. reported the effects of the hydroxylamine hydrochloride concentration with respect to reaction time [178]. The conversion of the nitrile groups of PAN increased as the concentration of hydroxylamine hydrochloride increased resulting in the nanofiber loss of flexibility. The PAN nanofibers are white in color and soft, which enables an easier manipulation. Moreover, the A-PAN nanofibers with similar yield or conversion rates (above 50%) showed brittle or even non-flexible nanofibers with a slight yellowish color in close agreement with the work of Liao et al. [179]. This can be related to the softer chemical treatment of the nanofibers as the temperature was raised gradually. This phenomenon is primarily due to the molecular diffusion of hydroxylamine hydrochloride moving from the solution onto the nanofiber [180].

The micrograph in Figure 12 illustrates the morphology of ZnO nanofiber and ZnO-PLLA nanocomposite. The structure of the nanofiber, before and after functionalization with ZnO, is intact and smooth. The PLLA nanofiber ranges from nanometers to approximately 4μm in diameter. Moreover, when ZnO was chemically grown onto the surface of PLLA, the size increased to 12μm in diameter. The size of the functionalized PLLA nanofiber is in

agreement with the literature, where the ZnO-PLLA nanofibers growth is affected by the parameters such as temperature and concentration during the synthesis of ZnO onto PLLA nanofibers [181].

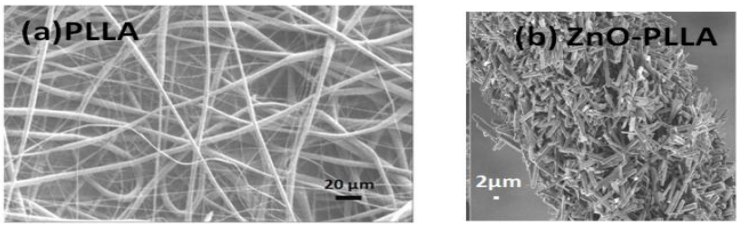

Figure 12. SEM micrographs of SEM micrographs of the (a) electrospun PLLA nanofibers (b) assembled ZnO-electrospun PLLA nanofibers

3.2 Mechanism of reagents on adsorbents

Thermogravimetric analysis (TGA) coupled with FT-IR was performed on SPION and SPION–Cyanex-301 samples in nitrogen atmosphere (Figure 13). A weight loss of 3% over the entire temperature range, most likely due to removal of absorbed water, was observed during the decomposition of SPION (Fig 13a, dotted line). The decomposition of SPION coated with Cyanex-301 occurred in two steps; a 15 wt% loss up to 250°C and an 18 wt% loss in the final step up to about 500°C (Figures 13a and b). The first step resulted in a DTG peak broader than in the second step at 450°C. The gases evolved from the decomposing sample were detected by FTIR. Carbon dioxide (2364cm^{-1}) and 2,4,4-trimethylpentane (2956cm^{-1}) were identified to desorb in the first step and 2,4,4-trimethylpentane in the final step (Figure 13c). The evolved gas analysis suggests decomposition of Cyanex via oxidation to carbon dioxide in the first step followed by release of aliphatic chains as 2,4,4-trimethylpentane molecules in the second step. Based on the TGA data, the amount of Cyanex-301 coated on the surface of SPION was determined to be 0.8 mmol g^{-1}. Assuming a complete coating of SPION, and spheres with 9±2nm diameters, the thickness of the Cyanex-301 layer on SPION was calculated to be 1nm in good agreement with values reported in the literature [182]. Moreover, the manufacturer of Cyanex 301 reported the decomposition temperature as ~220°C.

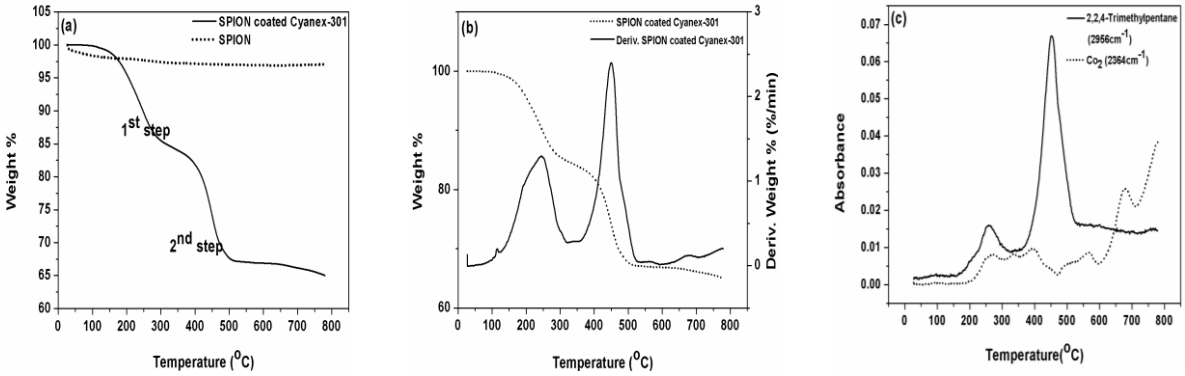

Figure 13. TGA curves of SPION and SPION–Cyanex-301

The amount of 3-MPA bound to the surface of SPION was determined from the weight loss measured by the thermogravimetric analysis (TGA). As depicted in Figure 13, the TGA curve for SPION shows about 3% weight loss over a temperature range of 100-300 °C. The weight loss is most likely attributed to the loss of absorbed water from the surface of the crystalline structure. Awwad et al. reported that Fe_3O_4 nanoparticles experience a weight loss around 100°C and was due to water loss [183]. Also, other researchers have

illustrated based upon the thermograph curve as T<200°C was attributed to water bound to the nanoparticles [184]. In addition Galeotti et al. reported that over a temperature range T= 50-300°C for iron oxide nanoparticles experienced a 1% weight loss which was due to both physically and chemically adsorbed water [185]. Pan et al. reported when 3-MPA is bonded to Fe_3O_4, then occurs decomposition at T=100°C, where the weight loss is ascribed to the evaporation of physically adsorbed water in the sample [186].
The TGA curve for 3-MPA coated SPION shows two weight loss steps. A total of 6 % weight loss was observed in two steps over the temperature range of 150-500^{o}C, corresponding to the decomposition of 3-MPA bound to the surface of SPION. The temperature range for the decomposition of 3-MPA was consistent with the work presented by Pan et al., who stated that the temperature of 260-340°C was attributed to the initial decomposition of 3-MPA groups on the surface of Fe_3O_4. Moreover, further decomposition of 3-MPA and its conversion to CO_2 and H_2O starts at T=350°C until T=510°C [186].
Based on the TGA data, the amount of 3-MPA bound to the surface of SPION is determined to be 0.24 ± 0.02mmol g^{-1}. Figure 14 shows there is a similarity between the TGA curves for 3-MPA coated SPION prepared using different initial 3-MPA concentration (0.05-1.0mol L^{-1}).

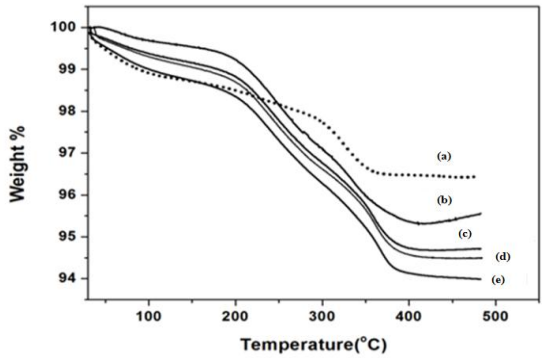

Figure 14. TGA curves of (a) SPION, and (b, c, d,e) 3-MPA coated SPION- at different 3-MPA concentrations of 0.05mol L^{-1}, 0.15mol L^{-1}, 0.5mol L^{-1} and 1.0mol L^{-1} ;respectively.

FT-IR was used to check whether the material and reagents were identified and bound to the surface of the material (iron oxide and nanofibers); respectively. The FT-IR spectra of SPION, Cyanex-301 coated SPION, Cyanex-301 and Cyanex-301-Cr(VI) are shown in Figure 15. SPION spectra showed a broad band at 3400 cm^{-1} that is attenuated in the Cyanex-301 coated SPION. This band is due to the stretching vibration of OH groups of the magnetite nanoparticles in the hydrated form. All materials containing Cyanex-301 showed a sharp band at 2950cm^{-1} and 2903cm^{-1} assigned to the (CH_2) or (CH_3) groups of Cyanex-301. The spectra of Cyanex-301 showed a broad band at 2385cm^{-1} and a sharp band at 2580cm^{-1} assigned to the S-H stretching vibration and bands at 711cm^{-1}, 731cm^{-1} and 805cm^{-1} assigned to the P=S vibrations [182,187,188]. In the chromium-Cyanex-301 spectrum, the peaks appear to be shifted to the right (694cm^{-1} and 726cm^{-1}) and are much sharper than those of plain Cyanex-301 due to the presence of Cr(VI) bonded to the thiol group.

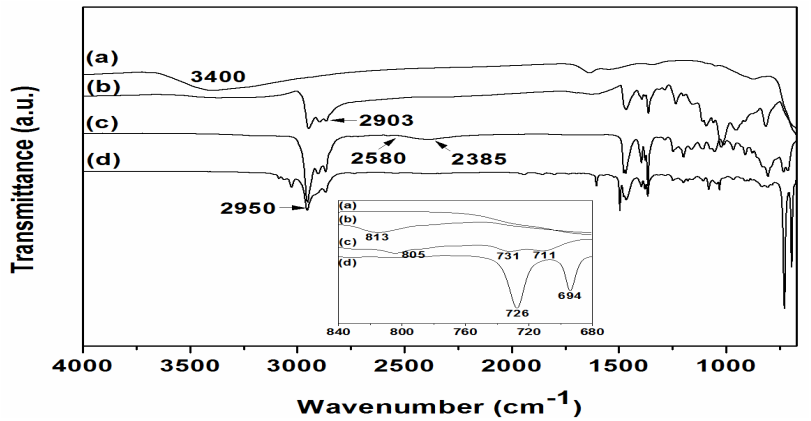

Figure 15. FTIR spectra of (a) SPION, (b) Cyanex-301 coated SPION, (c), Cyanex-301 and (d) Cyanex-301-Cr(VI). The inset shows the FTIR spectra in the wavenumber range of 650-850cm^{-1}.

Figure 16 shows the FT-IR spectra of SPION, 3-MPA and 3-MPA coated SPION at 3-MPA initial concentrations of 0.05M and 1.0M. The spectra corresponding to 3-MPA coated SPION at different initial 3-MPA concentrations point to small differences in structure and concentration of 3-MPA coated SPION. Few similarities are observed between SPION and 3-MPA coated SPION. The broad band at 3400cm^{-1} (stretching vibration of OH groups) is due to water bound to the surface of the magnetite nanoparticles. This peak is attenuated in the 3-MPA coated SPION spectra mainly due to the presence of 3-MPA coating on the SPION surface; whilst the broad peak at approximately 570cm^{-1} corresponds to Fe-O lattice vibrations and this was observed for all samples containing SPION. 3-MPA spectra showed two peaks at 2550 and 2557cm^{-1} and could be assigned to S-H [188]. In addition, a sharp peak at 1470cm^{-1} assigned to COO^- appears weaker in the 3-MPA coated spectra. The band at 1730 cm^{-1} could be assigned to C=O vibration (asymmetric stretching) of 3-MPA, which disappears in the spectrum of 3-MPA coated SPION revealing the binding of 3-MPA to the surface of SPION by chemisorption of carboxylate ions. Similar observation has been reported by other research groups [187,189,190]. The obtained FT-IR results suggest a successful surface modification of SPION with 3-MPA.

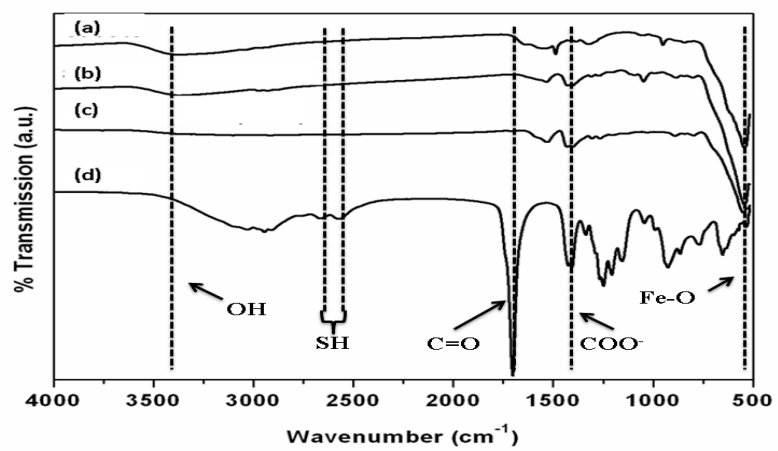

Figure 16. FTIR spectra of (a) SPION, (b & c) 3-MPA coated SPION at different 3-MPA concentrations (0.05mol L^{-1}, 1.0mol L^{-1}), and (d) 3-MPA.

The FT-IR spectra of PAN and A-PAN nanofibers are shown in Figure 17. The spectrum for the as-prepared PAN nanofibers exhibited characteristic peaks of nitrile (2242cm^{-1}), carbonyl (1660cm^{-1}) and C–H stretching (2941cm^{-1}). Generally, the carbonyl peak is observed at 1700cm^{-1}. However, when PAN was dissolved in the solvent DMF, the carboxyl transmission band is shifted towards lower wavenumber (1667cm^{-1}) in

comparison to the pure solvent. These results indicated that DMF residues remained onto the PAN nanofibers after drying [191]**.** After the functionalization of PAN to A-PAN by the reaction with hydroxylamine hydrochloride, the spectra show different changes. The peak corresponding to nitrile was markedly decreased due to the conversion of nitrile to amidoxime. In addition to the peaks of PAN nanofibers, the characteristic peaks of amidoxime, from the A-PAN spectrum, can be observed at 3100–3700cm^{-1} (assigned to both N–H and O–H), 917–927cm^{-1} (assigned to N–O) and the bending vibrations of the amine group NH or NH_2 (1570cm^{-1}) confirming the conversion of the nitrile group to amidoxime [192]. After the adsorption of Cr(VI) at pH=2, two new peaks at 783 and 906cm^{-1} are attributed to the Cr-O and Cr=O bonds from the Cr(VI) species appearing in the spectrum of A-PAN. In addition, the band at 1200-1470cm^{-1} with a large intensity corresponding to N-H and O-H bending was considerably increased due to the presence of Cr(VI) suggesting that the amine and oxime group of amidoxime are involved in the binding of chromium during Cr(VI) uptake [193].

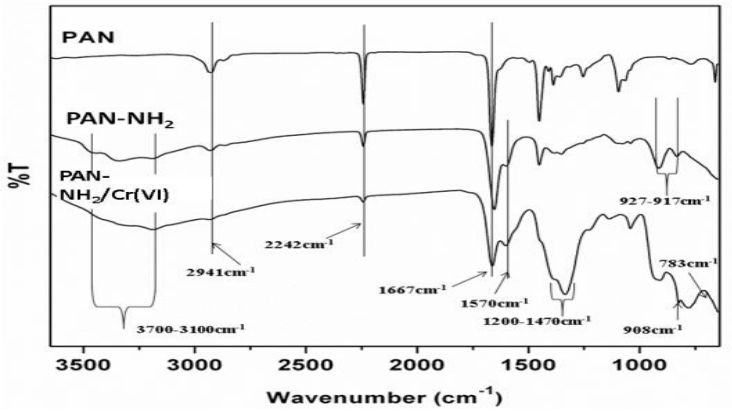

Figure 17. FT-IR spectra of the PAN and PAN-NH_2(A-PAN) nanofibers without interaction and with Cr(VI) solution, PAN-NH_2(A-PAN)/Cr(VI) nanofibers T=23±1°C, V=40mL, 100mg L^{-1}, pH=2 and A-PAN nanofiber = 20mg.

3.3 pH and adsorption behavior

The pH is an important parameter in the extraction process due to its influence on both the extractant and the metal species in solution. The experiments were carried out in the pH range from 2 to 11, while keeping all other parameters constant: [Cr(VI)]=10mg L^{-1}, [Cyanex-301 coated SPION]=1mg mL^{-1}, contact time=120min, T=23ºC. The removal of Cr(VI) as a function of solution pH is shown in Figure 18(a). Maximum removal is observed at pH=1 and pH=2 for 3-MPA and Cyanex-301; respectively (Figure 18(b) and (C)). Therefore, it was used as the optimum pH value for further adsorption experiments. The pH dependence of metal adsorption is related to the optimum pH range of the extractant Cyanex-301 and 3-MPA as reported in the literature [194,195]. At the optimum pH, the predominating form of Cr(VI) in solution is the acid chromate ion ($HCrO_4^-$). A more in depth understanding of the role of pH in the interaction of extractants (Cyanex-301 and 3-MPA) coated SPION and Cr(VI) is obtained by considering the findings from FT-IR and XPS. It can be observed that at lower pH the maximum extraction occurred; specifically at optimal pH 1 and 2. Conversely, at higher pH the extracting capabilities of SPION-extractants (3-MPA and Cyanex-301) are decreased; therefore, reducing the removal efficiency by causing the surfaces to be less positively charged. Furthermore, this competing effect greatly weakens the electrostatic attraction between the extractants coated SPION and negatively charged Cr(VI) anions. Interaction between SPION and Cyanex-301 and 3-MPA occurs primarily through the P=S bond, while the chromate ion is covalently bonded to sulfur via the thiol functionality. The maximum adsorption by the

extractants coated SPION is mainly ascribed to ion exchange of the SH bond of 3-MPA and Cyanex-301 with Cr(VI). Cr(VI) is a typical class (a) metal according to Hard Soft Acid Base (HSAB) principle. Hence, it has a strong tendency to be extracted with chelating agents which coordinate through oxygen, nitrogen or sulphur donor atoms. Moreover, 3-MPA has a sulfur as a donor atom with subsequent extraction of these metal ions (Cr(VI)) being possible. The reaction between Cr(VI) and SH functional group from 3-Mercaptoproprionic acid (3-MPA) was studied by P.H. Connett et al. When SH groups from 3-MPA was reacted with the hydrogen chromate ion, the reaction was very slow because the leaving group was the hydroxide (OH) from ($HCrO_4^-$). Hence, a mechanism was proposed resulting in the reaction [15].

$$(HOOC)RSH + -O\text{-}CrO_3^- \leftrightarrow (-OOC)RSCrO_3^- + H_2O \qquad (15)$$

According to the speciation diagram of Cr(VI) at low pH, the predominating species is the chromate ion ($HCrO_4^-$) [197-198]. One thought that needs to be addressed is if at low pH (acidic regime) the carrier material, SPION, does dissolve? To address this question, while performing the study of pH, the dissolution of iron in SPION was measured using ICP-OES. The results represented, on the left axis in Figure 18c, illustrated that the highest dissolution of iron occurred at maximum Cr(VI) extraction; the amount of dissolution of iron throughout the study was found to be less than 1%. Abramson et al. stated that it is known that metals (iron) dissolve faster in nitric acid than other diluted acids [199]. Moreover, nitrate acts as a depolarizer and nitro compounds are reduced by iron and acid without hydrogen evolution.

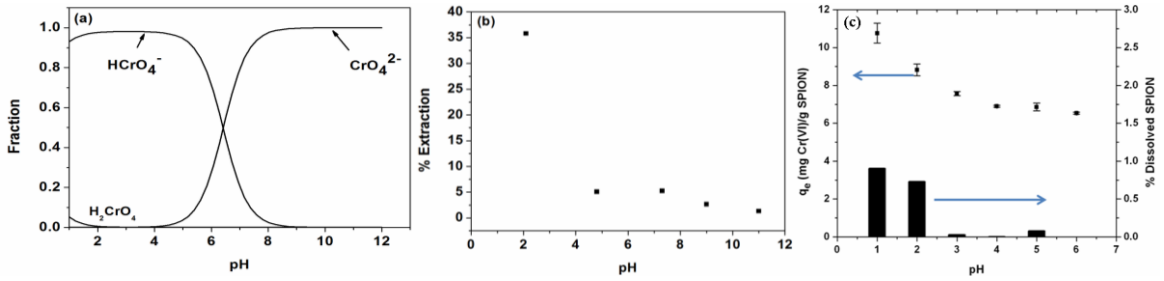

Figure 18. (a) speciation diagram of Cr(VI) and Effect of pH on the removal of Cr(VI) (b) Cyanex-301 (c) 3-MPA and % Dissolved SPION (bars, right axis).

When applying the adsorption technique, one of the key parameters to study is pH, as the pH is responsible for controlling the process. The uptake of Cr(VI) by this highly flexible nanofiber nanocomposite from solutions was studied as a function of contact time, pH and Cr(VI) concentration. The amount of Cr(VI) adsorbed on the flexible nanofiber nanocomposite platform as a function of pH in the range from 2 to 9 was experimentally determined and the data was illustrated in Fig 19a. The optimum pH for the adsorption of Cr(VI) species by the flexible ZnO-PLLA nanofiber nanocomposite was ≤ 3.5. This may be attributed to the substantial amount of hydrogen ions (H+) present. The pH level can neutralize the negatively charged ZnO adsorbent surface; subsequently, reducing the hindrance to the diffusion of Cr(VI) anions. Bhattacharyya et al. and Kumar et al. showed that when pH is less than 6, at low pH the molecular form of Cr(VI) is the predominantly adsorbed species, whereas as the pH increases above 6, the ionized form, CrO_4^{2-} was preferentially adsorbed due to the abundance of hydroxide ions (OH^-) hindering the diffusion of Cr (VI) anions, thereby reducing the removal efficiency [200-201]. As illustrated in Figure 19b, the point of zero charge, PZC, can be observed. As ZnO reaches the PZC the surface charge of the oxide becomes neutral. Subsequently, very little to no

adsorption of the Cr(VI) from wastewater was obtained, which can be the result of the pH being below the pzc; resulting in the surface of the adsorbent becoming positive.

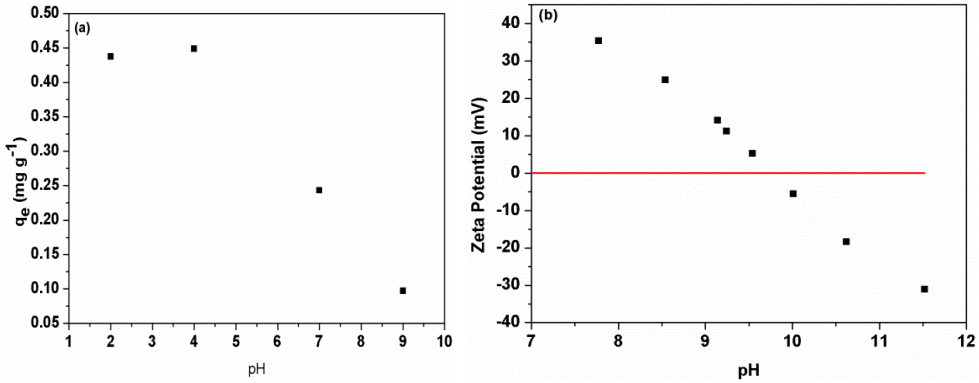

Figure 19. (a). pH Dependence; Cr(VI) initial concentration=2.3ppm Contact time=24hr, Total volume=100ml and Flow rate=2mL min^{-1} (b). Zeta potential for ZnO nanostructures.

The effect of solution pH on the adsorption of Cr(VI) ions onto A-PAN nanofibers is presented in Figure 20. As observed, the adsorption capacity was highly dependent on the pH with maximum adsorption at pH=2, which is consistent with literature [202]. The highest adsorption capacity achieved for the extraction of Cr(VI) at pH=2 was due to large number of H^+ ions present at low pH values, which in turn neutralizes the negatively charged adsorbent surface,.and also reducing the hindrance to the diffusion of chromate ions [203-205]. Lowering the pH below 2 will shift the concentration of $HCrO_4^-$ to H_2CrO_4 and that might reduce the adsorption of $HCrO_4^-$ form of Cr(VI) on the A-PAN adsorbent [203].

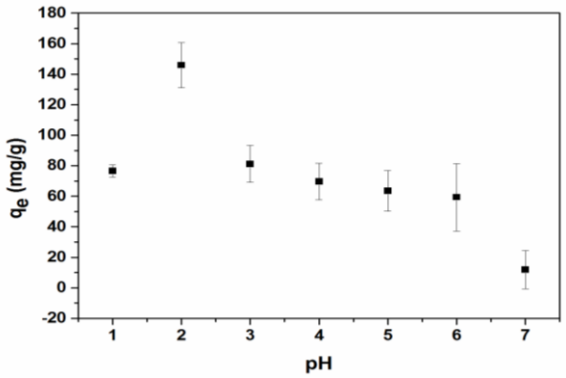

Figure 20. The loading capacity of Cr(VI) adsorbed onto A-PAN nanofibers as a function of pH. T=23±1°C, V=25mL, weight of A-PAN nanofiber ~20mg and [Cr(VI)]=100 mg L^{-1}.

The amount of Cr(VI) removed from the solution decreased with increasing pH (pH>3). As shown in equation (16), it is in agreement with the expectations that at low pH the majority of the NH_2 of the amidoxime group (pKa≤6) on the fiber are protonated to form NH_3^+ favoring the adsorption of negatively charged Cr(VI) complex ions through electrostatic bonds [206-208].

$$R_1 - NH_2 + H^+ \leftrightarrow R_1 - NH_3^+ \qquad (16)$$

At pH=1.0, hexavalent chromium ions mainly exist in the form of chromic acid (H_2CrO_4) with no electrostatic charge hindering its interaction towards NH_3^+ groups. In the pH range 2.0–6.0, different forms of chromium ions with negative charge such as: dichromate ($Cr_2O_7^{2-}$), hydrochromate ($HCrO_4^-$), and polychromates ($Cr_3O_{10}^{2-}$, $Cr_4O_{13}^{2-}$) coexist, of which $HCrO_4^-$ predominates. At pH above 7.0, the predominant species are CrO_4^{2-} and

$Cr_2O_7^{2-}$ at chromium concentration above ~1g L^{-1} [209]. However, at pH>3, a considerable decrease in the adsorption was observed mainly due to the protonation of amidoxime groups on the nanofibers surface diminishing considerably. This effect is markedly observed at pH above 7 where the adsorption is close to 0 as depicted in equation 17.

$$R_1 - NH_2 + OH^- \leftrightarrow R_1 - NH_2 \cdots\cdots OH^- \quad (17)$$

The variation in adsorption capacity of Cr(VI) ions at different pH values may be attributed to the affinities of A-PAN nanofibers for the different species of Cr(VI) existing at acidic pH values namely H_2CrO_4, $HCrO_4^-$, CrO_4^{2-}, and $Cr_2O_7^{2-}$ [210].

The NH_2 groups on the surface of the PAN nanofibers can either be protonated to form NH_3^+ at low pH (Eq. 16) or be deprotonated to form $NH_2\cdots\cdots OH^-$ at high pH (Eq. 17). Negatively charged $HCrO_4^-$ and $Cr_2O_7^{2-}$ ions are easily adsorbed to positively charged A-PAN nanofibers at low pH values due to the electronic attraction. The electrostatic repulsion between negative Cr(VI) species and negatively charged A-PAN nanofibers increased with increasing pH values, and thereby resulted in the decrease of the adsorption of Cr(VI).

For the functionalization of PAN, partial hydrolysis is a method that is important and frequently used in the adsorption of heavy metals; owing to the ease and likeability for modification of PAN. When PAN was exposed to acids, it has the remarkable ability to mainitain its composition and structure. However, when considering hydrolysis, the conversion of PAN can be considerably slow.

The effect of contact time on Cr(VI) adsorption onto the Cyanex-301 coated SPION was investigated at pH 2.0 with a concentration of Cyanex-301 coated SPION of 1.0mg mL^{-1} and initial Cr(VI) concentrations of 8.3ppm, 10.5ppm, or 50.8ppm. The amount Cr-removal observed as a function of contact time is depicted in Figure 21. Equilibrium was reached for all tested concentrations of Cr(VI) after 1h. The adsorption of Cr(VI) on Cyanex-301 coated SPION was faster than those reported for other adsorbents such as activated carbon.

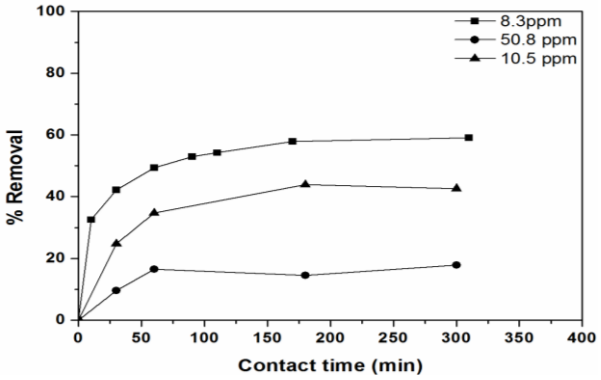

Figure 21. Effect of contact time on the removal percentage of Cr(VI) at different initial concentrations

The adsorption behavior of Cr(VI) onto 3-MPA coated SPION at initial Cr(VI) concentration, 10, 20, 30, 40 and 50mg L^{-1}, at pH=1.0 and room temperature as a function of contact time is shown in Figure 22. As depicted from the results, the adsorption rate of Cr(VI) on the 3-MPA coated SPION was initially quite high and thus obtaining equilibrium in 100min for all concentrations tested. Moreover, the loading capacity increased as the initial Cr(VI) concentration increase reaching 45.2mg Cr(VI)/g SPION with an initial concentration of 50ppm.

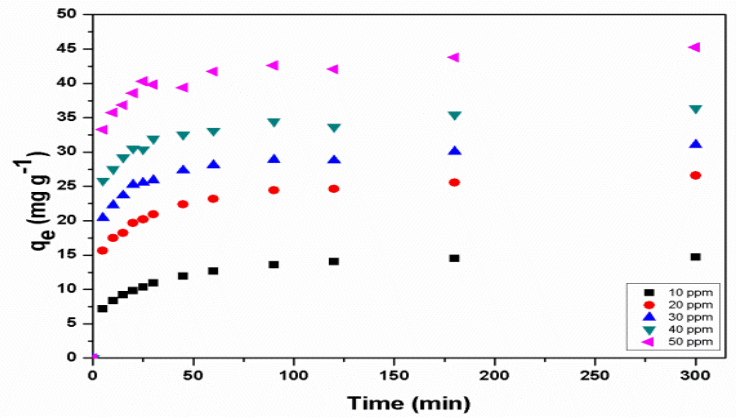

Figure 22. The amount of Cr(VI) adsorbed onto 3-MPA coated SPION (mg g^{-1}) as a function of contact time, at solution pH=3.0 and different initial Cr(VI) concentrations (10mg L^{-1} -50mg L^{-1}).

The A-PAN nanofibers after interaction with a certain concentration of Cr(VI) ions removed over a specified time range gives an indication that the surface functionalization of PAN works. This was a direct result of the interaction between the metal ions and the NH_2 group from the strong reducing agent, hydroxylamine hydrochloride. Initially, the rate of adsorption of Cr(VI) was fast in the initial stage of the process. After 20 minutes ~90% of Cr(VI) was extracted from solution; but, gradually reached a plateau indicating saturation. Hence, equilibrium was reached for all tested concentrations of Cr(VI) after 180 minutes (Figure 23). Kampalanonwat et al. stated the adsorption of the metal ions of Cr(VI) occurred in two steps. In the first step, the adsorption was relatively quick because of the great number of free adsorptive sites coupled with the high metal ion concentration. Furthermore, in the second step, the extraction of the metal ions in question decreased as equilibria was achieved [211]. This was due to the fact that the adsorption sites were depleted as well as the metal ion concentration in aqueous solution was decreased.

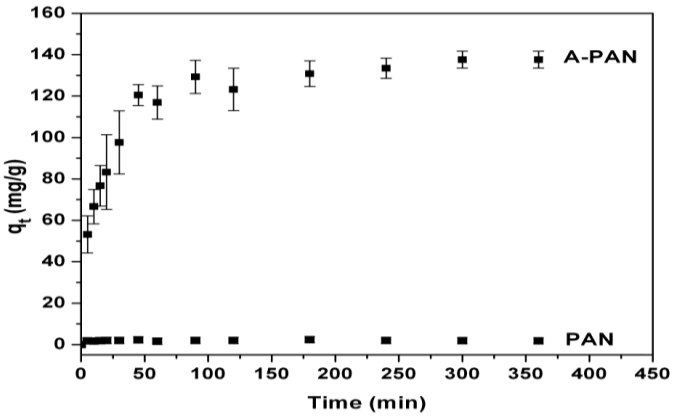

Figure 23. PAN and A-PAN adsorption equilibrium vs. time of [Cr(VI)]=100ppm, pH=2 and V=20mL

Hydroxylamine hydrochloride, a reducing agent, was used to convert aldehydes and carbonyls (ketones) into oximes in the presence of weak bases [180]. PAN nanofibers are reacted with hydroxylamine hydrochloride and further reaction with sodium hydroxide to produce ion exchange materials with high adsorption capacity [212]. The conversion of the nitrile groups of PAN increased as the concentration of hydroxylamine hydrochloride increased resulting in the nanofiber loss of flexibility and shows as a rather slow process as

compared to that of sodium hydroxide. This phenomenon was because of the molecular diffusion of hydroxylamine hydrochloride moving from the solution onto the nanofiber [213].

3.4 Adsorption isotherm and kinetics

The adsorption isotherms describe the interaction between the adsorbent and the pollutants. Adsorption isotherm models can be applied to a wide range of adsorbate concentrations in order to provide pertinent and important information for design and scale-up. These isotherms are critical for optimization of the adsorption mechanism and the loading capacity of the adsorbent.

Freundlich and Langmuir are extensively used classical adsorption isothermal models that offer an understanding of how equilibrium is established between the adsorbate and adsorbent. When the Langmuir model is applied a plot of C_e vs C_e/q_e results in a straight line with slope = $1/q_m$ and intercept =$1/(K_L\ q_m)$. As for the Freundlich model, a plot of log C_e vs log q_e a straight line is obtained with slope =1/n and an intercept =logK_F. The plots in Figure 24 obtained are the results of the estimated loading capacities of Langmuir and Freundlich models in comparison with the experimental loading capacity. It can be shown that the adsorption takes place following the linear fit using the Langmuir model.

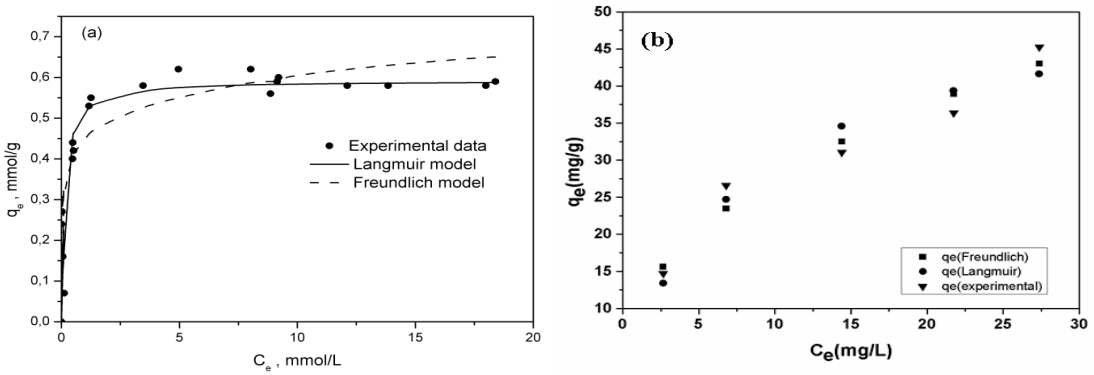

Figure 24. Maximum loading capacity of Cr(VI) adsorption data by (a) Cyanex-301 coated SPION and (b) 3-MPA coated SPION to the estimated loading capacities from Freundlich and Langmuir isotherms.

When compared to other adsorbent materials (Table 8) our system shows enhanced maximum loading capacity; comparatively. This could be attributed to the fact that the surface areas are much higher causing an increase in binding sites for the adsorbent material.

Table 8. Comparison of Cr(VI) maximum loading capacity using extractants (Cyanex-301 and 3-MPA) coated SPION and other reported adsorbents

Adsorbent	pH	T (°C)	Adsorption capacity (mg/g)	Source
Cyanex-301 coated SPION	2	25	30.8	This work
3-MPA coated SPION	1	25	45.2	This work
Granular activated carbon	3	25	7	[214]
Carbon slurry	2	30	14.2	[215]
Sawdust	3	25	8.3	[216]
Ethylenediamine-modified cross-linked magnetic chitosan resin	3	20	39.7	[217]
Chestnut tannins immobilized on chrome shavings	4	25	9.2	[218]
Mimosa tannins immobilized on chrome shavings	4	25	0.26	[219]

Magnetite nanoparticles	2.5	25	19.2	[220]
Fe^{3+} oxide/hydroxide NP agglomerates	4	25	31.5	[221]
Nano γ-Fe_2O_3	2.5	25	19.4	[222]

The effect of equilibrium adsorption data of Cr(VI) onto A-PAN nanofibers are illustrated in Figure 25. The adsorption capacity q_e increased with an initial increase in C_e and reached a plateau at 150±2mg L^{-1} as C_e increased further. The obtained experimental results were fitted using Langmuir and Freundlich models. The Langmuir model was derived to describe the adsorption of a monolayer of adsorbate on a homogeneous, flat surface of an adsorbent. The mathematical expression of the model was given in eq. 6.

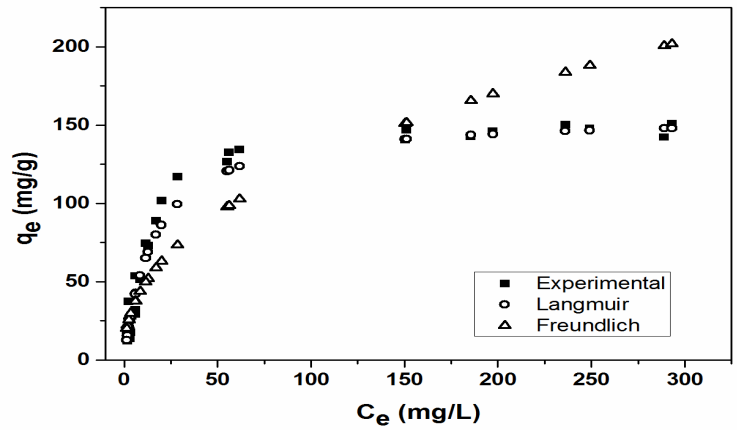

Figure 25. Comparison of Langmuir and Freundlich adsorption isotherm models for the adsorption of Cr(VI) on A-PAN nanofibers with experimental results. T=23±1°C, V=40 mL, pH=2 and A-PAN nanofiber =20mg.

The obtained values of Langmuir and Freundlich parameters as well as the correlation coefficient (R^2) were summarized in Table 9. The experimental data obtained correlated very well to the Langmuir model based on R^2 values indicating homogeneous distribution of adsorptive sites and monolayer adsorption.

Table 9. Mathematical models of Langmuir and Freundlich empirical results

Model	**Parameters**		
Langmuir	q_{max},(mg g^{-1})	K_L,(L g^{-1})	R^2
	156.3	0.061	0.995
	n	K_F, (mg g^{-1})/(mg L^{-1})$^{1/n}$	R^2
Freundlich	2.30	17.1	0.825

Difficulties are inherented in direct comparisons with other literature data because of the different experimental conditions used in each study. However, the data reported on hexavalent chromium removal include various adsorbents, such as activated carbons, low cost adsorbents (sawdust, lignite, peat, chars, coals), clay minerals, industrial waste/by-products (fly ash, waste sludge, mud, lignin), bio-sorbents (algae, fungi, bacteria, plants, peat, chitin, chitosan), commercial ion-exchange resins and polymers (natural or synthetic), etc. [223]. The values of some of these Cr(VI) adsorbents are given in Table 10 and compared with the results obtained in this work. The values obtained were higher than the majority of adsorbents reported coupled with addition of its ease of separation from the bulk solution for A-PAN nanofibers. When comparing the loading capacity of Cr(VI) of amidoximated nanofibers to that of amine fibers prepared by Deng et al., it could be observed that the performance of this work wass around 7-fold higher [224].

Table 10. Comparison of Cr(VI) adsorption capacity using amidoximated PAN with different reported adsorbents

Adsorbent	pH	T (°C)	Adsorption capacity (mg g^{-1})	Source
A-PAN nanofibers	2.0	23	137.61±4.1	This work
A-PAN fiber	2.5	25	20.7	[224]
Ppy/PANI	2.0	25	227	[225]
PAN/Ppy core shell nanofibers	2.0	45	74.91	[205]
Carbon nanotubes on Granular activated carbon	5.0	25	1.031, 0.853, 0.07	[226]
PAN (PVAm/PEI)	2.0	25	39.0/20.6	[227]
Surface modified tannery residual biomass	2.0	50	217.39	[228]
PEI-modified aerobic granular sludge	5.2	20	348.125	[229]
Magnetite nanoparticles	2.5	25	19.2	[230]
Chitosan-ionic liquid	3.5	25	63.69	[231]

Ppy= Polypyrrole; PANI=polyaniline, PEI=poly(ethyleneimine)

The empirical isotherm, Freundlich, considers the adsorption of Cr(VI) onto A-PAN a to be a monolayer (chemisorption) or multilayered (physisorption). From the linear equation, in Figure 24, the slope and intercept can be used to calculate the key parameters (Table 9) to determine the type of sorption in this work. If the value of n lies between 1 and 10 the adsorption is deemed as chemisorption.

The mechanism for adsorption of Cr(VI) onto the surface of 3-MPA coated SPION and A-PAN nanofibers involve three main steps: (i) migration of the target metal from the bulk of the solution to the surface of the adsorbent (bulk diffusion); (ii) diffusion of the metal ions through the boundary layer to the polymeric film of the adsorbent (diffusion); and (iii) adsorption of the metal ion to an active site on the surface of the material (chemisorption) [232]. Due to the agitation of the sample, bulk diffusion can be eliminated; therefore, diffusion and chemisorption can be the main rate limiting steps. To identify the rate-controlling mechanisms during the adsorption of Cr(VI), two simplified models were applied to evaluate the experimental data. The goodness of the fit was estimated in terms of the coefficient of determination, R^2. In this work, the pseudo-first-order (eq. 10) and pseudo-second order kinetic (eq. 12) models were selected to test the adsorption kinetics.

The kinetic parameters for pseudo-first and pseudo-second order models were determined by the linear plots of log (q_e-q_t) vs t and (t/q_t) vs t; respectively (Figure 26) to determine q_e theoretical in order to compare with q_e experimental. From the values obtained from the fitting of the data following the pseudo-first and pseudo-second order models (Table 11), it can be observed that at low Cr(VI) concentration such as 10mg L^{-1}, diffusion of Cr(VI) ions to the surface of the adsorbent plays an important role given the high correlation coefficient (R^2=0.9986). At 10mg L^{-1}, the results suggest that the fitting supports the pseudo-first order model. However, as the concentration of Cr(VI) increases diffusion becomes less important and the fitting with the pseudo-first order model declines. On the other hand, the correlation coefficients and theoretical q_e values obtained for the pseudo-second order are preferred over the pseudo-first order. Hence, the adsorption system follows the pseudo-second order kinetic model which considers chemisorption as the rate limiting step. The adsorption of Cr(VI) occurred most likely via complexation and/or chelation between the Cr(VI) ions and thiol group of 3-MPA.

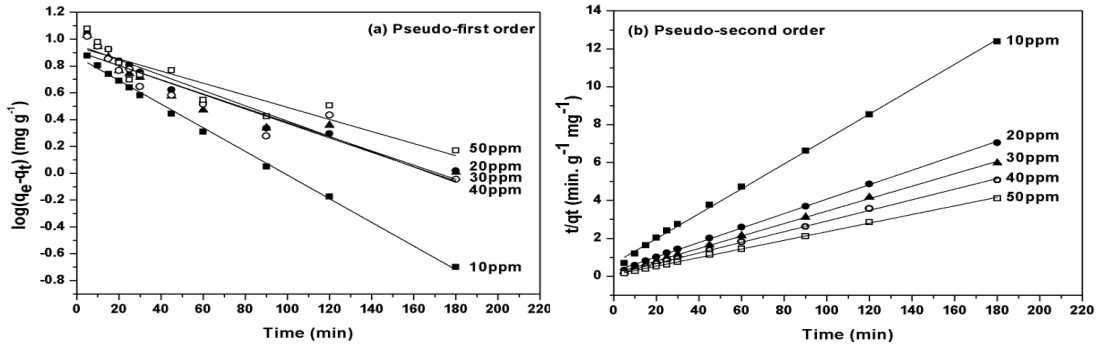

Figure 26. Kinetic models for the adsorption of Cr(VI) onto 3-MPA coated SPION, (a) Pseudo-first order model, and (b) Pseudo-second order model.

As shown in Figure 27, the pseudo-second order kinetic model has been explained from the linear plot time vs $\frac{t}{q_t}$ and the parameters achieved are summarized in Table 11. From the correlation factor (R^2), which is a validation point for model comparisons as the value of R^2 is closer to 1 determines the best fit model of choice.

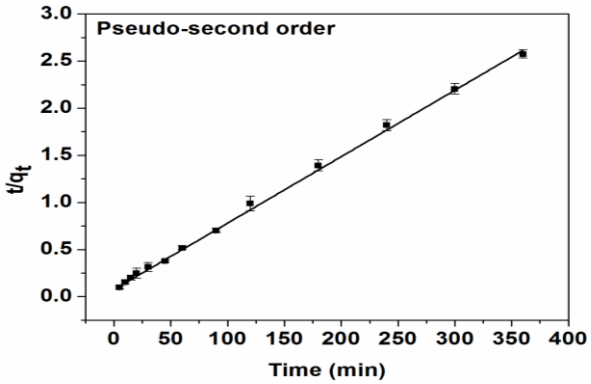

Figure 27. Pseudo-second order adsorption kinetics for Cr(VI) onto A-PAN nanofibers.

Table 11. Pseudo-first and pseudo-second order theoretical values along with the empirical results

	Pseudo-first order model			Pseudo-second order model			Experimental
Metal ions	R^2	k_1 (min^{-1})	q_e ($mg \cdot g^{-1}$)	R^2	k_2 ($g \cdot mg^1 \cdot min^{-1}$)	q_e ($mg \cdot g^{-1}$)	q_e ($mg \cdot g^{-1}$)
Cr(VI)	0.9148	$1.52 \cdot 10^{-2}$	68.34	0.9994	$5.6 \cdot 10^{-4}$	140.85	137.61±4.1

The results point to the fact that chemisorption was the rate limiting step through the complexation between the hydrochromate ion and the amine ion onto A-PAN nanofiber. Because the loading capacity was closer to the experimental maximum loading capacity and R^2 value from the pseudo-second order model was much closer to 1 than that of the pseudo-frst order model; hence, the model effectively described the kinetics of Cr(VI) being adsorbed onto A-PAN nanofibers.

Moreover, the contact time showed a very fast adsorption onto A-PAN which can be attributed to the number of readily available sites on the surface. The electrostatic interaction of Cr(VI) ions could also be considered as it is being attached to NH_2 effecting the transfer and attachment rates. Deng et al. reported chemisorption as the rate limiting step and attributed the very fast kinetics to Cr(VI) being adsorbed onto aminated nanofibers [224]. However, it was reported a different kinetics rate when compared

animated nanofibers to that of activated carbon. Because activated carbon is a porous material, the kinetics was driven by slow internal pore diffusion.

The interaction of Cr(VI) adsorbed onto adsorbents were studied using XPS. The spectrum is also in agreement with TEM that iron oxide was coated with the surfactants, Cyanex-301 and 3-MPA. Moreover, the chemical state of each element appearing in the sample is illustrated in Figure 28. XPS was used to support the fact that 3-MPA coated SPION efficiently and effectively removed Cr(VI) from solution. From the spectrum of Cr and S for both extractants analysis revealed when Cr(VI) is adsorbed onto the surface of each extractant, through chemical interactions, onto the surface of Fe_3O_4 could be changed mostly due to the shifts in the binding energies [233]. For the extractant 3-MPA, the binding energy for the S2p peak before and after contact with Cr(VI) is exhibited at 167 eV. In addition, a higher intensity and much narrower peak was similar to unreacted sulfur in 3-MPA, whereasinvestigating the second peak at 168.1 eV shows the intensity was much lower in comparison. The broader peak was found to be similar to that of SO_3 which can be attributed to the sulfur atom from 3-MPA molecule interacting with Cr(VI) species in solution. As in the case of the S atom for Cyanex-301, exhibited an elevated energy of 162eV as illustrated in Figure 28. Moreover, the sulfur 2p broad peak can be fitted into two subpeaks at 163.4eV and 164.6eV representing two types of sulfur binding to Cyanex 301.

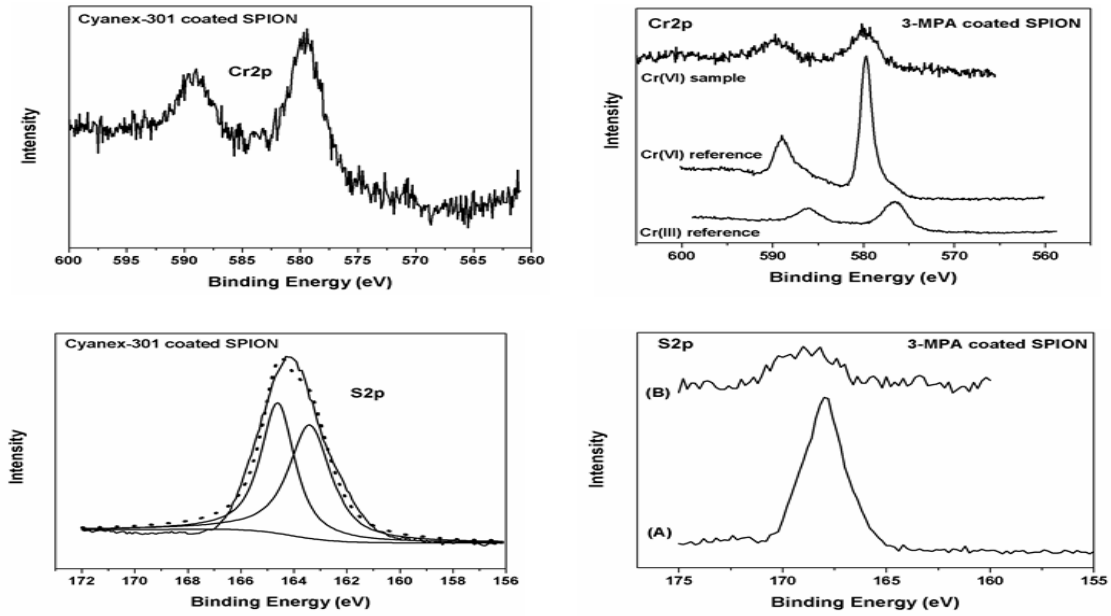

Figure 28. XPS spectrum of the Cr2p and S2p from SPION-Cyanex-301-Cr(VI). Spectrum Cr2p and S2p from SPION-3-MPA-Cr(VI). The circles present the raw data; the lines present the fitted subpeaks and the background.

More importantly, considering the Cr2p peaks for Cyanex-301 and 3-MPA, the Cr2p spectrum confirms 2 peaks with binding energies at 589 and 579eV; respectively, characteristically attributed to that of Cr(VI) [234]. Considering the two spin orbit split peaks for Cr(VI) from the sample, Cr(VI) from the reference material ($K_2Cr_2O_7$) and Cr(III) from the reference material ($CrCl_3$) are shown for 3-MPA. From the location of the binding peaks for each of the materials mentioned in the prior sentence, the results clearly show that in both cases chromium chemically bonded to was indeed Cr(VI). These results of the binding energies are consistent with the reference handbook [234]. Also, when observing the peaks from the samples there is a very small peak corresponding to a lower

binding peak. Subsequently, that binding energy is identified as that of Cr(III). Hence, there exist a clear difference between the binding energies for Cr(VI) and Cr(III). The difference between the width of the sample and the reference material could be attributed to non-uniformities and conductivities of the sample.

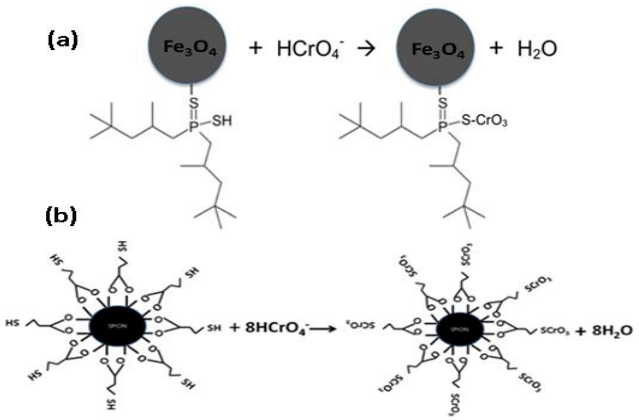

Figure 29. Schematic representation of the proposed mechanism on the interaction between $HCrO_4^-$ ion and sulfur atom on (a) Cyanex-301 and (b) 3-MPA.

Furthermore, the proposed mechanism in Figure 29 is shown as a result of the XPS analysis for the extraction of Cr(VI) from solution onto reagents (Cyanex-301 and 3-MPA) coated SPION. The mechanism describes that the –SH group from the two reagents are involved in a complexation reaction with the Cr(VI) ion species in the form of ($HCrO_4^-$). The XPS spectra are shown in Figures 30 and 31. The N1s spectra show that when A-PAN is interacted with Cr(VI) and or Cr(III) the nitrogen peak has shifted towards a higher bonding energy indicating that the adsorption has changed the chemical state of the nitrogen atoms in the amine groups as compared to the binding energy of triple bonded nitrogen in PAN (Figure 30).

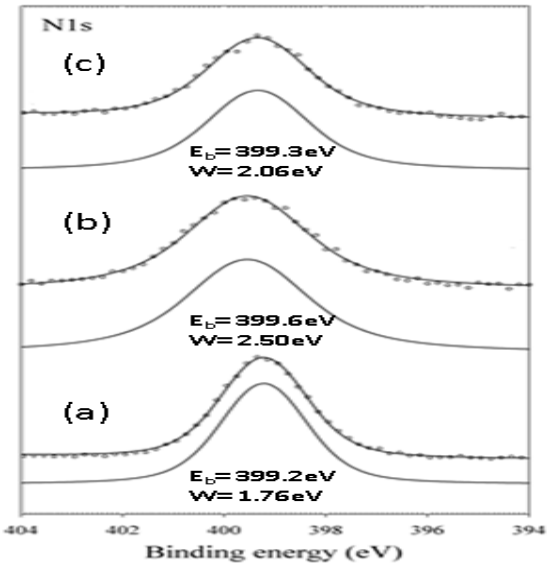

Figure 30. N1s XPS spectra from (a) A-PAN without Cr adsorption, (b) after reaction with Cr(III) and (c) after reaction with Cr(VI).

The Cr2p core-level XPS spectra of the chromium (Figure 31) can be observed by two peaks at 579eV and 589eV and is attributed to that of $K_2Cr_2O_7$. Meanwhile, there is a clear

difference between the two spectra in that the peaks observed at binding energies 577eV and 586eV can be attributed to $CrCl_3$. The results are in conformation when fibermats are reacted with HCl and NaOH; respectively, where the presence of Cr(III) and Cr(VI) are illustrated.

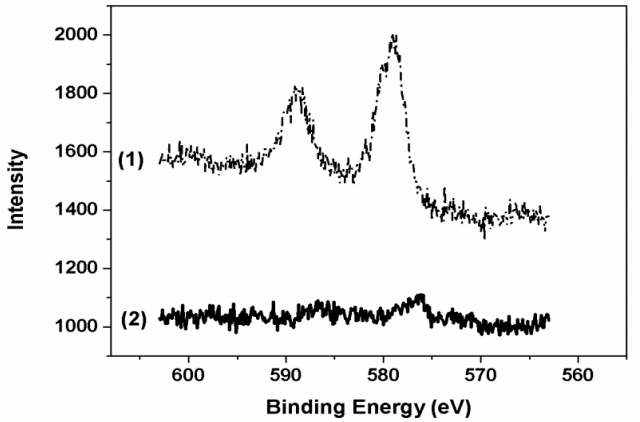

Figure 31. XPS spectra for (1) after interaction with HCl to produce Cr(III) and (b)after interaction with NaOH . V=5mL T=23±1ºC, C_o=100mg/L (for Cr(VI) and weight of A-PAN =20 mg.

The interaction of the hydrochromate ion ($HCrO_4^-$) via the nitrogen atom from the reagent is depicted as the proposed mechanism in Figure 32.

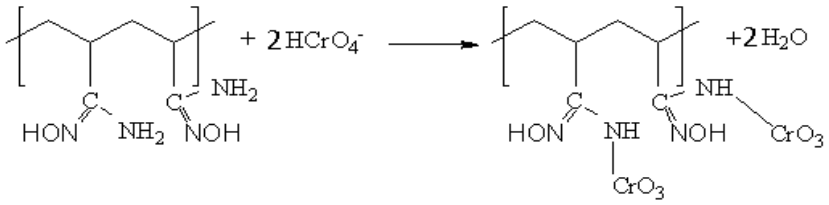

Figure 32. Proposed mechanism on the interaction between (a) $HCrO_4^-$ ion via nitrogen bond on A-PAN nanofiber.

3.5 Desorption from the adsorbent material

The recovery of Cr(VI) from the adsorbent can benefit both the environment as well as add economic value to the residue. To effectively recover the Cr(VI) contained in the adsorbant material, it is necessary to find the best eluting solvent. The desorption of Cr(VI) species from loaded SPION-Cyanex-301 was tested using HNO_3, NaOH, deionized H_2O and NaCl solutions. The results (Table 12) showed that for 2M HNO_3 eluting solution a high desorption percentage (> 70%) was achieved at pH=0, while the percentage of SPION dissolved by the acid at pH=0 was less than one percent (0.15%). Moreover, it is believed that Cr(VI) ions form more stable complexes with the acid than with the extractant. In the case of NaOH, the percentage recovery was determined to be 25 % at pH=13. As hydroxide ions are added to the system, they compete with Cr(VI) anions attached to the adsorption sites and consequently, increasing pH will cause the Cyanex-301 to be protonated so the adsorbed Cr(VI) will be transferred to the solution. The desorption percentage for H_2O and NaCl, respectively was almost negligible (< 2%) in comparison with HNO_3 and NaOH. A plausible explanation for the low desorption percentage is attributed to the lower electronegativity of sulphur resulting in electrons more readily shared in the Cr(VI)-S bond; therefore, resulting in a greater degree of covalencyby increasing the strength of the bond.

Table 12. Effect of elution solutions on the desorption percentage of Cr(VI).

Stripping Solution	Recovery (%)
HNO_3 2.0M	73
HNO_3 0.1M	20
0.1M NaOH	25
H_2O	2
0.1M NaCl	2

The best desorption results were achieved using 2M HNO_3. However, some studies reported in the literature indicate that at high concentrations of HNO_3 (>5M) Cyanex-301 begins to degrade thus basic conditions were chosen as the most appropriate desorption solution [187]. Finally, as the recovery at pH 13 was acceptable (~25%) but not complete, two more desorption cycles were performed. Negligible desorption was observed in these further steps while also SPION dissolution began to occur indicating that the chromate ion is strongly covalently bonded to the sulfur atom of Cyanex-301. The obtained results from the desorption study were consistent with the reported results by others such as Gupta *et.al* [235] who illustrated the use of cyanobacteria with different eluting solutions and found that HNO_3 was among the most efficient desorbents studied while desorption with deionised water was almost negligible.

For the desorption of Cr(VI) species from loaded A-PAN nanofibers, A-PAN nanofibers were tested using different concentrations of HCl and NaOH solutions. The results showed that for 0.01M NaOH eluting solution a high desorption percentage (> 80%) was achieved (Figure 33). As hydroxide ions are added to the system, they compete with Cr(VI) anions attached to the adsorption sites; consequently, instead of regenerating $HCrO_4^-$ the hydroxide will convert the nitrile group onto PAN nanofibers into COOH groups. Moreover, as the concentration of NaOH is added to the system the amount of $HCrO_4^-$ ions regenerated will decrease. On the other hand, a plausible explanation for the relatively high desorption percentage of Cr(III) in elevated concentrations of HCl solution maybe due to what Pezzin et al. proposes that the reduction from Cr(VI) to Cr(III) due to a three - electron reduction after the formation of a diester [236] . The obtained results from the desorption study were consistent with the reported results by others, such as Deng et al., who illustrated that after 3 cycles of regenerating Cr(VI) in the presence of NaOH ~96% was regenerated [224]. The results indicated that Cr(VI) has a strong affinity to NH_2 groups from A-PAN nanofibers.

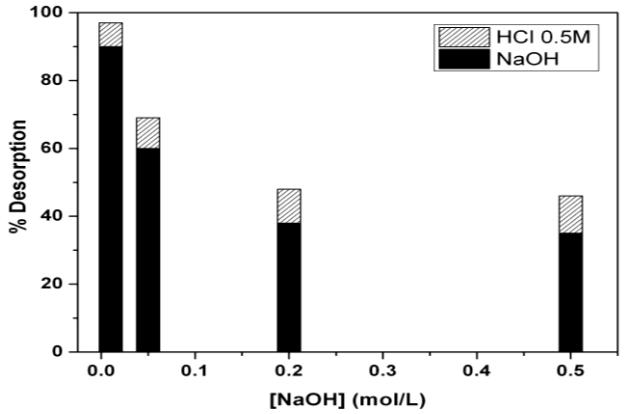

Figure 33. Desorption of total Cr(III) and Cr(VI) speciation from A-PAN nanofibers at different NaOH and HCl concentrations.

The composition of the samples shown in Figure 34 was determined by chemical analysis to fully understand the adsorption mechanism of chromium species on the surface of the A-PAN nanofibers. Prior to analysis, the difference in the color change of A-PAN without adsorption of Cr(VI) appears as a very flexible white mat (Figure 34(1) and the yellow-brownish mat from A-PAN after adsorption of Cr(VI) (Figure 34(2) were displayed. This work was carried out to obtain spectrum in order to illustrate the adsorption of Cr(VI) onto A-PAN. Also, the characteristic spectrum can be used to explain the desorption of Cr(III) or Cr(VI) from A-PAN nanofibers.

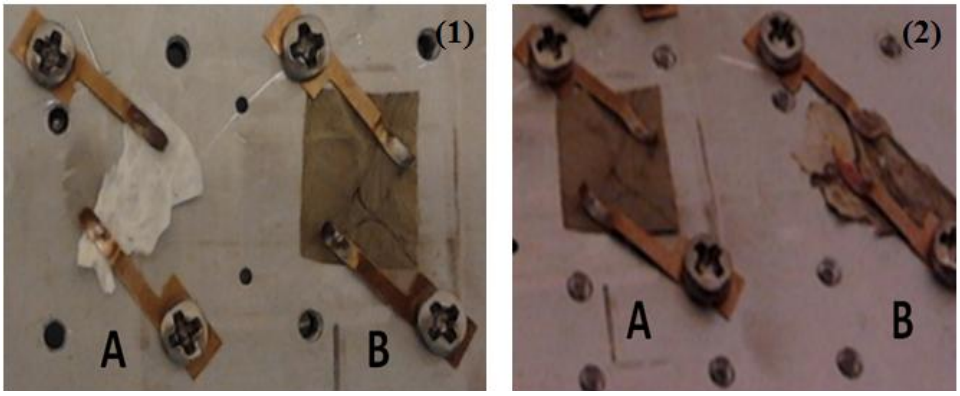

Figure 34. Sample preparation for (1) (A) A-PAN and (B) A-PAN-Cr(VI) nanofibers and (2) Prepared samples for (A) A-PAN-Cr(VI) in HCl and (B) A-PAN-Cr(VI) in NaOH nanofibers

Figure 34(1 and 2) shows A-PAN nanofiber after interaction with HCl and NaOH, respectively. Based upon visually inspecting the fiber mat in Figure 34(1B) the fiber has almost the same color as the fiber from Figure 34(2A). Conversely, the fiber mat from Figure 34(2B) appears to have lost the majority of its yellowish-brown color.

3.6 Elemental ionic concentration and particle size effect in different media: Dissolution study for biological applications

The metal ions concentration in aqueous solutions were investigated after ultrahigh centrifugation using ICP, where further analysis were prepared and conducted for Dynamic Light Scattering (DLS) analysis as shown in Tables 13, 14 and 15; respectively. The experiments were conducted with the high speed of stirring whereas the concentration was kept constant. As the surface to volume ratio decreases, the behavior of nanoparticles is influenced [237]. It has been shown that nanomaterials have different toxicity profiles compared with larger particles because of their small size and high reactivity. In addition, when particle size decreases there is a tendency to increase the toxicity; even if some materials are relatively inert in bulk form (e.g. ZnO, TiO_2 and SiO_2) [238]. In this work, a series of experiments were preformed to investigate the dissolution of lab-made and commercial metal oxide nanoparticles dispersed in different media (i.e.water, cell media and PBS). The temperatures selected for these experiments were 25 ^{o}C and 37 ^{o}C, respectively.

From the results shown in Table 13, it can be observed that the extent of dissolution can be varied according to the type of material as well as the matrix. In the case of elements, Ce, Fe and Ti, there is no significant increase in the dissolution in all conditions. On the contrary, in the case of the element Si, the extent of the dissolution for both manufacturers showed relatively the same effect despite the media used in this work. The dissolution for Zn was the highest when water was used as a dissolution medium. This may be attributed

to the effect of pH. Also, the speciation of Zn ions in solution is dependent upon temperature and concentration. It is of the utmost importance to ensure the nanomaterial can be effective at neutral pH (7) because the pH of the human body is slightly alkaline (pH=7.4). At biological pH, the precipitation of zinc hydroxide appears to be independent of the concentration of zinc [239].
According to the thermodynamic calculation software (Medusa), it was found that the solubility of Zn increases as the pH decreases. Subsequently, the negligible extent of dissolution of Zn in PBS media can be due to the existence of phosphate ions that may prevent the dissolution process from taking place.

Table 13: ICP analysis results of the four commercial samples (paper IV)

	Concentration (mg/L) @ Temperature 25°C			Concentration (mg/L) @ Temperature 37°C	% Dissolution			
Metals	H_2O	PBS	Cell Media	Cell Media	H_2O 25°C	PBS@ 25°C	Cell Media@ 25°C	Cell Media @ 37°C
Fe	6.8	0.42	3.2	1.8	1.0	0.1	0.5	0.3
Ti	0	0.005	24.4	1.3	0.0	0.0	2.8	0.2
*Si	52	54.38	58.2	65.4	11.1	11.6	12.4	14.0
Zn	207.8	0.21	97.6	114.8	25.9	0.0	12.1	14.3

* from Nanologica

	Concentration (mg/L) @ Temperature 25°C		Concentration (mg/L) @ Temperature 37°C		% Dissolution			
Metals	Cell Media w/serum	Cell Media w/o serum	Cell Media w/serum	Cell Media w/o serum	Cell Media w/serum @ 25°C	Cell Media w/ serum @ 37°C	Cell Media w/o serum @ 25°C	Cell Media w/o serum @ 37°C
*Si	38.2	37.6	42.7	46.1	5.7	6.4	5.6	6.9
Ce	13.8	0.0	14.5	0.0	1.2	1.2	0.0	0.0

* from Ludox

Table14: DLS characterization of commercial metal oxide nanoparticles used in this study (paper V).

	Particle Size (Hydrodynamic) (nm)			Particle Size (Dry form) (nm)	
Material	H_2O	Cell Media	PBS		Supplier
TiO_2	754.5 ± 89.1	263.0 ± 123.1	1424.3 ± 103.4	29.15 ± 9.76	Degussa
SiO_2	942.4 ± 148.4	575.4 ± 320.2	563.7 ± 320.2	348 ± 102	Lanxess
ZnO	252.6 ± 230.2	361.6 ± 240.7	1698.2 ± 204.7	15.49 ± 3.87	IBU/tec
α-Fe_2O_3	214.5 ± 183.1	338.4 ± 158.8	672.4 ± 35.2	90	Nanologica

The hydrodynamic particle size measurements from DLS are detailed in Table 14. Particle size can be affected by the intrinsic higher scattering intensity due to larger particles, which in this experiment means the interaction between silica and DMEM. Also, an increasing concentration can affect the interparticle interactions for the experiments as the concentration was kept constant at 1.0mg mL^{-1}.

The results shown in Table 15 illustrates that the hydrodynamic particle size increases when interacted with DMEM cell media. For those particles less than 100nm with the exception of silica at 20nm, resulted in an average cluster or agglomerate size (which is TEM dry size/DLS hydrodynamic size) of 29, 22 and 4 for silica 5-15nm, 7-14nm and 80nm, respectively. Silica of 20nm showed the highest effect of all the samples investigated. The increased hydrodynamic size may be due to the fact that according to the suppliers because of the large amount of atoms on the surface, the atomic ratio of Si to O for SiO_2 nanoparticles being not 2:1. Subsequently, this can cause increased agglomeration when interacted with DMEM, but the mechanism as to how this interaction occurs was not studied. The results for Sigma- μm, NLAB 40S and 85 silica particles according to the suppliers depict a TEM average size of these particles as <8μm, 2-4μm and 3μm, respectively. Because these particles are in the micron range and insoluble in water, NLAB 40S and 85, it is difficult to accurately determine how much agglomeration due to DMEM and electrostatic interactions may have occurred.

Table 15: DLS results of samples with maximum intensity peak.

Product	Size from supplier	Results Maximum Intensity
	SiO_2	Average
Sigma Aldrich	5-15nm	422±23.0 nm
Plasma Chem	7-14nm	336±17.7 nm
NanoStructured and Amorphous Materials	20nm	5653.7±404.6 μm
NanoStructured and Amorphous Materials	80nm	329±63.0 nm
Sigma Aldrich	Sigma um <8 μm	2924.5±464.6 μm
NanoLab	NLAB-Si 40S (2-4) μm	2843±142.8 μm
NanoLab	NLAB-Si 85 (3) μm	5384±984 μm

Bath sonication can attribute to the size of the particle diameter by breaking the agglomeration locally, but it can also promote agglomeration due to enhanced particle-particle interaction. Under certain experimental conditions, there have been studies showing that ultrasonication of silica particles greater than 100nm [240].

Table 16 below shows the particle size measured by TEM (dry form) and the hydrodynamic particle size measured by DLS (suspension) for the commercial and lab made SPION coated dextran. The nanoparticle was studied to understand the effects of each nanoparticle on 2 human epidermal cell lines: murin and keratinocytes in both under ultraviolet and non-ultraviolet light. The results conclude that the cells exposed to the commercial dextran coated nanoparticles 1 and lab-made nanoparticles 2 had a decline in cell viability. Conversely, the other nanoparticles did not exhibit any keratinocyte cellular behavior.

Table 16: particle size measurements using DLS techniques.

Material	**Particle size (nm) (TEM)**	**Particle size (nm) (DLS)***	
		Water	**Cell Culture Media**
KTH SPION-DEX 1 (Commercial)	21.1 ± 4.7	346	87
KTH SPION-DEX 2 (Commercial)	54.9 ± 16.6	428	103
KTH SPION-DEX 1 (Lab made)	15 ± 3.7	100	134
KTH SPION-DEX 2 (Lab made)	20.4 ± 7.5	111	160

When the nanoparticles (both lab-made and commercial dextran 2) were exposed to UV light in the presence of the murin cells affirmed the hypothesis that particle uptake and induction of oxidative stress in which these two actions led to NF-κB being activated [241].

4. Conclusions

The utilization of specific engineered nanomaterials either in the form of nanoparticles or fibers (functionalized or non-functionalized) are a powerful platform that can substantially enhance environmental quality through pollution prevention, water treatment and remediation. Moreover, as these known advantages are a benefit to those industrialized countries it would be an enormous asset to countries that are also in the development process. Nanotechnology has gathered much attention in the treatment of water due to its unique properties.

A successful preparation of functionalized nanoadsorbents (Cyanex-301 and 3-MPA) onto SPION for the removal of Cr(VI) from aqueous solutions were carried out. The nanoparticles were synthesized by the co-precipitation method. The extracted reagents both contained a thiol group that served as an important molecule in this work. TEM and EDX characterization showed that the reagents were attached to SPION.

pH played an important role in determining what pH regime and speciation of the adsorbate in the removal of Cr(VI). The maximum adsorption of Cr(VI) was achieved with less than 1% of iron dissolution from SPION. Moreover, the adsorption was better described by the Langmuir isotherm resulting in a maximum loading capacity as compared to other materials found in the literature.

XPS analysis for both reagents via thiol group gave conclusive evidence that the chromium analyzed was in the form of Cr(VI). Also, the difference in the binding energies for sulfur supported the chemical bonding with Cr(VI) in the form of $HCrO_4^-$.

The production of a fast, simple and efficient nanofiber to address the issue of Cr(VI) introduced into aqueous systems was investigated. Nanofibers, particularly functionalized PAN nanofibers, play an important role in the adsorption process. Electrospunned PAN nanofibers were produced and further reacted with hydroxylamine hydrochloride to produce amidoxime PAN nanofibers (A-PAN). This chemical reaction was only possible because of the nitrile group from PAN. The behavior of the metal ion, Cr(VI), was greatly influenced by pH and initial concentration. The conversion of the nitrile group to amine increased as the reaction time increased. Additionally, the adsorption of the metal ions fitted well to the Langmuir isotherm model resulting in a homogeneous monolayer with an estimated maximum loading capacity exceeding well above some materials reported in the literature for the adsorption for Cr(VI). The dominant mechanism was ascribed to chemisorption as the behavior of the metal ion onto A-PAN better described with the pseudo-second-order kinetic model. The analysis revealed that the amine groups on the surface of A-PAN was responsible for the extraction of Cr(VI) through electrostatic interaction between the positively protonated amine group and the negative ion of Cr(VI). As pH and other parameters are key in the successful adsorption, concentration of adsorbents was adjusted while keeping pH, temperature and adsorbate concentration constant. The results show that the greatest adsorption took place when the adsorbent concentration was the lowest in comparison to the other parameters.

Electrostatic and surface attractions between ZnO and Cr(VI) species control the interactions between the flexible nanocomposite platform and the Cr (VI) species. The adsorption equilibrium was obtained within 1300 minutes when the pH was kept less than 3.5. pH was found as a key parameter for the study of ZnO-PLLA nanofibers in the adsorption of Cr(VI). Moreover, this work also found out that using a base solution, 60% of Cr(VI) can be regenerated from the nanocomposite.

The dissolution medium showed little to no significant effect on the dissolution of the metal oxide nanoparticles with the exception being ZnO. The particle size is believed to have significant influence on the dissolution of the metal oxide nanoparticles.

Unfortunately, in this study, the particle size was not varied with respect to the same metal oxides used. It was observed that the temperature at ($25^{o}C$ and $37^{o}C$) indicated no significant effect on the dissolution. Despite using a high stirring rate, a significant dissolution was not observed except for ZnO in water media.

Nanomaterials that have been used in the dissolution have shown interesting results. When introduced to different media, the engineered nanoparticles were agglomerated before being interacted with human lung cells. DLS results for silica from both manufacturers showed the greatest agglomeration and dissolution.

The dextran coated nanoparticles with the smallest TEM dry particle size for the lab-made and commercial samples exhibited a decline in cell viability. The activation of NF-κB was determined to have occurred from the induction of UV light on the samples.

The study involving the synthesis, preparation, characterization and utilization of nanomaterials for the removal of heavy metals from industrial applications such as treatment of wastewater or biological systems have proven to be promising.

Future work

In the future, there are several routes that can be taken to further investigate the improvement of the materials depicted in this thesis in order to provide a deeper understanding of wastewater treatment systems. To apply indepth study of the mechanism of adsorption dynamics, it is recommended that different isotherms and kinetic models should be sought for. Until now, our study has not encompassed models such as BET model and other isotherms such as the Temkin and the Dubinin-Raduskevich. Also, investigation into how adsorption thermodynamics affect our system is vital. In wastewater treatment industries, development of novel adsorbents that can be used for large scale applications are needed and this should be done in close collaboration with academic research insititutions. Synthesis of new materials and applications of them for heavy metal removal should be given a priority considering the release of such metals and their toxic effects on humans and the environment.

The present work has focused on the batch mode, which is a method that has worked well in carrying out laboratory experiments. The disadvantage of this method is that it does not mimic real-world applications, therefore other methods such as continuous, fixed and packed bed reactor systems should be investigated to find out the effects of nanomaterials for adsoption of different concentrations.

Acknowledgements

I would like to say thank you to Professor Michael Fokine for all you have done for me throughout my PhD studies. You have shown courage and steadfastness to take a stand on my behalf when others walked away. Associate Professor Yohannes Kiros thank you for taking on the role as my supervisor when I thought all was lost. I know it has not been easy; but, I thank you for believing in myself when I no longer felt the same. You have taught me how to become confident in my research abilities and to pay attention to the details. Professor Inger Odnevall Wallinder, thank you for taking a decision when you did not have to. You generosity will never be forgotten. Professor Farid Akhtar words can not express my gratitude. You have encouraged me to continue this work by taking the time to sit with me despite my not being your student. Thank you for the conversations that I will take with me for the remainder of my life. Dr. Mohsin Saleemi (Asima and Jr.) my best friend I thank you and your family for adopting me into your family. Your support has been invaluable. I hope to someday role-model those attributes to someone as you have done for me. Professor Illona Kretzchmar my professor who introduced me to Sweden through research in New York. I have come to say thank you for encouraging me to dream beyond my circumstances and to enjoy the process while being unapologetic about it. Dr. Claude Brathwaite thank you for introducing me to Professor Kretzchmar through the LSAMP program and initially tricking me into going to Sweden. You are one of the most respected directors that I have come to know. Thank you for not accepting my response of 'no' because I would not be in this moment had it not been for you. Dr. Bengt Fadeel thank you for the opportunities forwarded to me throughout my PhD and the conversations you have imparted to me are priceless. Dr. Hanna Karlsson thank you for the assistance and the chance to learn some nuggets regarding toxicity and cell viability that have been ingrained in my mind. Dr. and Mrs Lynn Hales the advice you have given me over the years have been so important to me throughout my life. Thank you for understanding and supporting me. Also, the chocolate pies are to die for☺. Dr. Marta Avila thank you for all the times you spent as my supervisor during our time in FNM. You taught me so much about the world of chemistry and how to be an effective and efficient lab student. Dr. Salima at our girl…Salima thank you for just being you. I am so honored to call you one of my best friends. Dan and Julie Colston, Scott Barritt, Eddie Thomas, Michael Boady, Felix Melenciano, Washington Moreira, Matt Lopez and Lawrence Stellmon thank you for teaching me the value of being a friend. It has been your support and love that has gotten me this far. Andy Horn I have come to appreciate the critical conversations about life, career and what we will leave to world. You have a gift that the world will definitely benefit from.

Pastor Dr.Casey and Michelle Fisher, Dr. Goodman, Ms. Peaches and Mrs. Wilson thank you for loving and feeding me with the word. No amount of money, time or gratitude could come close to the enrichment and self awareness freely granted by our Lord and Savior.

Dr. Ana Lopez and Dr. Anosh, Dr. Yi and Dr. Yuzhe (son), AnnaLisa (Smiley) and Alberto, Sofie and Ove, Gozie, Charles and Dr. Angela (Jr. I and II), Sheryar, Dr. Fredrik, Estaban, Dr.Tobias, Dr. Reyhaneh, Dr. Reza, Dr. Benjamin and Anna (Robert), Stina and Andreas (little Ms. Andreas Jr.), Alberto Recalenda, Dr. Peter, Dr. Pontus, Maria and Marcus (Sir Hiss), Lotten, Igor, Silke, Mario, Katarina, Dr. Gina, Dr. Usman thank you all for the wonderful time spent in Sweden with you each of you hold a special place in my heart.My Swedish family The Hammarstrands: Gunnar and Pia, Sandra and Henrik (Malte and Albert), Felix and Mårten words are not enough to share my gratitude to you for all

you have done. You have been such a rock for me during my stay in Sweden…thank you for all you have done.
Dr Maureen Corcoran, Professor James Dickerson and Dr. Steve Gerberding thank you for the wonderful talks about science and life after the PhD. You calm and direct approach in the form of advice has been greatly appreciated and much needed. Once again thank you and God bless you.
Debora, Melat, Benjamin, Fabio, MaryAnn, Jeffrey, Alfred, Fernand, Gabriel, Karin, Collins, Samuel, Tony, Anton, Gabriel, Alejandro, Pastor Fava, David, Abraham, Femi, Daniel, Matabel, Rachel, Jacqueline,Alex and Kasia, Bon and Elizabeth (little Ms. Bon), Dotun and Suki (Michelle),Marcus, Sol, Davida, Muyuki, Ile and Kenny (Joel), Roy and Amanda, thank you for the prayers and awesome fun shared with each of you at church, never forgotten always cherished my dear Hillsong Connect group and Host team. Robert Oscarsson I have been so honored to have be in your presence. You have taught me so much about your life, God and your desire to change the world. You are like a son to me. I pray that all of your desires will be granted. Petrus and Matteus (brothers on a mission for God) and family (especially grandparents), Nathan, Helena and husband, Samuel and Mikael thank you for your prayers and opening your homes and heart to me during my stay in Sweden. I have learned more about myself and my relationship with God because of you. Hugo Kylberg thank you for allowing me to see Sweden through the eyes of an amazing and talented young man. I am so proud of you and Viktor Carlsson the both of you have become great friends and I look forward to seeing how you will set the world on fire with your gifts. Patrick and twins, Jonathan and Nina you and your family have been such a blessing I know it was God who introduced us in the airport of Malaysia and Iceland…God bless you for a wonderful and fruitful friendship. My brothers (W.L. Jr, Shun, Fabian, Blake, Todd, Dr.O. and Bobby) and sisters (Bridget, Brigette, Brittany, Keshia, Lindy, Cherrie, Tameka, Wheat and Stacey) thank you for the unconditional love given to me, which is irreplaceable. I dedidicate this thesis to my nephews (Jeremye, MarKeith, ShunTerrance, Trajan, Kendrick, Patrick Terrance, W.L:III, Jaylon, Fabian Jr., Braylen, Landon, Jason, Barritt, Harrison, Land, Brandon, Hayden, Holt, Beckett, JohnWallace, Hudson) and nieces (Britericka, BriCharlassey, BriTasia, Te'Lia, BriNaya, Caitlin, N'Dasha, Tiana, Briah, Morgan, Emme, Hadley, Hayes, Helen) never give up on your dreams because it is the world who is going to benefit from your existence. Dr. Naeem and Dr. Shugufta, Muhammed and Zain I am so grateful to call you my extended family your love and unwaivered support has carried me throughout our PhD together. It is my prayer that God will move us close to one another so we can have the priviledge of seeing my best buddies (the boys) grow up.
My goddaughters (Mia and Julia) papa is very proud of the awesome godly ladies you have become and my godson (Baby DII) no more fighting papa only love and dancing ok☺.
Vonta and Jesse (DoLove) I am looking forward to watching life unfold before your very eyes, keep up the great work and watch God bless you beyond your wildest dreams. Ms. Thelma Rush my mentor, friend, Aunt, I love you to life…you have enriched my life beyond expectations. You live the life that all wish they could with respect, love and brutal honesty with God being at the head. Uncle Rod and Aunt Linda, Robert and Charlene, Ken and Murial Bunch-Jones, Lisa Bunch and Rosie Burks thank you for helping me find myself and introducing me to fantastic world of science. No amount of money can repay you for your investment in me. I love you. Also, my aunts, uncles and cousins I thank and love you even though I did not specifically call your names individually because I would still be writing☺. Felicia and April (2 members of the 3 musketeers) simply I love you both to life….

References

[1] N. Savage and M. Diallo, "Nanomaterials and Water Purification: Opportunities and Challenges", Journal of Nanoparticle Research, vol. 7, no. 4–5, pp. 331–342, 2005.

[2] J. Bartram, K. Lewis, R. Lenton, and A. Wright, "Focusing On Improved Water and Sanitation for Health", 2005.

[3] WHO/UNICEF, "Drinking Water Equity, Safety and Sustainability", 2011, http://www.wssinfo.org/fileadmin/user_upload/resources/report_wash_low.pdf. Accessed online Sept. 20, 2013.

[4] Rabia Ahmed, "Drinking Water Contamination and Its Effects on Human Health", 2010. http://www.cwru.edu/med/epidbio/mphp439/Drinking_Water.pdf. Accessed online June 6, 2013.

[5] WHO/UNICEF, "Progress on sanitation and drinking-water 2010 update", 2010. http://www.who.int/water_sanitation_health/publications/9789241563956/en/.Accessed online Oct. 10, 2013.

[6] J. Harris, "Consumption and the Environment", 1996. http://ase.tufts.edu/gdae/publications/frontier_series/consum-pt8.pdf. Accessed online Nov 2, 2013.

[7] R. A. Kraemer, K. Choudhury, and E. Kampa, "Protecting Water Resources: Pollution Prevention", 2001.

[8] European Environment Agency, "Water pollution —overview", 2008. http://www.eea.europa.eu/themes/water/water-pollution. Accessed online June 17, 2013.

[9] G. O'Conner, "Organic compounds in sludge-amended soils and their potential for uptake by crop plants", Sci Total Environ, vol. 185, no. 1, pp. 71–81, 1996.

[10] K. Fatta, I. Kalavrouziotis, P. Koukoulakis and M. Vasquez, "The risks associated with wastewater reuse and xenobiotics in the agroecological environment", Sci Total Environ, vol. 409, no. 19, pp. 3555–63, 2011.

[11] X. Li, J. Huang, D. Zhang, L. Shi and S. He, "Simultaneous removal of cadmium ions and phenol with MEUF using SDS and mixed surfactants", Desalination, vol. 276, pp. 136–41, 2011.

[12] Y. Ming-Ho, "Environmental Toxicology: Biological and Health Effects of Polluntants", Chapter 12, CRC Press LLC, 2nd Edition, BocaRaton, USA.

[13] R. Khlifi and H. Chaffai, "Head and neck cancer due to heavy metal exposure via tobacco smoking and professional exposure: A review", Toxicology and Applied Pharmacology, vol. 248, pp.71-88, 2010.

[14] S. Morais, F. Costa and M. Pereira, "Heavy metals and human health", In. Oosthuizen J (ed) Environmental Health Emerging Issues and Practice, InTech, Rijeka, Croatia, pp. 227-246, 2012.

[15] J. Roberts, "Metal toxicity in children. In Training Manual on Pediatric Environmental Health: Putting It into Practice", 1999.

[16] U. Farooq, J. Kozinski, M. Khan, and M. Athar, "Biosorption of heavy metal ions using wheat based biosorbents – A review of the recent literature", Bioresource technology, vol. 101, pp. 5043–5053, 2010.

[17] I. Gaballah and G. Kilbertus, "Recovery of heavy metal ions through decontamination of synthetic solutions and industrial effluents using modified barks", Journal of Geochemical Exploration, vol. 62, pp. 241–286, 1998.

[18] K. Low, C. Lee, and S. Liew, "Soprtion of cadmium and lead from aqueous solutions by spent grain", Process Biochem., vol. 36, pp. 59–64, 2000.

[19] B. Volesky, "Removal of lead from aqueous solution by Penicillium biomass. Biotechnol. Bioeng", Biotechnol. Bioeng., vol. 42, pp. 785–787, 1993.

[20] J. Chen and O. Hao, "Microbial chromium (VI) reduction Critic. Rev.", Environ. Sci. Technol., vol. 28, pp. 219–251, 1998.

[21] J. Godt, F. Scheidig, C. Grosse-Siestrup, V. Esche, P. Brandenburg, A. Reich, and D. Groneberg, "The toxicity of cadmium and resulting hazards for human health", J. Occup. Med. Toxicol., vol. 1, pp. 1–6, 2006.

[22] Y. Sharma, "Economic treatment of cadmium (II)-rich hazardous waste by indigenous materials", J. Colloid Interfac. Sci., vol. 173, pp. 66–70, 1995.

[23] K. Singh, A. Singh, and S. Hasan, "Low cost bio-sorbent ‘wheat bran’ for the removal of cadmium from wastewater: kinetic and equilibrium studies", Biores. Technol., vol. 97, pp. 994–1001, 2006.

[24] D. Boening, "Ecological effects, transport, and fate of mercury: a general review", Chemosphere, vol. 40, pp. 1335–1351, 2000.

[25] D. Manohar, K. Krishnan, and T. Anirudhan, "Removal of mercury (II) from aqueous solutions and chlor-alkali industry wastewater using 2-mercaptobenzimidazole-clay", Water Res., vol. 36, pp. 1609–1619, 2002.

[26] F. Morel, A. Kraepiel, and M. Amyot, "The chemical cycle and bioaccumulation of mercury",, Ann. Rev. Ecol. Syst., vol. 29, pp. 543–566, 1998.

[27] L. Dupont and E. Guillon, "Removal of hexavalent chromium with a lignocellulosic substrate extracted from wheat bran", Environ. Sci. Technol., vol. 37, pp. 4235–4241, 2003.

[28] F. Granados-Correa and J. Serrano-Gómez, "CrO_4^{2-} ions adsorption by Fe-modified pozzolane", Sep. Sci. Technol., vol. 44, pp. 924–936, 2009.

[29] M. Kobya, "Adsorption, kinetic and equilibrium studies of Cr(VI) by hazelnut shell activated carbon.", Adsorp. Sci. Technol., vol. 22, pp. 51–64, 2004.

[30] K. Singh, H. Hasan, M. Talat, V. Singh, and S. Gangwar, "Removal of Cr(VI) from aqueous solutions using wheat bran", Chem. Eng. J., vol. 151, pp. 113–121, 2009.

[31] D. Chilvers and P. Peterson, Global cycling of arsenic. In: Lead, Mercury, Cadmium and Arsenic in the Environment, John Wiley & Sons, Chichester, 1987.

[32] S. Dudka and B. Markert, "Baseline concentrations of As, Ba, Be, Li, Nb, Sr and V in surface soils of Poland", Sci. Total Environ., vol. 122, pp. 279–290, 1992.

[33] F. Robertson, "Arsenic in ground water under oxidizing conditions, southwest United States", Environ. Geochem. Health, vol. 11, pp. 171–176, 1989.

[34] T. Chuah, A. Jumasiah, I. Azni, S. Katayon, and S. Choong, "Rice husk as a potentially low-cost biosorbent for heavy metal and dye removal: an overview", Desalination, vol. 175, pp. 305–316, 2005.

[35] A. Papandreou, C. Stournaras, and D. Panias, "Copper and cadmium adsorption on pellets made from fired coal fly ash", J. Hazard. Mater, vol. 148, no. 3, pp. 538–547, 2007.

[36] B. Yu, Y. Zhang, A. Shukla, S. Shukla, and K. Dorris, "The removal of heavy metal from aqueous solutions by sawdust adsorption—removal of copper", J. Hazard. Mater B, vol 80, pp. 33–42, 2000.

[37] WHO, "Environmental Health Criteria 221: Zinc", Geneva, 2001. http://whqlibdoc.who.int/ehc/who_ehc_221.pdf. Accessed online Aug. 9, 2013.

[38] N. Akhtar, J. Iqbal, and M. Iqbal, "Removal and recovery of nickel (II) from aqueous solution by loofa sponge-immobilized biomass of Chlorella sorokiniana: characterization studies", J. Hazard. Mater B, vol. 108, pp. 85–94, 2004.

[39] A. Ozturk, "Removal of nickel from aqueous solution by the bacterium Bacillus thuringiensis", J. Hazard. Mater, vol. 147, pp. 518–523, 2007.

[40] WHO, "Guidelines for Drinking Water Quality 4th edition", Geneva, 2011.

[41] W. H. Organization, "WHO's drinking water standards", Geneva, 1993..http://www.lenntech.com/applications/drinking/standards/who-s-drinking-water-standards.htm. Accessed Sept. 5, 2015.

[42] D. Drury. " Report on regulations and standards for drinking-water quality", Draft 12,2013.http://www.who.int/water_sanitation_health/Draft_RegScan_May_2014.pdf . Accessed Sept. 5, 2015.

[43] S. Sundaram and P. Raghavan, "Chromium-VI: Reagents Synthetic Applications", Springer Briefs in Molecular Science, DOI: 10.1007/978-3-642-20817-1_1, 2011.

[44] W. Motzer and T. Engineers, Chemistry, Geochemistry, and Geology of Chromium and Chromium Compounds, no. 6, USA: Chromium (VI) Handbook, CRC Press, pp. 23–91, 2005.

[45] D. Kimbrough, Y. Cohen, A. Winer, L. Creelman, and C. Mabuni, "A critical assessment of chromium in the environment", Crit. Rev. Environ. Sci. Technol., vol. 29, pp. 1–46, 1999.

[46] J. Jacobs and S. Testa, "Overview of Chromium(VI) in the Environment: Background and History", no. 6i, pp. 1–22, 2004.

[47] W. J. Priestley, "Chromium and Its Alloys", Industrial & Engineering Chemistry, vol. 28, no. 12, 1936.

[48] J. Barnhart, "Chromium chemistry and implications for environment", Journal of Soil Contamination, vol. 6, no. 6, pp. 561–568, 2008.

[49] C. Wei, D. Zhi, C. Yang, L. Gui-Ning, L. Yun-Feng, H. Se-Yan, and Z. Liu-Chun, "Removal of chromium (VI) from electroplating wastewater using an anion exchanger derived from rice straw", Environmental Technology, 2012.

[50] S. Farag and Z. Sahar, "Identification of bacterial strains from tannery effluent and reduction of hexavalent chromium", Journal of Environmental Biology, vol. 31, no. 5, pp. 877–882, 2010.

[51] G. Lautner, J. Carver, and R. Konzen, "Measurement of chromium VI and chromium III in stainless steel welding fumes with Electron Spectroscopy for Chemical Analysis and Neutron Activation Analysis", American Industrial Hygiene Association Journal, vol. 39, no. 8, pp. 651–660, 1978.

[52] A. D. Dayan and A. J. Paine, "Mechanisms of chromium toxicity, carcinogenicity and allergenicity: review of the literature from 1985 to 2000", Hum. Exp. Toxicol., vol. 20, pp. 439–451, 2001.

[53] "Final Report of Toxicological Profile for Chromium", Atlanta, Georgia, 2000.http://www.atsdr.cdc.gov/toxprofiles/tp.asp?id=62&tid=17. Accessed online July 27, 2013.

[54] D. Kimbrough, Y. Cohen, A. Winer, L. Creelman, and C. Mabuni, "A critical assessment of chromium in the environment", Crit. Rev. Environ. Sci. Technol., vol. 29, pp. 1–46, 1999.

[55] Z. Chen, R. Naidu, and S. Avudainayagam, "Separation of chromium (III) and chromium (VI) by capillary electrophoresis using 2,6-pyridinedicarboxylic acid as a pre-column complexation agent", Journal of Chromatography A, vol. 927, pp. 219–227, 2001.

[56] A. Léonard and R. Lauwerys, "Carcinogenicity and mutagenicity of chromium", Mutation Research/Reviews in Genetic Toxicology, vol. 76, no. 3, pp. 227–239, 1980.

[57] S. Sonia and R. Abbasia, "Teratogenic effects of chromium (vi) in environment as evidenced by the impact on larvae of amphibian Rana Tigrina: implications in the environmental management of chromium", International Journal of Environmental Studies, vol. 23, no. 2, 1984.

[58] WHO, "Access to safe drinking water improving; sanitation needs greater efforts", Geneva, Switzerland, 2010. http://www.who.int/mediacentre/news/releases/2010/water_20100315/en/. Accessed online June 28, 2013.

[59] G. Khitrov and R. Jaeger, "Chromium Toxicity", The Ronald O. Perlman Department of Dermatology, Department of Toxicology NYU Grad School of Arts and Science. [Online]. Available: http://www.nyu.edu/classes/jaeger/chromium_toxicity.htm. Accessed Nov. 20, 2013.

[60] L. Deling, T. Turi, A. Schuck, G. Khitrov, M. Blumenberg, and I. Freedberg, "Rays and Arrays: the transcriptional program in the response of human epidermal keratinocytes to UVB illumination", The FASEB Journal, vol. 15, no. 13, pp. 2533–2535, 2001.

[61] B. Finley, B. Kerger, G. Corbett, and D. Paustenbach, "Pharmacokinetics of drinking water exposure to selected chromium (Ifl and VI) compounds in human volunteers", The Toxicologist, vol. 30, no. 1, p. 14, 1996.

[62] P. Sheehan, D. Meyer, M. Sauer, and D. Paustenbach, "Assessment of the Human Health Risks Posed by Exposure to Chromium Contaminated Soils at Residential Sites", J. Tox. Environ. Health, vol. 32, no. 2, pp. 161–201, 1991.

[63] Nanofutures, European Technology Integrating and Innovation Platform on Nanotechnology, "Integrated Research and Industrial Roadmap for European Nanotechnology", Nanofutures Coordination and Support action , Grant agreement no. 266789, 2012, http://www.nanofutures.eu/sites/default/files/NANOfutures_Roadmap%20july%202012_0.pdf, Accessed online July 2015

[64] K. Savolainen, U. Backman, D. Brouwer, B. Fadeel, T. Fernandes, T. Kuhlbusch, R. Landsiedel, I. Lynch and L. Pylkkänen, "Nanosafety in Europe 2015-2025: Towards Safe and Sustainable Nanomaterials and Nanotechnology Innovations", Finnish Institute of Occupational Health, 2013,

www.ttl.fi/en/publications/...in_europe.../nanosafety_2015-2025.pdf, Accessed online August 2015

[65] "Center for Responsible Nanotechnology," Available: http://www.crnano.org/whatis.htm. Accessed Sept. 2013.

[66] N. Taniguchi, "Nanomaterials", in Proc. of International Conference on Precision Engineering (ICPE), pp. 18–23, 1974.

[67] "National Research Council: Small wonders – endless frontiers, a review of the National Nanotechnology Initiative", Washington, D.C., 2002.

[68] "Scientific Committee On Emerging And Newly Identified Health Risks (SCENIHR).", 2006.http://ec.europa.eu/health/scientific_committees/consultations/public_consultations/scenihr_cons_06_en.htm. Accessed online Nov. 3, 2013

[69] E. Roduner, "Size matters: why nanomaterials are different", Chem. Soc. Rev., vol. 35, pp. 583–592, 2006.

[70] M. Lundqvist, J. Stigler, G. Eliia, I. Lynch, T. Cedervall, and K. Dawson, "Nanoparticle size and surface properties determine the protein corona with possible implications for biological impacts", in Proceedings of the National Academy of Sciences, pp. 14265–14270, 2008.

[71] S. Lanone and J. Boczkowski,"Biomedical applications and potential health risks of nanomaterials: Molecular mechanisms, Curr. Mol. Med., vol. 6, pp. 651–663, 2006.

[72] P. Khanna, C. Ong, B. Bay and G. Baeg," Nanotoxicity: an interplay of oxidative stress, inflammation and cell death a review", Nanomaterials, vol.5, pp. 1163-1180, 2015.

[73] Y. Chen, H. Chen and J. Shi, "Drug delivery/imaging multifunctionality of mesoporous silica-based composite nanostructures". Expert Opin. Drug Deliv., vol.11, pp.917-930, 2014.

[74] A. Nemmar, P. Yuvaraju, S. Beegam, J. Yasin, R. Dhaheri, M. Fahim, B. Ali," *In vitro* platelet aggregation and oxidative stress caused by amorphous silica nanoparticles", Int. J. Physiol. Pathophysiol. Pharmacol., vol.7, pp. 27-33, 2015.

[75] Y. Xu, N. Wang, Y. Yu, Y. Li, Y. Li, Y. Yu, X. Zhou and Z. Sun, "Exposure to silica nanoparticles causes reversible damage of the spermatogenic process in mice", PLoS ONE, vol.9, 2014.

[76] A. Gupta and M. Gupta,"Synthesis and surface engineering of iron oxide nanoparticles for biomedical applications", Biomaterials, vol. 26, pp. 3995–4021, 2005.

[77] M. Peng, H. Li, Z. Luo, J. Kong, Y. Wan, L. Zheng, Q. Zhang, H. Niu, A. Vermorken and W. van de Ven,"Dextran-coated superparamagnetic nanoparticles as potential cancer drug carriers in vitro", Nanoscale, vol.7, pp.11155–11162, 2015.

[78] S. Laurent, A. Saei, S. Behzadi, A. Panahifar and M. Mahmoudi," Superparamagnetic iron oxide nanoparticles for delivery of therapeutic agents: Opportunities and challenges", Expert Opin. Drug Deliv., vol. 11, pp.1449–1470, 2014.

[79] H. Zhang, C. Wang, B. Chen and X. Wang," Daunorubicin-TiO_2 nanocomposites as a "smart" ph-responsive drug delivery system", Int. J. Nanomed., vol. 7, pp.235–242, 2012.

[80] N. Younes, S. Amara, I. Mrad, I. Ben-Slama, M. Jeljeli, K. Omri, J. El Ghoul, L. El Mir, K. Rhouma and H. Abdelmelek," Subacute toxicity of titanium dioxide (TiO_2)nanoparticles", Nanomaterials, vol. 5, 2015.

[81] R. Shrivastava, S. Raza, A. Yadav, P. Kushwaha and S. Flora," Effects of sub-acute exposure toTiO_2, ZnO and Al_2O_3 nanoparticles on oxidative stress and histological changes in mouse liver and brain", Drug Chem. Toxicol., vol. 37, pp. 336–347, 2014.

[82] M. Auffan, J. Rose, J. Bottero, G. Lowry, J. Jolivet, and M. Wiesner, "Towards a definition of inorganic nanoparticles from an environmental, health and safety perspective: A review", Nature Nanotechnology, vol. 4, pp. 634-641, 2009.

[83] J. Ramsden, "What is nanotechnology ?", vol. 1, pp. 3–17, 2005.

[84] J. Hristov and L. Fachikov, "An overview of separation by magnetically stabilized beds: State-of-the-art and potential applications", China Particuology, vol. 5, no. 1–2, pp. 11–18, 2007

[85] T. Takeshima, Y. Tada, N. Sakaguchi, F. Watari and B. Fugetsu, "DNA/Ag Nanoparticles as Antibacterial Agents against Gram-Negative Bacteria", Nanomaterials, vol. 5, pp. 284-297, 2015.

[86] S. Raj, S. Jose, U. Sumod and M. Sabitha, " Nanotechnology in cosmetics: Opportunties and challenges", J. Pharm Bioallied Sci., vol. 4, no. 3, pp. 186-193, 2012

[87] "Nanotechnology and Suncreens", A consumer guide for avoiding nano-sunscreens, 2007,http://www.foe.org/system/storage/877/23/9/634/Nanotechnology_and_sunscreens.pdf Accessed August 2015.

[88] Z. Renyun and H. Olin, "Carbon nanomaterials as drug carriers: Real time drug release investigation", Materials Science and Engineering C, vol. 32, pp. 1247–1252, 2012.

[89] D. Agatino, G.Elisa, M. Giuseppe, and P. Leonardo, "A survey of photocatalytic materials for environmental remediation: A review", J. Hazard. Mater., vol. 3, no. 29, pp. 211–212, 2012.

[90] N. Sanpo, J. Wang, and C. Berndt, "Influence of Chelating Agents on the Microstructure and Antibacterial Property of Cobalt Ferrite Nanopowders", Journal of the Australian Ceramic Society, vol. 49, no. 1, pp. 84–91, 2013.

[91] H. Ghandoor, H. Zidan, M. Khalil, and M. Ismail, "Synthesis and Some Physical Properties of Magnetite (Fe_3O_4)Nanoparticles", Int. J. Electrochem. Sci., vol. 7, pp. 5734–5745, 2012.

[92] R. Cornell and U. Schwertmann, The Iron Oxides: Structure, Properties, Reactions Occurences and Uses, Wiley-VCH, Weinheim, 2003.

[93] A. Lu, E. Salabas, and F. Schüth, "Magnetic Nanoparticles: Synthesis, Protection, Functionalization, and Application", Angew. Chem. Int. Ed., vol. 46, pp. 1222–1244, 2007.

[94] A. Ranaware and S. Satpute, "Correlation between effects of cerium oxide nanoparticle and ferrofluid on the performance and emission characteristics of a C.I. engine", International Journal of Modern Engineering Research, vol. 3, pp. 2831-2835, 2013.

[95] S.Stewart, R. Borup, M. Wilson, A. Datye and F. Garzon, "Ceria and doped ceria nanoparticle additives for polymer fuel cell lifetime improvement", ECS Trans., vol. 63, no. 3, pp. 403–411, 2014.

[96] D. Girija, H. Naik, C. Sudhamani and B. Kumar,"Cerium oxide nanoparticles a green, reusable, and highly efficient heterogeneous catalyst for the synthesis of polyhydroquinolines under solvent free conditions", Applied Science Research, vol.3, no.3, pp.373-382, 2011.

[97] J.Shi, H.Karlsson, K.Johansson, V.Gogvadze, L.Xiao, J.Li, T.Burks, A. Uheida, M.Muhammed, S.Mathur, R.Morgenstern, V.Kagan, B.Fadeel, "Microsomal Glutathione Transferase1 Protects Against Silica Nanoparticle-Induced Cytotoxicity", ACS Nano, vol.6, no.3, pp.1925-38, 2012.

[98] M. Wason and J. Zhao, "Cerium oxide nanoparticles:potential applications for cancer and other diseases", Am. J. Transl. Res., vol. 5, no.2, pp. 126-131, 2013.

[99] L. Weisheng, Y. Huang, X. Zhou and Y. Ma,"Toxicity of cerium oxide nanoparticles in human lung cancer cells", International Journal of Toxicology, vol.25, pp.451-457, 2006.

[100] USGS Mineral Information Titanium http://minerals.usgs.gov/minerals/pubs/commodity/titanium, Accessed Sept. 2015.

[101] A. Popov, A. Priezzhev, J. Lademann and R. Myllyla, "TiO_2 nanoparticles as an effective UV-B radiation skin-protective compound in sunscreens", J. Phys. D: Appl. Physics, vol. 38, no. 15, 2005,

[102] G. Nohynek, J. Lademann, C. Ribaud and M. Roberts, "Grey goo on the skin? Nanotechnology, cosmetic and sunscreen safety", Crit. Rev. Toxicol., vol. 37, no. 3. pp. 251-77, 2007.

[103] M. Kiser, P. Westerhoff, T. Benn, Y. Wang, J. Perez-Rivera and K. Hristovski," Titanium nanomaterial removal release from wastewater treatment plants", Environ. Sci. Technol., vol. 43, pp. 6757-6763, 2009

[104] T. Benn and P. Westerhoff, " Nanoparticle silver released into water from commercially available sock fabrics", Environ. Sci.Technol., vol. 42, no. 11, pp. 4133–4139, 2008.

[105] B. Nowack, T. Bucheli, " Occurrence, behavior and effects ofnanoparticles in the environment", Environ. Pollut., vol. 150, no. 1, pp. 5–22, 2007.

[106] American Conference of Governmental Industrial Hygienists (ACGIH):Threshold limit values and biological exposure indices for 1992–1993. Cincinnati: Ohio: American Conference of Governmental industrial hygienists; 1992.

[107] P. Maness, S. Smolinski, D. Blake, Z. Huang, E. Wolfrum and W. Jacoby," Bactericidal activity of photocatalytic TiO2 reaction : toward an understanding of its killink mechanism", Appl. Environ. Microbiol., vol.65, no.9, pp. 4094-4098, 1999.

[108] K. Wong, " Silver nanoparticles-The real "silver bullet" in clinical medicine", Medicinal Chemistry Communication, vol.1, no.2, 2012.

[109] C. Tsai, Y. Hung, Y. Chou, D. Huang, J. Hsiao and C. Chang," High-contrast paramagnetic fluorescent mesoporous silica nanorods as a multifunctional cell-imaging probe", Small, vol.4, no.2, pp. 186–191, 2008.

[110] L. Ingunn, C. Sandberg, T. Gao, B. Jelle and A. Gustavsen," Synthesis of hollow silica nanospheres by sacrificial polystyrene templates for thermal insulation application", Advances in Materials Science and Engineering, vol. 2013, 2013.

[111] P. More, S. Jeong, J. Lee, Y. Seo, B. Ryu and Y. Choi," Printable electronics-compatible silicon nanoparticles prepared by the facile decomposition of SiS_2 and their application in a back-to-back Schottky diode", Journal of Materials Chemistry, no.44, 2012.

[112] S. Bet and A. Kar," Thin film deposition on plastic substrates using silicon nanoparticles and laser nanoforming, vol. 130, no. 1-3, pp. 228-236, 2006.

[113] S. Ramakrishna, K. Fujihara, W. Teo, T. Yong, Z. Ma and R. Ramaseshan,"Electrospun nanofibers: solving global issues", vol.9, no.3, pp.40-50, 2006

[114] Wahyudiono, S. Machmudah, K. Murakami, S. Okubayashi and M. Goto," Generation of PVP fibers by eletrospinning in one-step process under high-pressure CO_2", International Journal of Industrial Chemistry, vol.4, no. 27, 2013.

[115] T. Kowalewski, S. Blonski and S. Barral," Expeiments and modelling of electrospinning process", Bulletin of the Polish Academy of Sciences, vol.53, no.4, 2005.

[116] H. Rajabinejad, R. Khajavi, A. Rashidi, N. Mansouri and M. Yazdanshenas,"Recycling of used bottle grade poly ethyleneterephthalate to nanofibers by melt-electrospinning method", Int. J. Environ. Res., vol.3, no.4, pp.663-670, 2009.

[117] A. Luzio, E. Canesi, C. Bertarelli and M. Caironi,"Electrospun polymer fibers for electronic applications: a review", Materials, vol.7, 2014.

[118] C. Martin," Membrane-based synthesis of nanomaterials", Chem. Mater., vol.8, pp.1739-1746, 1996.

[119] T. Ondarcuhu and C. Joachim,"Drawing a single nanofibre over hundreds of microns", Europhys. Lett., vol.42. no.2, pp.215-220, 1998.

[120] P. Ma and R. Zhang,"Synthetic nano-scale fibrous extracellular matrix", J. Biomed Mat. Res., vol.46, pp.60-72, 1999.

[121] G. Whitesides and B. Grzybowski,"Self-assembly at all scales", Science, vol.295, pp.2418-2421, 2002.

[122] J. Doshi and D. Reneker, "Electrospinning process and applications of electrospun fibers", J. Electrost., vol. 35, pp. 151–160, 1995.

[123] Z. Huang, Y. Zhang, M. Kotaki, and S. Ramakrishna, "A review on polymer nanofibers by electrospinning and their applications in nanocomposites", Composites Science and Technology, vol. 63, pp. 2223–2253, 2003.

[124] J. Cooley, "Apparatus for electrically dispersing fluids", U.S. Patent 6926311902.

[125] W. Morton, "Apparatus for electrically dispersing fluids", U.S. Patent 7056911902.

[126] P. Baumgarten, "Electrostatic spinning of acrylic microfibers", J. Colloid Interface Sci., vol. 36, pp. 71–79, 1971.

[127] J. Deitzel, J. Kleinmeyer, D. Harris, and N. Tan, "The effect of processing variables on the morphology of electrospun nanofibers and textiles", Polymer, vol. 42, pp. 261–272, 2001.

[128] C. Thompson, G. Chase, A. Yarin, and D. Reneker, "Effects of parameters on nanofiber diameter determined from electrospinning model", Polymer, vol. 48, pp. 6913–6922, 2007.

[129] Z. Shin, Y. Wanli, J. Wang, L. Guiwu, G. Qiaon, and J. Zhihao, "Effect of interfacial structure on the thermal conductivity of carbon nanofibers reinforced aluminum nitride composites", Ceramics International, vol. 39, no. 3, pp. 3365–3370, 2012.

[130] A. MacDiarmid, W. Jones Jr, I. Norris, J. Gao, A. Johnson Jr, N. Pinto, J. Hone, B. Han, F. Ko, H. Okuzaki, and M. Llaguno, "Electrostatically-generated nanofibers of electronic polymers", Synthetic Metals, vol. 119, pp. 27–30, 2001

[131] Y. Ryua, H. Kima, K. Leeb, H. Parka, and D.Lee, "Transport properties of electrospun nylon 6 nonwoven mats", European Polymer Journal, vol. 39, no. 9, pp. 1883–1889, 2003.

[132] M. Hajra, K. Mehta, and G. Chase, "Effects of humidity, temperature, and nanofibers on drop coalescence in glass fiber media", Separation and Purification Technology, vol. 30, no. 1, pp. 79–88, 2003

[133] A. Yarin, "Taylor cone and jetting from liquid droplets in electrospinning of nanofibers", Journal of Applied Physics, vol. 90, no. 9, pp. 4836–4847, 2001.

[134] S. Ramakrishna, K. Fujihara, W. Teo, T. Lim, and Z. Ma, "An Introduction to Electrospinning and Nanofibers", Singapore:World Scientific, 2005.

[135] S. Rengaraj, K. Yeon, and S. Moon, "Removal of chromium from water and wastewater by ion exchange resins", Journal Hazardous Materials, vol. 87, no. 1–3, pp. 273–287, 2001

[136] E. Salazar, M. Ortiz, A. Urtiaga, and J. Irabien, "Equilibrium and kinetics of the Cr(VI) extraction with Aliquat 336", Ind. Eng. Chem. Res, vol. 31, pp. 1516–1522, 1992

[137] B. Al-Rashdi, D. Johnson, and N. Hilal, "Removal of heavy metal ions by nanofiltration", Desalination, vol. 315, no. 15, pp. 2-17, 2012.

[138] M. Ahmed, S. Taha, T. Chaabane, D. Akretche, R. Maachi, and G. Dorange, "Nanofiltration process applied to the tannery solutions", Desalination, vol. 200, pp. 419–420, 2006

[139] J.Zuo, S.Tong, X.Yu, L.Wu, C.Cao, M.Ge, and W.Song, "Fe^{3+} and amino functioned mesoporous silica: preparation, structural analysis and arsenic adsorption", J. Hazard. Mater., vol. 235–236, pp. 336–342, 2012.

[140] Q. Li, X. Xu, H. Cui, J. Pang, Z. Wei, Z. Sun, and J. Zhai, "Comparison of two adsorbents for the removal of pentavalent arsenic from aqueous solutions", Journal of Environmental Management, vol. 98, pp. 98–106, 2012.

[141] A. Hariharan, "Solvent Extraction Of Chromium (VI) From Aqueous Acid Solutions By Tricaprylamine Oxide", International Journal of ChemTech Research, vol. 2, no. 1, pp. 690–694, 2010.

[142] L. Rafati, A. Mahvi, A. Asgari, and S. Hosseini, "Removal of chromium (VI) from aqueous solutions using Lewatit FO36 nano ion exchange resin", Int. J. Environ. Sci. Tech., vol. 7, no. 1, pp. 147–156, 2010.

[143] A. Yavuz, E. Dincturk-Atalay, A. Uygun, F. Gode, and E. Aslan, "A comparison study of adsorption of Cr(VI) from aqueous solutions ontoalkyl-substituted polyaniline/chitosan composites", Desalination, vol. 279, no. 1-3, pp. 325-331, 2011.

[144] M. Barakat, "New Trends in removing heavy metals from industrial wastewater", Arabian Journal of Chemistry, vol. 4, pp. 361–377, 2010.

[145] T. Kurniawan, G. Chan, W. Lo, and S. Babel, "Physicochemical treatment techniques for wastewater laden with heavy metals", Chemical Engineering Journal, vol. 118, pp. 83–98, 2006.

[146] S. Babel and T. Kurniawan, "Low-cost adsorbents for heavy metals uptake from contaminated water: a review", Journal Hazardous Materials, vol. B97, pp. 219–243, 2003

[147] A. Aklil, M. Mouflihb and S. Sebti, "Removal of heavy metal ions from water by using calcined phosphate as a new adsorbent", Journal Hazardous Materials, vol. A112, pp. 183–190, 2004.

[148] T. Mohammadi, A. Mohebb, M. Sadrzadeh, and A. Razmi, "Modeling of metal ion removal from wastewater by electrodialysis", Separation and Purification Technology, vol. 41, pp. 73–82, 2005.

[149] M. Barakat, Y. Chen, and C. Huang, "Removal of toxic cyanide and Cu(II) ions from water by illuminated TiO_2 catalyst", J. Appl. Catal. B: Environ, vol. 53, pp. 574–578, 2004.

[150] P. Kajitvichyanukula, J. Ananpattarachaia, and S. Pongpom, "Sol–gel preparation and properties study of TiO2 thin film for photocatalytic reduction of chromium(VI) in photocatalysis process", Sci. Technol. Adv. Mater., vol. 6, pp. 352–358, 2005.

[151] B. Nowack and J. VanBriesen, "Chelating Agents in the Environment", in Biogeochemistry of Chelating Agents, B. Nowack and J. M. VanBriesen, Eds. Washington: American Chemical Society, 2003.

[152] J. Huang, Y. Cao, Z. Liu, Z. Deng, F. Tang, and W. Wang, "Efficient removal of heavy metal ions from water system by titanate nanoflowers", Chemical Engineering Journal, vol. 180, pp. 75–80, 2012.

[153] P. Chingombe, B. Saha, and R. Wakeman, "Surface modification and characterisation of a coal-based activated carbo", Carbon, vol. 43, pp. 3132–3143, 2005.

[154] G. Crini, "Non-conventional low-cost adsorbents for dye removal: A review," Bioresource Technology, vol. 97, pp. 1061–1085, 2006.

[155] T. Burks, A. Uheida, M. Saleemi, M. Eita, M. Toprak, and M. Muhammed, "Selective Removal of Chromium (VI) using Superparamagnetic Iron Oxide Nanoparticles coated with Cyanex-301", Separation Science and Technology, vol. 48, pp. 1243–1251, 2013.

[156] M. Owlad, M. Aroua, W. Daud, and S. Baroutian, "Removal of Hexavalent Chromium-Contaminated Water and Wastewater: A Review", Water, Air, and Soil Pollution, vol. 200, no. 1–4, pp. 59–77, Nov. 2008.

[157] A. SenGupta and M. Yizhak, Ion Exchange and Solvent Extraction A Series of Advances, vol. 16 . New York: Marcel Dekker, Inc, 2004.

[158] D. Neumann and F. Phil, "Principles of Ion Exchange in Wastewater Treatment", Asian Water, vol. 19, 2009

[159] F. Helfferich, Ion Exchange, 1st Edition. New York, NY: McGraw Hill, 1995.

[160] T. Kurniawan and S. Babel, "A research study on Cr(VI) removal from contaminated wastewater using low-cost adsorbents and commercial activated carbon", pp. 1110–1117, 2003.

[161] G. Raj, Surface Chemistry (Adsorption), 4th ed. Krishna Prakashan Media, 2002.

[162] S. Yadla, V. Sridevil, and M. Lakshmi, "Journal of Chemical, Biological and Physical Sciences", J. Chem. Bio. Phy. Sci. Sec. D., vol. 2, no. 3, pp. 1585–1593, 2012.

[163] D. W. Green and R. H. Perry, Perry's Chemical Engineers' Handbook, 8th ed. McGraw Hill.

[164] D. L. Sparks, "Kinetics and Mechanisms of Soil Chemical Reactions", in Handbook of Soil Sciences Properties and Processes, Second Edi., P. M. Huang, Y. Li, and M. E. Sumner, Eds. Boca-Raton: CRC Press, pp. 1–30, 2011,.

[165] G. Limousin, J. Gaudet, L. Charlet, S. Szenknect, V. Barthes, and M. Krimissa, "Sorption isotherms: a review on physical bases, modeling and measurement", Applied Geochemistry, vol. 22, pp. 249–275, 2007.

[166] A. Dada, A. Olalekan, A. Olatunya and O.Dada,"Langmuir, Freundlich, Temkin and Dubinin-Radushkevich Isotherms studies of Equilibrium Sorption of Zn^{2+} unto Phosphoric Acid Modified Rice Husk", Journal of Applied Chemistry, Vol.3, no.1, pp. 38-45, 2012.

[167] S. F. Fendorf, "Surface reactions of Chromium in Soils and Waters," Geoderma, vol. 67, pp. 55–71, 1995.

[168] D. Lakherwal, "Adsorption of heavy metals: a review," International Journal of Environmental Research and Development, vol. 4, no. 1, pp. 41–48, 2014.

[169] J. Robles-Camacho and A. M. Armienta, "Natural chromium contamination of groundwater at Leo'n Valley, Mexico," Journal of Geochemical Exploration, vol. 68, pp. 167–181, 2000.

[170] D. E. Kimbrough, Y. Cohen, A. M. Winer, L. Creelman, and C. Mabuni, "A critical assessment of chromium in the environment," Crit. Rev. Environ. Sci. Technol., vol. 29, pp. 1–46, 1999.

[171] "Final Report of Toxicological Profile for Chromium," Atlanta, Georgia, 2000.http://www.atsdr.cdc.gov/toxprofiles/tp.asp?id=62&tid=17. Accessed online July 27, 2013.

[172] J. Igwe and A. Abia, "Adsorption kinetics and intraparticulate diffusivities for bioremediation of Co (II), Fe (II) and Cu (II) ions from wastewater using modified

and unmodified maize cob," International Journal of Physical Sciences, vol. 2, no. 5, pp. 119–127, 2007.

[173] H. Kazemzadeh, A. Ataie, and F. Rashchi, "Synthesis of magnetite nano-particles by reverse co-precipitation," International Journal of Modern Physics: Conference Series, vol. 5, pp. 160–167, 2012.

[174] D. Bahnemann, C. Kormann and R. Hofmann, "Preparation and characterization of quantum size zinc oxide: a detailed spectroscopic study ", J. Phys. Chem., vol. 91, no. 14 , pp. 3789–3798, 1987.

[175] N.Oh, J. Jegal, and K. Lee, "Preparation and characterization of nanofiltration composite membranes using polyacrylonitrile (PAN). II. Preparation and characterization of polyamide composite membranes", Journal of Applied Polymer Science, vol. 80, no. 14, pp. 2729–2736, 2001

[176] L. Chen, L. Bromberg, H. Schreuder-Gibson, J. Walker, T. Hatton, and G. Rutledge, "Chemical protection fabrics via surface oximation of electrospun polyacrylonitrile fiber mats", *Journal of Materials Chemistry*, vol. 19, no. 16, p. 2432, 2009

[177] V. Ishtchenko, K. Huddersman, and R. Vitkovskaya, "Part 1. Production of a modified PAN fibrous catalyst and its optimisation towards the decomposition of hydrogen peroxide", Applied Catalysis A: General, vol. 242, no. 1, pp. 123–137, 2003.

[178] K. Saeed, S. Haider, T. Oh, and S. Park, "Preparation of amidoxime-modified polyacrylonitrile (PAN-oxime) nanofibers and their applications to metal ions adsorption", Journal of Membrane Science, vol. 322, no. 2, pp. 400–405, 2008.

[179] S. Liao, Q. Feng, P. Zhang, F. Huang and Q. Wei, "Preparation of amidoxime polyacrylonitrile chelating nanofibers for the adsorption of metal ions", 2012.

[180] Hydroxylamine·HCl, G-Biosciences,www.Gbiosciences.com. Accessed August, 2015.

[181] A. Sugunan, V. Guduru, A. Uheida, M. Toprak and M. Muhammed, "Radially Oriented ZnO Nanowires on Flexible Poly-L-Lactide Nanofibers for Continuous-Flow Photocatalytic Water Purification", J. Am. Ceram. Soc., vol. 93, no. 11, pp. 3740-3744, 2010.

[182] H. Shi, X. Fu, X. Zhou, D. Wang and Z. Hu, "A low temperature extraction-solvothermal route to the fabrication of micro-sized MoS2 spheres modified by Cyanex 301", Journal of Solid State Chemistry, vol. 179, no. 6, pp. 1690-1697, 2006.

[183] A. Awwad and N. Salem, "A green and facile approach for synthesis of magnetite nanoparticles," Nanosci. Nanotechnol., vol. 2, no. 6, pp. 208–213, 2012.

[184] W. Xiao, H. Gu, D. Li, D. Chen, X. Deng, Z. Jiao, and J. Lin, "Microwave-assisted synthesis of magnetite nanoparticles for MR blood pool contrast agents," J. Magn. Magn. Mater., vol. 324, pp. 488–494, 2012.

[185] F. Galeotti, F. Bertini, G. Scavia, and A. Bolognesi, "A controlled approach to iron oxide nanoparticles functionalization for magnetic polymer brushes," J. Colloid Interface Sci., vol. 360, pp. 540–547, 2011.

[186] S. Pan, H. Shen, Q. Shu, J. Luo, and M. Hu, "Surface mercapto engineered magnetic Fe3O4 nanoadsorbent for the removal of mercury from aqueous solutions," J. Colloid Interface Sci., vol. 365, pp. 204–212, 2012.

[187] J. Kumar, B.R: Reddy, K.J. Reddy and A.V. Reddy, Liquid-liquid extraction of tetravalent hafnium from acidic chloride solutions using bis(2,4,4-trimethylpentyl) dithiophosphinic acid (Cyanex 301) Separ. Sci. Technol. 42(2006) 865-877.

[188] B. Menoyo, M.Elizalde, A. Almela, Determination of the degradation compounds formed by the oxidation of thiophosphinic acids and phosphine sulfides with nitric acid, Anal. Sci. 18 (2002) 799-804.

[189] L. Rossi, L. Vono, F. Silva, P. Kiyohara, E. Duarte, and J. Matos, "A magnetically recoverable scavenger for palladium based on thiol magnetite nanoparticles," Appl. Catal., A, vol. 330, pp. 139–144, 2007.

[190] S. Singh, K. Barick, and D. Bahadur, "Surface engineered magnetic nanoparticles for removal of toxic metal ions and bacterial pathogens," J. Hazard. Mater, vol. 192, pp. 1539–1547, 2011.

[191] H.Siesler, "Polymer–solvent interaction: the IR-dichroic behaviour of DMF residues in drawn films of polyacrylonitrile", Colloid Polym. Sci., vol. 255, pp. ,321–326, 1977.

[192] L. Zhang, J. Luo, T.J. Menkhaus, H. Varadaraju, Y. Sun, H. Fong, "Antimicrobial nano-fibrous membranes developed from electrospun polyacrylonitrile nanofibers", J. Membr. Sci., vol. 369, pp. 499–505, 2011.

[193] S. Park, S. Jo, D. Kim, W. Lee and B. Kim, "Effects of iron catalyst on the formation of crystalline domain during carbonization of electrospun acrylic nanofibers", Synth. Met., vol. 150, pp. 265–270, 2005.

[194] K. Wieszczycka and W. Tomczyk," Degradation of organothiophosphorous extractant Cyanex 301", Journal of Hazardous Materials, vol 192, pp 530-537, 2011.

[195] D. Morillo, A. Uheida, G. Perex , M. Muhammed and M. Valiente, " Arsenate removal with 3-mercaptopropanoic acid-coated superparamagnetic iron oxide nanoparticles", Journal of Colloid and Interface Science, vol 438, pp 227-234, 2015.

[196] P. Connett and K. Wetterhahn, "Reaction of Chromium(V1) with Thiols: pH Dependence of Chromium(VI) Thio Ester Formation", J. Am. Chem. Soc., no. 11, pp. 1842–1847, 1986.

[197] L. Benefield, J. Judkins, and B. Wend, Process Chemistry for Water and Wastewater Treatment. Englewood Cliffs: Prentice Hall, 1982.

[198] D. Moha and C. U. Jr. Pittman, "Review: activated carbons and low cost adsorbents for remediation of tri- and hexavalent chromium from water," J. Hazard. Mater., vol. 137, pp. 762–811, 2006.

[199] M. Abramson and C. King, "The Rate of Dissolution of Iron in Acids," J. Am. Chem. Soc., vol. 61, no. 9, pp. 2290–2295, 1939.

[200] P. Bhattacharyya, K. Pradhan, S. Paul,A. Das, "Nano crystalline ZnO catalyzed one pot multicomponent reaction for an easy access of fully decorated 4 H-pyran scaffolds and its rearrangement to 2-pyridone nucleus in aqueous media", Tetrahedron Lett., vol. 53, pp. 4687–4691, 2012.

[201] A. Kumar, M. Gupta, M.Kumar, "L-Proline catalysed multicomponent synthesis of 3-amino alkylated indolesvia a mannich-type reaction under solvent-free conditions", Green Chem., vol. 14, pp. 290-295, 2012.

[202] M. Gholipour, H. Hashemipour, and M. Mollashahi, "Hexavalent chromium removal from aqueous solution via adsorption on granular activated carbon: adsorption, desorption, modeling and simulation studies," *ARPN J. Eng. Appl. Sci.*, vol. 6, no. 9, 2011.

[203] M. Dakiky, M. Khamis, A. Manassra, and M. Mer'eb, "Selective adsorption of chromium(VI) in industrial wastewater using low-cost abundantly available adsorbents," *Adv. Environ. Res.*, vol. 6, pp. 533–540, 2002.

[204] M. Bhaumik, A. Maity, V. V. Srinivasu, and M. Onyango, "Removal of hexavalent chromium from aqueous solution using polypyrrole-polyaniline nanofibers," *Chem. Eng. J.*, vol. 181–182, pp. 323–333, 2012.

[205] J. Wang, K. Pan, Q. He, and B. Cao, "Polyacrylonitrile/polypyrrole core/shell nanofiber mat for the removal of hexavalent chromium from aqueous solution," *J. Hazard. Mater.*, vol. 244–245, pp. 121–129, 2013.

[206] S. Zulfiqar, F. Karadas, J. Park, E. Deniz, G. D. Stucky, Y. Jung, M. Atilhan, and C. T. Yavuz, "Amidoximes: promising candidates for CO2 capture", Energy Environ. Sci., vol. 4, pp. 4528–4531, 2011.

[207] J. Bernal, M. del Nozal, L. Debán, J. del Valle, V. Cerdá, and J. Est, "Analytical properties of the amidoxime group. XII", J. Therm. Anal., vol. 31, pp. 931–940, 1986.

[208] A. Srinivasan and T. Viraraghavan, "Decolorization of dye wastewaters by biosorbents: a review", J. Environ. Manage., vol. 91, pp. 1915–1929, 2010.

[209] T. Karthikeyan, S. Rajgopal, and L. Miranda, "Chromium (VI) adsorption from aqueous solution by Hevea Brasilinesis sawdust activated carbon," J. Hazard. Mater., pp. 192–199, 2005.

[210] S. Parlayici, A. Yar, A. Avci and E. Pehlivan; " Removal of hexavalent chromium using polyacrylonitrile/titanium dioxide nanofiber membrane", Desalination and Water Treatment, pp.1-7, 2015.

[211] P. Kampalanonwat and P. Supaphol, "Preparation of Hydrolyzed Electrospun Polyacrylonitrile Fiber Mats as Chelating Substrates: A Case Study on Copper(II) Ions", Industrial & Engineering Chemistry Research, vol. 50, no. 21, pp. 11912–11921, Nov. 2011.

[212] S. Karaivanova and A. Badev, "Modification of polyacrylonitrile fibers with hydrazine and hydroxylamine in aqueous medium", Die Angewandte Macromolekulare Chemie, vol. 140, pp. 1-32, 1986.

[213] Z. Wang, L. Wan, and Z. Xu, "Surface engineerings of polyacrylonitrile-based asymmetric membranes towards biomedical applications: An overview", Journal of Membrane Science, vol 304, pp. 8-23, 2007.

[214] Y. Ho and G. Mckay, "Pseudo-second order model for sorption processes", Process Biochemistry, vol. 34, pp. 451–465, 1999.

[215] F. Di Natale, A. Lancia, A. Molino, and D. Musmarra, "Removal of chromium ions from aqueous solutions by adsorption on activated carbon and char", J. Hazard. Mater., vol. 145, pp. 381–390, 2007.

[216] V. Gupta, A. Rastogi, and A. Nayak, "Adsorption studies on the removal of hexavalent chromium from aqueous solution using a low cost fertilizer industry waste material," J. Colloid Interface Sci., vol. 342, pp. 135–141, 2010.

[217] F. Gode, E. D. Atalay, and E. Pehlivan, "Removal of Cr(VI) from aqueous solutions using modified red pine sawdust," J. Hazard. Mater., vol. 152, pp. 1201–1207, 2008.

[218] X. Hu, J. Wang, Y. Liu, X. Li, G. Zeng, Z. Bao, X. Zeng, A. Chen, and F. Long, "Adsorption of chromium (VI) by ethylenediamine-modified cross-linked magnetic chitosan resin: Isotherms, kinetics and thermodynamics," J. Hazard. Mater., vol. 185, pp. 306–314, 2011.

[219] L. Chabaane, S. Tahiri, A. Albizane, M. El Krati, M. L. Cervera, and M. de la Guardia, "Immobilization of vegetable tannins on tannery chrome shavings and their use for the removal of hexavalent chromium from contaminated water," Chem. Eng. J., vol. 174, pp. 310–317, 2011.

[220] P. Yuan, D. Liu, M. Fan, D. Yang, R. Zhu, F. Ge, J. Zhu, and H. He, "Removal of hexavalent chromium [Cr(VI)] from aqueous solutions by the diatomite supported/unsupported magnetite nanoparticles," J. Hazard. Mater., vol. 173, pp. 614–621, 2010.

[221] G. Zelmanov and R. Semiat, "Iron (Fe+3) oxide/hydroxide nanoparticles-based agglomerates suspension as adsorbent for chromium (Cr+6) removal from water and recovery," Sep. Purif. Technol., vol. 80, pp. 330–337, 2011.

[222] P. Yuan, M. Fan, D. Yang, H. He, D. Liu, A. Yuan, J. Zhu, and T. Chen, "Montmorillonite-supported magnetite nanoparticles for the removal of hexavalent chromium [Cr(VI)] from aqueous solutions," Journal Hazardous Materials, vol. 166, pp. 821–829, 2009.

[223] Y. Talokar, "Studies on removal of chromium from waste water by adsorption using low cost agricultural biomass as adsorbents", *Int. J. Adv. Biotechnol. Res.*, vol. 2, no. 4, pp. 425–456, 2011.

[224] S. Deng and R. Bai, "Adsorption and desorption of humic acid on amidoximated polyacrylonitrile fiber", J. Colloid Interface Sci., vol. 280, pp. 36–43, 2004

[225] M. Bhaumik, A. Maity, W. Srinivasu, and M. Onyango, "Enhanced removal of cr(VI) from aqueous solution using polypyrrole/Fe3O4 magnetic nanocomposite", *J. Hazard. Mater.*, vol. 190, pp. 381–390, 2011

[226] Y. Onundi, A. Mamun, M. Al Khatib and A. Suleyman, " Heavy metals removal from synthetic wastewater by a novel nano-size composite adsorbent" , Int. J. Environ. Sci. Tech., vol. 8, no. 4, pp. 799-806, 2011.

[227] K. Wong, B. Liu, S. McCalla, B. Chu and B. Hsiao, "Analysis of PAN and PEGDA coated membranes for filtering water with reduced fouling and increased heavy metal adsorption", The Journal of Experimental Secondary Science, vol. 1, no. 3, 2012.

[228] J. Anandkumara and B. Mandalb, "Adsorption of chromium(VI) and rhodamine B by surface modified tannery waste: kinetic, mechanistic and thermodynamic studies", J. Hazard. Mater., vol. 186, no. 2–3, pp. 1088–1096, 2011.

[229] X. Sun, C. Liu, Y. Ma, S. Wang, B. Gao, and X. Li, "Enhanced Cu(II) and Cr(VI) biosorption capacity on poly(ethylenimine) grafted aerobic granular sludge", Colloids Surfaces B Biointerfaces, vol. 82, no. 2, pp. 456–462, 2011

[230] P. Yuan, D. Liu, M. Fan, D. Yang, R. Zhu, F. Ge, J. Zhu, and H. He, "Removal of hexavalent chromium (Cr(VI)) from aqueous solutions by the diatomite-supported/unsupported magnetite nanoparticles.", J. Hazard. Mater., vol. 173, no. 1–3, pp. 614–21, 2010.

[231] A. Kumar, T. Gupta, S. Kakan, S. Kalidhasan, V. Manasi, and N. Rajesh, "Effective adsorption of hexavalent chromium through a three center (3c) co-operative interaction with an ionic liquid and biopolymer", J. Hazard. Mater, vol. 239–240, pp. 213–224, 2012.

[232] S. Pan, H. Shen, Q. Xu, J. Luo and M. Hu, "Surface mercapto engineered magnetic Fe3O4 nanoadsorbent for the removal of mercury from aqueous solutions", J. Colloid Interface Sci., vol. 365, no. 1, pp. 204–212, 2012.

[233] T. Fujii, F.M.F de Groot, G.A. Sawatzky, F.C. Voogt, T. Hibma and K. Okada, " In situ XPS analysis of various iron oxide films grown by NO2-assisted molecular-beam epitaxy". Phys Rev B, vol. 59, pp. 3195-3202, 1999.

[234] C. Wanger, W. Riggs, L. Davis, J. Moulder, and G. Mullenberg, Handbook of X-ray Photoelectron Spectroscopy. Eden Prairie: Perkin Elmer Corp., pp. 190, 1979.

[235] V. Gupta and A. Rastogi, "Biosorption of Lead from aqueous solutions by green algae Spirogyra species: Equilibrium and adsorption kinetics", J. Hazard. Mater, vol. 154, pp. 347-354, 2008.

[236] S. Pezzin, J. Rivera, C. Collins, and K. Collins, "Reduction of Trace Quantities of Chromium(VI) by Strong Acids", J. Braz. Chem. Soc., vol. 15, no. 1, pp. 58–65, 2004.

[237] B. Issa, I. Obaidat, B. Albiss and Y. Haik," Magnetic nanoparticles: surface effects and properties related to biomedicine applications", Int. J. Mol. Sci., vol. 14, pp. 21266-21305, 2013.

[288] C. Buzea, I. Blandino and K. Robbie," Nanomaterials and nanoparticles:sources and toxicity", Biointerphases, vol.2, no.4, pp.17-172, 2007.

[239] T. Albrecht, J. Addai-Mensah and D. Fornasiero,"Effect of pH, concentration and temperature on copper and zinc hydroxide formation/precipitation in solution", Ian Wark Research Institute, University pf South Australia,

[240] N. Enomoto, S. Maruyama and Z.Nakagawa," Agglomerization of silica spheres under ultrasonication", J. Mater. Res., vol. 12, no. 5, pp. 1410-1415, 1997.

[241] A. Murray, E. Kisin, A. Inman, S. Young, M. Muhammed, T. Burks, A. Uheida, A. Tkach, M. Waltz, V. Castranova, B. Fadeel, V. Kagan, J. Riviere, N. Riviere and A. Shedova," Oxidative stress and dermal toxicity of iron oxide nanoparticles in vitro", Cell Biochem Biophys, vol. 67, pp. 461-476, 2013.